

DOCUMENT RESUME

ED 072 646

EM 010 739

AUTHOR King, Barry C.; Fowler, Frank D.
TITLE Relative Effectiveness of Two and Three Dimensional
Image Storage Media. Technical Report.
INSTITUTION Naval Training Equipment Center, Orlando, Fla.
REPORT NO NAVTRAEQUIPCEN-70-C-0238-1
PUB DATE Sep 72
NOTE 128p.; Prepared under contract by Martin Marietta
Corporation, Orlando, Fla

EDRS PRICE MF-\$0.65 HC-\$6.58
DESCRIPTORS Comparative Analysis; *Flight Training; Military
Training; Navigation; *Simulators; *Stereopsis;
*Visual Aids; Visual Perception

ABSTRACT

In the design of visual simulation equipment for training systems, one key decision is the nature of the image storage medium to be used. One consideration in this complex issue is the adequacy of the depth cues which can be derived from imagery based on two- rather than three-dimensional sources. Although motion parallax is a relatively minor cue, it is the essential difference between imagery derived from two- and three-dimensional sources. This study was designed to investigate the role of motion parallax in the perception of apparent depth on a dynamic television display. Subjects were tested on their ability to perceive dimensionality as a function of altitude. The results showed that motion parallax provides a useful cue to depth only at very close ranges. It was concluded that for training problems which require simulation of television navigation and/or targeting imagery there is little or no advantage in the more expensive three-dimensional image storage devices for altitudes above 750 feet. (Author/JK)

FILMED FROM BEST AVAILABLE COPY



U S DEPARTMENT OF HEALTH
EDUCATION & WELFARE
OFFICE OF EDUCATION
THIS DOCUMENT HAS BEEN REPRO-
DUCED EXACTLY AS RECEIVED FROM
THE PERSON OR ORGANIZATION ORIGIN-
ATING IT POINTS OF VIEW OR OPIN-
IONS STATED DO NOT NECESSARILY
REPRESENT OFFICIAL OFFICE OF EDU-
CATION POSITION OR POLICY

Technical Report: NAVTRAEQUIPCEN 70-C-0238-1

RELATIVE EFFECTIVENESS OF TWO AND THREE
DIMENSIONAL IMAGE STORAGE MEDIA

Barry C. King
Frank D. Fowler

Martin Marietta Corporation
Orlando, Florida
Contract N61339-70-C-0238
NAVTRADEVCCEN Task No. 8424

September 1972

DoD Distribution Statement

Approved for public release;
distribution is unlimited.

NAVAL TRAINING EQUIPMENT CENTER
ORLANDO, FLORIDA 32813

04071007

Ac. 1. 010 W

NAVTRAEQUIPCEN 70-C-0238-1

ABSTRACT

An experiment consisting of two series of tests is described. Both tests were designed to evaluate the ability of subjects to perceive the dimensionality of source material used to generate dynamic TV images of simulated military targets. The first series of tests, designated the Dive Approach series, was designed to investigate the perception of motion-dependent cues to apparent depth during an approach to the target area at a constant dive angle. This type of approach was selected to represent the final flight path of a TV guided missile. Behavioral techniques were used to assess the ability of observers to detect these cues in dynamic imagery presented via TV. The stimulus material used in these behavioral tests consisted of video recordings of target convergence runs made in the Martin Marietta Guidance Development Center (GDC) using 3 dimensional (3-D) and optically simulated 2 dimensional (2-D) target areas.

The second series of tests, designated the Constant Altitude Approach series, was designed to investigate the perception of motion-dependent cues to dimensionality derived from simulated horizontal flight at various altitudes. Again, the materials used in the behavioral analysis were video recordings of selected target runs made on the GDC terrain model.

The imagery used in these two series of tests included a wide variety of manmade targets and natural terrain features. Both tests were conducted as complete factorial designs.

The results show that movement parallax provides a useful cue to depth only at very close ranges. This was true whether the target area appeared to expand radially around the aim point as in the constant dive angle tests, or appeared to progress from top to bottom of the TV screen as in the tests designed to simulate horizontal flight. This finding has significant implications for the design of visual simulation equipment to be used for training. Thus, for training problems which require simulation of TV navigation and/or targeting imagery, serious consideration should be given to the use of relatively inexpensive 2-D image storage devices for altitudes in excess of 750 feet.

GOVERNMENT RIGHTS IN DATA STATEMENT

Reproduction of this publication in whole or in part is permitted for any purpose of the United States Government.

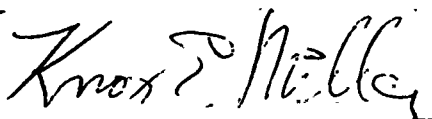
FOREWORD

In the design of visual simulation equipment for training systems one key decision is the nature of the image storage medium to be employed. This is a complex issue involving many diverse considerations one of which is the adequacy of the depth cues which can be derived from imagery based on 2 as opposed to 3 dimensional sources.

Many of the obvious and compelling cues to depth such as interposition, relative size, aerial perspective, etc., are independent of both source dimensionality and dynamic conditions. Others however, such as movement parallax and vertical perspective change can only occur as a result of relative movement between the observer and that which is observed. Thus, although motion parallax is a relatively minor cue to depth it is the principal subject of this study since it constitutes the essential difference between imagery derived from 2 and 3 dimensional sources.

Specifically, this study was designed to investigate the role of motion parallax in the perception of apparent depth on a dynamic TV display. This was accomplished in two steps. Video recordings were obtained of both 3 dimensional and optically simulated 2 dimensional target areas using two basically different approach geometries. The resulting imagery was then used in a series of behavioral tests to assess the ability of subjects to perceive dimensionality as a function of altitude.

The results of these analyses show that movement parallax provides a useful cue to depth only at very close ranges. It was concluded that for the training problems which require simulation of TV navigation and/or targeting imagery there is little or no advantage in the more expensive 3 dimensional image storage devices for altitudes above 750 feet.



KNOX E. MILLER
Project Psychologist

TABLE OF CONTENTS

Section	Page
I INTRODUCTION	1
1 Background	1
2 Objectives	2
II METHOD	3
1 Introduction	3
2 Dive Approach Tests	3
2.1 Experimental Design	3
2.2 Behavioral Test Procedures	8
3 Constant Altitude Tests	9
3.1 Experimental Design	9
3.2 Behavioral Test Procedures	12
III DISCUSSION OF RESULTS	14
1 Dive Approach Tests	14
1.1 Target Area	14
1.2 Velocity	16
1.3 Shadow Versus Nonshadow Effects	17
1.4 Display Viewing Distance	17
1.5 Subjective Responses	17
2 Constant Altitude Tests	17
2.1 Target Area	18
2.2 FOV/SR/Alt.	22
2.3 Experience	23
2.4 Velocity	24
3 Related Analyses	24
3.1 Comparisons Between the Dive Approach and Constant Altitude Tests	24
3.2 Comparison With Other Psychophysical Data	26
3.3 Notes on Perspective Change	26
IV CONCLUSIONS	27
V RECOMMENDATIONS	29
References	30

NAVTRAEQUIPCEN 70-C-0238-1

APPENDICES	Page
A Statistical Analysis	31
B Generation of Two-Dimensional Dive Approach Runs by Using an Optical Zoom Technique	36
C Test Facilities and Equipment	40
D Target Preparation and Target Characteristics	46
E Approach Geometries	54
F Stimulus Tape Generation	65
G Movement Parallax and Target Perspective Calculations	70
H Subject Instructions	108

NAVTRAEQUIPCEN 70-C-0238-1

LIST OF TABLES

Table	Page
1 Analysis of Variance Summary for Dive Approach Test for the Slant Range Dependent Variable.	14
2 Analysis of Variance Summary for Dive Approach Test for the Average Correct Response Dependent Variable	15
3 Analysis of Variance Summary for Constant Altitude Test	17
4 TV System Operating Characteristics Summary	43
5 Zoom Focal Lengths and FOV Corresponding to 3-D Ranges.	61
6 Dive Approach Stimulus Presentation Sequence.	66
7 Constant Altitude Stimulus Presentation Sequence.	68
8 Comparison of VTR Stimulus Material Fidelities.	69
9 Critical Displayed Target Image Measurements - Dive Approach.	98
10 Heights of Critical Target Elements - Dive Approach	96
11 Critical Target Element Measurements - Constant Altitude Approach .	96
12 Percent Target Image Displacements Relative to Sensor FOV - Dive Approach	97
13 Displayed Image Angular Displacements - Dive Approach	99
14 Percent Image Displacements Relative to Sensor FOV - Constant Altitude Approach	99
15 Displayed Image Angular Displacements - Constant Altitude Ap- proach	102
16 Relative Displayed Image Rates During Terminal Phase of Run - Dive Approach	106

LIST OF ILLUSTRATIONS

Figure	Page
1 Basic Guidance Development Center (GDC) Test Stimulus Generation Setup.	4
2 Target Areas for Dive Approach Tests	5
3 Profile of Basic 2-D 3-D Dive Approach Geometry.	7
4 Complete Factorial Layout for Dive Approach Test (2-D Case).	8
5 Profile of Constant Altitude Approach Geometry	10
6 Terrain Model Ground Track Paths for Constant Altitude Approach Tests.	10
7 Complete Factorial Layout for Constant Altitude Test	12
8 Slant Range/Altitude at Response as a Function of Target Area for 650 and 1,100 Feet per Second Velocities for Pilot Subjects: Dive Approach Test	15
9 Percent Correct Response as a Function of Target Area for 650 and 1,100 Feet per Second Velocities for Pilot Subjects: Dive Approach Tests	16
10 Percent Judged 3-D as a Function of Target Area with SR/Alt Noted as Bar Graph Divisions (for Both Pilot and Naive Subjects) - Constant Altitude Test	19
11 Interaction of Target Areas as a Function of Range/Altitude for Areas 5, 6 and 3 - Constant Altitude Test.	20
12 Percent Judged 3-D for Pilot Subjects: Performance on each Area as a Function of FOV/SR/Alt - Constant Altitude Test.	21
13 Percent Judged 3-D for Pilot Subjects; Averaged Over Areas as a Function of SR/Alt for the Constant Altitude Test.	22
14 Pilot-Naive Subject Interaction as a Function of FOV/SR/Alt Averaged Over All Areas for Constant Altitude Test	23
15 Indication of Large Within - and Small Between - Groups Variance	32
16 Indication of Small Within - and Large Between - Groups Variance	33
17 Comparison of 2-D and 3-D Target Convergence Geometries (Vertical View)	38
18 Martin Marietta's Guidance Development Center.	40
19 TV Camera Mounted in GDC Gimbal Assembly	42
20 Airport Target Area.	48
21 Truss Bridge Target Area	48
22 Industrial Complex Target Area	50
23 POL Storage Facility Target Area	50
24 Mountain Storage Facility Target Area	51
25 Test Target Area	51
26 Profile of Basic 2-D 3-D Dive Approach Geometry.	55
27 Lat'ral and Longitudinal Distances Viewed by Sensor with Fixed FOV	56
28 2-D and 3-D Run Geometry Relationships	57
29 Zoom Focal Length Required as a Function of Slant Range and Normalized Time	61

NAVTRAEQUIPCEN 70-C-0238-1

Figure	Page
30 Profile of the Constant Altitude Approach Geometry.	62
31 Dive Approach - Longitudinal Image Displacement Geometry (Full Image Displacement) - Profile View.	71
32 Dive Approach - Lateral Image Displacement Geometry (Full Image Displacement) - Plan View	73
33 Constant Altitude Approach Geometry - Flat Terrain Case	75
34 Constant Altitude Approach Geometry - Vertical Background Case.	77
35 Perspective Change Geometry - Constant Altitude Approach.	80
36 Basic Display Viewing Geometry.	83
37 Sensor and TV Display Relationships for Maximum LOS Displacement Case in Dive Approach Runs.	84
38 Sensor and TV Display Relationships for Partial LOS Displacement Case in Dive Approach Runs.	85
39 Sensor Geometry Related to Dive Approach Absolute Growth Rate	88
40 Constant Altitude Geometry (for use in Image Rate Computations)	91
41 General Relationship Between Slant Ranges and Projected Target LOS Slant Distances to Terrain.	94
42 Percent Target Image Horizontal and Vertical Displacement Versus Target Height - Dive Approach	98
43 Vertical and Horizontal Displayed Target Angular Displacements - Dive Approach	100
44 Percent Target Image Longitudinal Displacement Versus Target Height for Different Altitudes - Constant Altitude Approaches - Flat Terrain Background Case	101
45 Percent Target Image Longitudinal Displacement Versus Target-to- Vertical Background Separation for Different Altitudes - Vertical Background Case.	102
46 Displayed Target Image Angular Displacement Versus Altitude - Constant Altitude Approach.	103

SECTION I

INTRODUCTION

1. BACKGROUND

The purpose of this study is to acquire quantitative behavioral data which will help resolve an important and persistent design issue in the development of visual simulation equipment for training systems. One of the key decisions to be made in the design of visual simulation equipment is the nature of the image storage medium, i.e., 3-dimensional terrain model, 2-dimensional transparency, or mathematical model (for computer based displays). This is obviously a complex issue involving many engineering, human factors, economic, and mission considerations. One such consideration is the adequacy of the depth cues which can be derived from imagery based on 2- as opposed to 3-dimensional sources.

The various cues to depth can be classified in terms of their dependence on motion. That is, many of the most compelling cues such as interposition, relative size, aerial perspective, etc., can be considered essentially static since they are present under both static and dynamic conditions. Others, however, such as movement parallax and vertical perspective change can only occur as a result of relative movement between the observer (sensor) and that which is observed. Although motion parallax is a relatively minor cue to depth, it represents the essential difference between imagery derived from a 3-dimensional source (terrain model) as opposed to imagery derived from a 2-dimensional source (transparency).

Therefore, this study was specifically designed to investigate the role of motion parallax in the perception of apparent depth on a dynamic TV display. To accomplish this objective, it was first necessary to acquire simulated target imagery under a variety of experimental conditions for use as stimulus material in a series of behavioral tests.

These stimulus materials required the development of a special optical technique to provide sets of equivalent target runs differing only in the presence or absence of motion dependent depth cues. This technique, which simulates a 2-dimensional image source by eliminating relative motion within the visual field, is described in detail in a subsequent section.

This study was primarily designed to investigate the perceptual processes involved in viewing target imagery by means of a TV display. It was, however, considered desirable from the standpoint of potential application to utilize representative real world conditions in terms of flight trajectory, sensor viewing geometry, and ground imagery. Therefore, both constant dive angle and constant altitude approaches were employed at simulated velocities consistent with operational training problems. An optical zoom technique was employed in the Dive Approach runs to obtain the equivalent of 2-dimensionally based imagery using the same target models as the 3-dimensionally based imagery. The Constant Altitude series

of tests was based on 3-dimensional imagery exclusively. However, the video tapes used in this series of tests included motion dependent cues to depth ranging from well below to well above threshold in each of the target areas.

2. OBJECTIVES

The primary objectives of this study were:

a. To evaluate the ability of subjects to perceive the dimensionality of the source used to generate dynamic target imagery on a TV display.

b. To identify the motion dependent cues responsible for the illusion of depth on a 2-dimensional screen.

c. To determine the relative importance of certain selected variables in providing these cues.

SECTION II

METHOD

1. INTRODUCTION

Two series of tests were conducted in this experiment - both designed to evaluate the ability of subjects to identify the dimensionality of the source of target imagery viewed under dynamic conditions on a TV monitor. The first series of tests, identified as the Dive Approach, was designed to determine the point at which subjects can perceive the dimensionality of imagery typical of the final flight path of a TV guided missile, i.e., from a simulated 10,000 feet down to within 1,500 feet of impact. In the Dive Approach tests, the target area appears to expand radially from the aim point at the center of the display. The behavioral tests were based on recordings of target convergence runs made in the Martin Marietta Guidance Development Center (GDC) - see Figure 1 - using 3-dimensional and optically simulated 2-dimensional target areas. (The method of target image generation is described in Appendix F.) Prior to preparation of the video tapes used in the behavioral analysis, a pilot study was performed to select the most appropriate target runs in terms of realism, approach velocity, flight times, and illumination conditions. The Dive Approach runs which were selected were then dubbed from the master video tapes onto the final stimulus tapes in an irregular sequence. The second series of tests, designated the Constant Altitude Approach, was designed to investigate the ability to perceive motion dependent depth cues as a function of altitude/slant range in simulated horizontal flight. As above, the behavioral stimuli were video recordings of selected target runs on the GDC terrain model. These two series of tests included a wide variety of dynamic imagery in which a number of manmade targets and natural terrain features were available. Both tests were conducted as complete factorial designs.

2. DIVE APPROACH TESTS

2.1 EXPERIMENTAL DESIGN. The following variables were expected to be the most important determiners of the perception of apparent depth under dynamic conditions and are discussed in detail in the following section.

- a. Target Areas: Containing various types of dimensional cues
- b. Approach Velocity: Two approach speeds, 650 and 1,100 ft/s
- c. Subjects: Experienced military pilots and naive subjects
- d. Stored Image Dimensionality: 2-D and 3-D
- e. Shadow Conditions: Shadowed or nonshadowed.

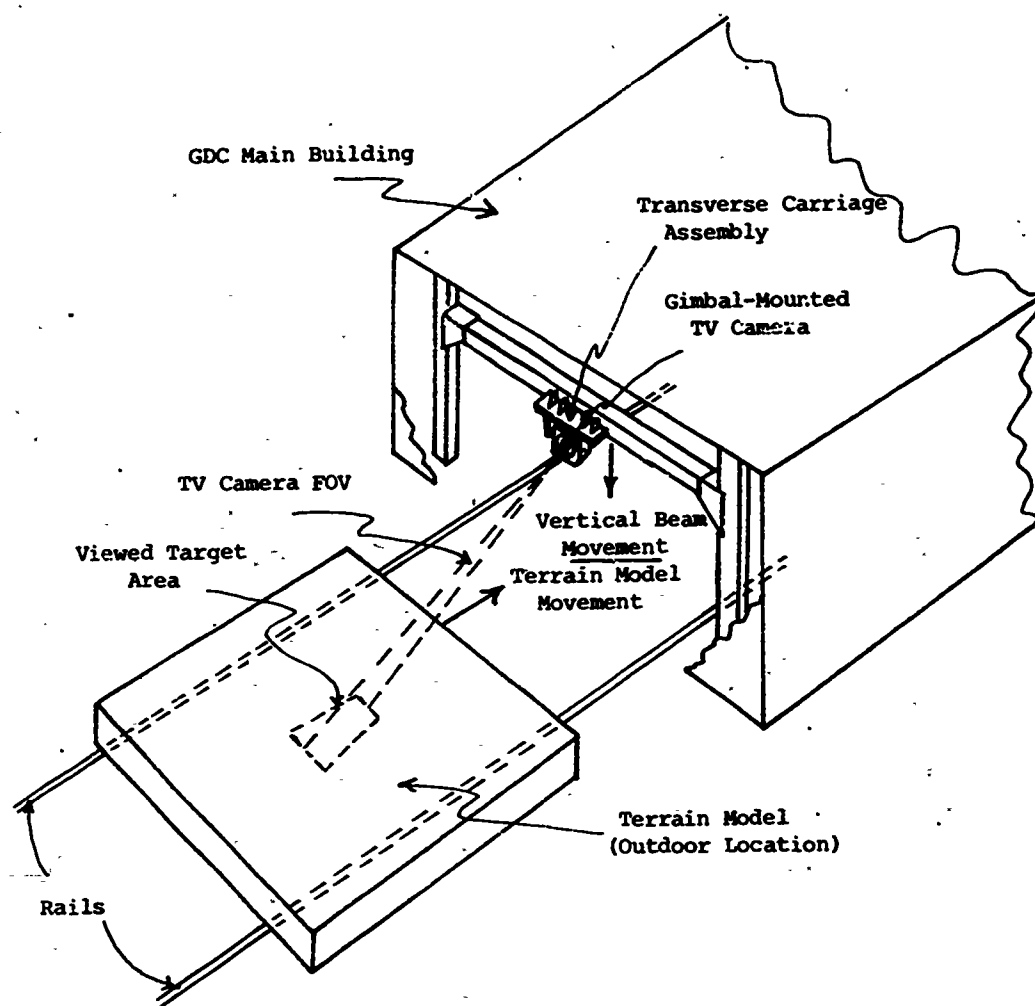


Figure 1. Basic Guidance Development Center (GDC) Test Stimulus Generation Setup

2.1.1 Independent Variables.

2.1.1.1 Target Areas. Five areas, each containing typical military targets as well as varied terrain features, were used. These areas, plus a practice area, are shown in Figure 2. The target objects were selected to provide a wide range of representative sizes, orientations, vertical heights, and spacings. Average contrast levels and linear measurements of selected target features were recorded for each of the target areas. These measurements were then used in the calculations of angular displacement and percentage field of view (FOV) movement as discussed in the Results section. The five areas are briefly described below. (Appendix D provides more detailed information on their physical characteristics.)

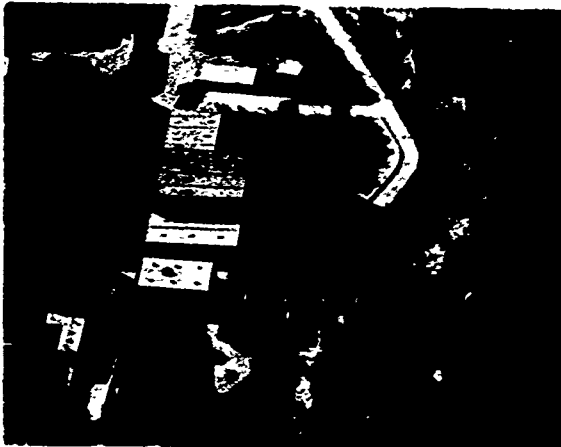
- a. Airport: Contained hangars, operations shack and various aircraft placed in close proximity to enhance movement parallax effects.



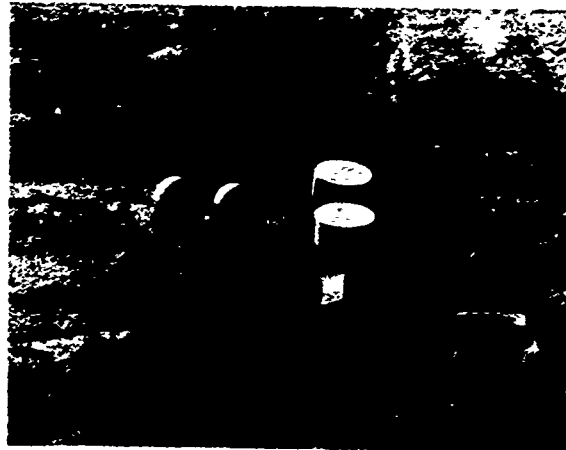
Airport



Truss Bridge



Industrial Area



POL Storage Facility



Mountain Storage Facility



Practice Area

Figure 2. Target Areas for Dive Approach Tests

NAVTRAEQUIPCEN 70-C-0238-1

b. **Truss Bridge:** Open framework structure that provided prominent motion-dependent cues in a rolling terrain background.

c. **Industrial Area:** Consisted of typical building, streets, and vehicles.

d. **POL Storage Facility:** Placed in a desert area containing few features and no elevation differences.

e. **Mountain Storage Facility:** Provided pronounced terrain variations as well as dimensional cues peculiar to manmade objects.

In addition, an area was selected which provided obvious cues to dimensionality for the purpose of demonstration. This area is also shown in Figure 2 and consisted of a large suspension bridge, tall buildings, and critical street orientations relative to the buildings.

2.1.1.2 **Velocity.** Two realistic approach velocities were selected: 650 and 1100 feet per second (380 and 650 knots). This resulted in an image sequence length of approximately 13 seconds for the lower and 8 seconds for the higher simulated approach velocity.

2.1.1.3 **Subjects.** Two groups of subjects consisting of both operationally experienced pilots and naive college students were used.

2.1.1.4 **Stored Image Dimensionality.** The techniques used to generate the master video tapes are described in detail in Appendices E and F. The most critical aspect of this effort was the production of target imagery differing only in the presence or absence of motion-dependent depth cues. This was accomplished in the 2-D runs by continuously controlling the TV camera optics to provide the same image growth rates as in the 3-D runs. Figure 3 depicts the 2-D and 3-D Dive Approach geometries. The scale factor employed in these runs was 250:1. (Appendix D describes the method of converting from the basic 600:1 GDC scale to the 250:1 scale factor.)

In the 3-D runs, constant velocity closure was accomplished by decreasing the camera-to-target range at a constant rate, i.e., the terrain model moved longitudinally and the gimbal-mounted TV camera descended at the proper speed (under computer control) to simulate a diving trajectory. The approach geometry was defined by a 30-degree dive angle from a simulated 10,000 foot slant range down to 1,500 feet, with corresponding altitudes of 5,000 to 750 feet, respectively. In the 2-D runs, a zoom lens was used to simulate a constant velocity dive without relative motion within the visual field (see Appendix B). This was done by positioning the gimbal-mounted TV camera at a fixed point along the descent path used for the 3-D stimulus generation and carefully aligning it with the same target aim points. The zoom lens focal length was adjusted under computer control to produce apparent closure at the same scaled velocities used for the 3-D cases. These differences in the 2-D and 3-D approach geometries resulted in the display of slightly different areas in the longitudinal axis. In addition, the 2-D aspect angle remained constant while the 3-D convergence runs produced small changes in aspect

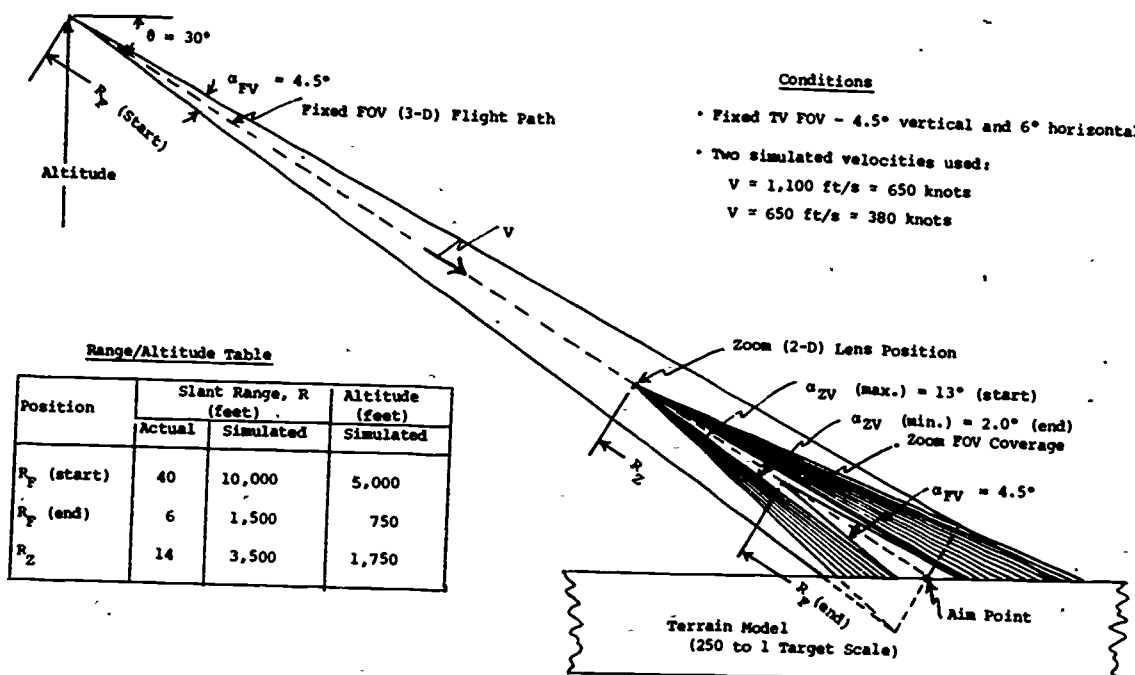


Figure 3. Profile of Basic 2-D 3-D Dive Approach Geometry angles. Preliminary tests showed, however, that the differences in longitudinal coverage between the 2-D and 3-D imagery were not detected by any of the subjects. The only usable cues to dimensionality then were those of motion parallax, and, to a much lesser degree, perspective change (see Appendix B).

2.1.1.5 Shadow Conditions. Since useful depth information can often be derived from shadows, several target areas were studied under shadowed and nonshadowed conditions.

2.1.1.6 Display Viewing Distance. Two viewing distances were used: 20 inches and 59 inches. The closer distance represented a normal subject-to-TV monitor separation for ease of viewing. The longer distance was used in a portion of the tests to achieve a display magnification* of unity. This was done in order to provide equivalence between the motion parallax values available via the TV display and those which could be directly observed on the terrain model.

2.1.2 Factorial Layout. These independent variables were presented in a complete factorial design. Five target areas, two velocities**, two subject categories, and two types of imagery (2-D and 3-D) were used. Shadow and

* Ratio of total displayed visual angle to TV camera fixed FOV in the 3-D runs.

** Four target areas were tested at both velocities (see Figure 4).

nonshadow conditions were provided for two areas and were analyzed as a subtest. The main test layout for the 2-D case is shown in Figure 4.

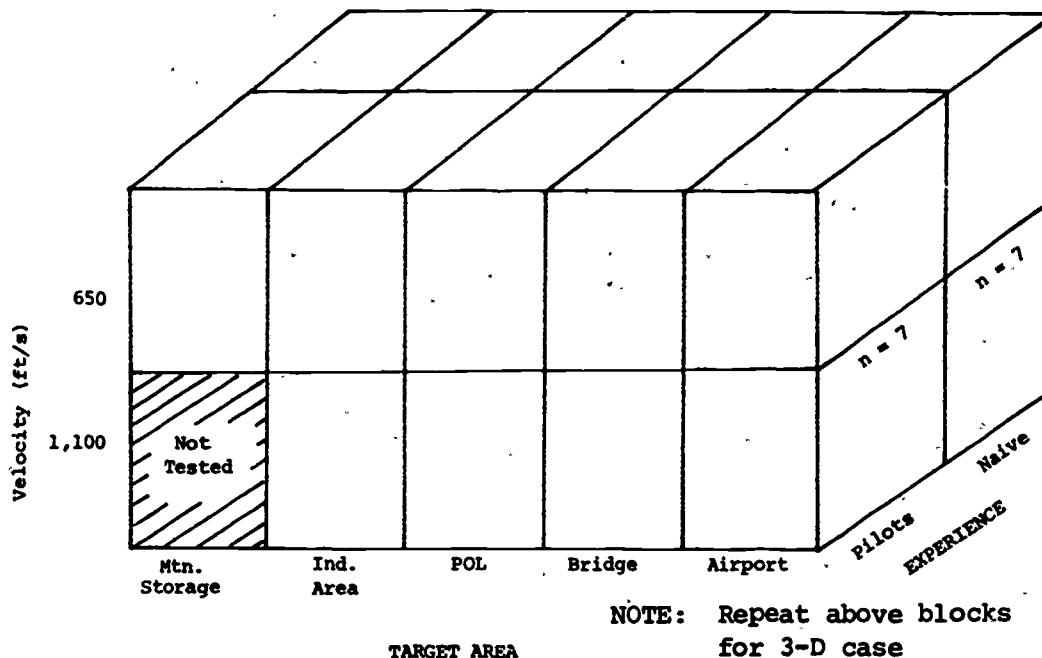


Figure 4. Complete Factorial Layout for Dive Approach Test (2-D Case)

2.2 BEHAVIORAL TEST PROCEDURES. The equipment used in the behavioral tests consisted of a high quality 8 inch display, a helical scan video recorder, a chin rest for maintaining eye height and distance from the display, and an audio tape recorder to record subject responses.

2.2.1 Stimulus Presentation Sequence. The stimulus tapes were dubbed from a master video tape in an irregular sequence of targets and other test parameters. Calculated slant ranges were dubbed onto the audio track of the video tape at 1,000 foot intervals. The presentation sequence is given in Table 6 of Appendix F.

2.2.2 Data Recording. The subject was asked to respond verbally (2-D, 3-D, or Don't Know) as soon as he made his decision concerning the dimensionality of the particular presentation. This response was recorded in synchrony with the video tape sound track which provided slant range data. This data was then reduced by reviewing the audio tape and determining at what range (in thousands of feet) the subject made his determination. As a back-up procedure, the test conductor also recorded the subject's response on a separate data sheet.

2.2.3 Dependent Variables. Two dependent variables were used in this test: range at time of response, and accuracy of the subject's judgment. The subject was urged to make the earliest possible determination but was

allowed to change his mind at the end of the run. The purpose of this approach was to encourage responses at the maximum ranges while maintaining a high percentage of correct final answers. At the end of the test, each subject was asked to identify and describe specific features of the target areas that provided cues to dimensionality.

3. CONSTANT ALTITUDE TESTS

3.1 EXPERIMENTAL DESIGN. The independent variables in this test were:

- a. Target Areas
- b. Velocity
- c. Experience of the Subjects
- d. Field-of-View/Slant Range/Altitude Combinations

This test was designed to evaluate the ability of subjects to detect the cues to depth which are present in a dynamic TV presentation as a function of altitude in simulated horizontal flight. Using many of the same targets employed in the Dive Approach tests, video tape recordings were made at four different altitudes. The fields of view (FOV) were adjusted by use of the zoom lens so that the camera recorded the same lateral dimension at each altitude. Under these conditions, the only cues present were motion parallax and perspective change as in the first test. The details of the image generation techniques are discussed in Appendix E. However, Figure 5 is presented here as an aid in visualizing the technique. The TV camera was fixed at a 30-degree depression angle, as in the previous test series, providing slant ranges equal to twice the corresponding altitudes. The terrain model was driven beneath the camera at the desired constant velocity. This test was designed as a supplement to the Dive Approach test to cover a wider range of operational conditions.

3.1.1 Independent Variables.

3.1.1.1 Target Areas. Seven target areas were used. These consisted of constant altitude flight paths across the length of GDC terrain model. Figure 6 shows the entire terrain model* with the flight paths superimposed. An attempt was made to include all areas used as targets on the Dive Approach test so that direct comparisons could be made. The areas ranged from those containing predominantly manmade objects, to mountainous terrain, to flat featureless terrain containing almost no manmade targets. The seven areas, including summaries of their general composition, are listed below: (These are listed in order from left to right as shown in Figure 6.)

* The view is from an elevated position representative of that at which the TV camera was located. The terrain model is in the GDC outdoor test area and is illuminated by sunlight.

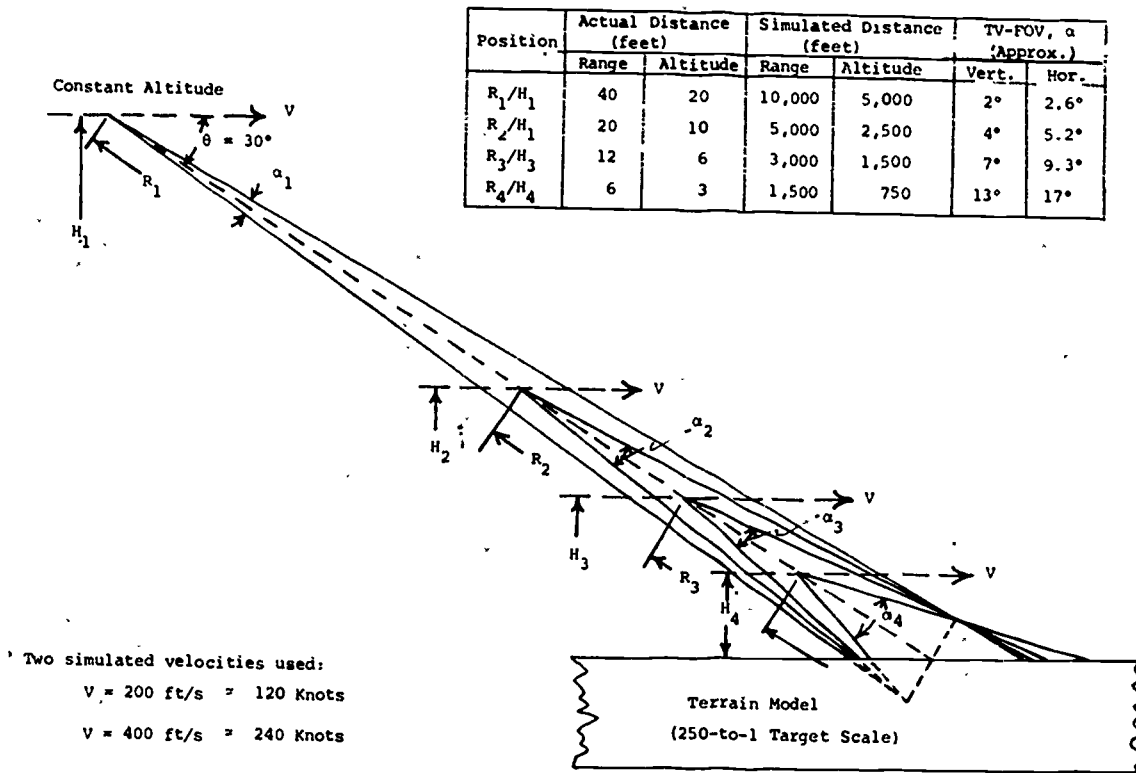


Figure 5. Profile of Constant Altitude Approach Geometry

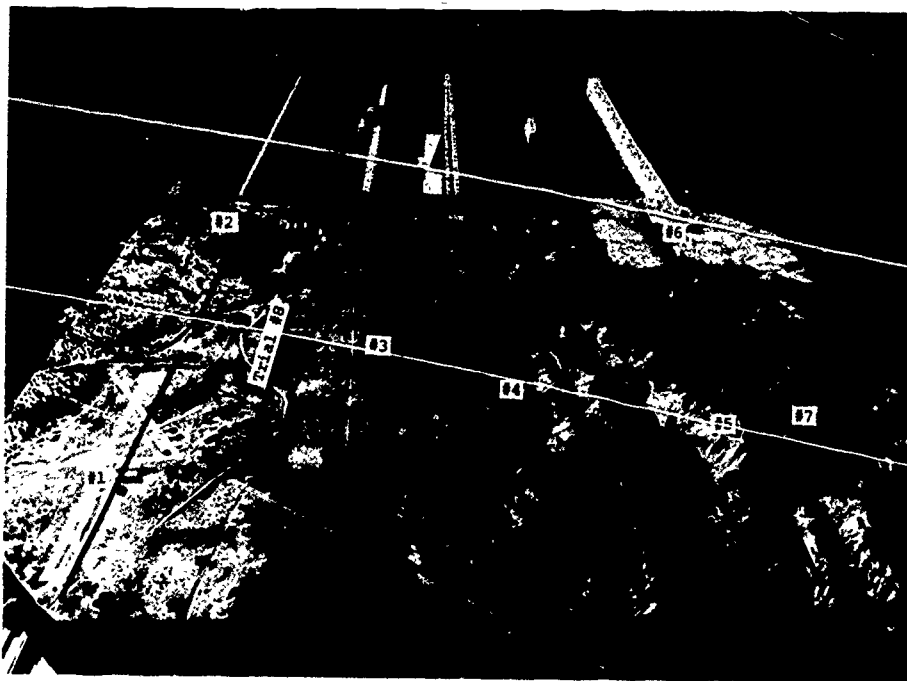


Figure 6. Terrain Model Ground Track Paths for Constant Altitude Approach Tests

NAVTRAEQUIPCEN 70-C-0238-1

- a. Airport: Included the same area and structures used as the airport target for the Dive Approach test.
- b. Harbor: A continuation of the flight path containing the airport target. It offered little in the way of vertical structures and contained a considerable expanse of water with only a few ships visible.
- c. Practice Area: Same as that used in the Dive Approach tests. This was selected because it contained the tallest vertical manmade structures available on the GDC model.
- d. General Terrain: Essentially featureless, with only a few trees, almost no elevation changes and a large lake. This area was similar to much of the area that a pilot might cruise over on his way to a target.
- e. Bridge: Included the same truss bridge used in the first test.
- f. Mountain Top: Included flight over a mountain peak. It was expected that the most obvious depth cues would be present on this flight path.
- g. POL Facility: Included the same POL target area used in the Dive test. However, it was necessary to avoid the elevated terrain shown in the initial portion of the 3-D Dive Approach run since it would provide an exaggerated clue inconsistent with the rest of the flight path.
- h. Mountain Storage Facility: Included the same area and structures used in the Dive test.

3.1.1.2 Velocity. Two simulated flight velocities were used: 120 and 240 knots. These relatively slow velocities were chosen to provide minimum image smear on the TV display. The slower velocity was used in the factorial analysis of all target and FOV/SR/Alt combinations and the faster velocity was tested over two target areas and at two FOV/SR/Alt conditions.

3.1.1.3 Experience. Two groups of subjects were selected to provide a basis for generalizing the results: experienced ex-military or active reserve pilots and a naive group consisting of company secretaries.

3.1.1.4 FOV/Slant Range/Altitude. Five FOV/SR/Alt combinations were used: 2°/10,000/5,000 ft., 4°/5,000/2,500 ft., 7°/3,000/1,500 ft., 13°/1,500/750 ft., and 13°/3,000/1,500 ft. The first four FOV's were chosen to provide approximately the same amount of terrain area exposure for each altitude. The last FOV/SR/Alt combination was selected to evaluate response at a given altitude with different FOV's: 13°/3,000/1,500 ft. vs. 7°/3,000/1,500 ft. When not referring to this particular case, these

NAVTRAEQUIPCEN 70-C-0238-1

combined parameters are considered only in terms of slant range/altitude values, i.e., the subjects were responding to dimensionality effects primarily associated with viewing range and altitude, not FOV.

3.1.2 Factorial Layout. Figure 7 depicts the complete factorial layout with seven target areas, five FOV/SR/Alt combinations and two subject experience levels. As noted above, the higher velocity condition was analyzed as a subtest and is shown as an insert. Seven experienced pilots and four naive subjects were used.

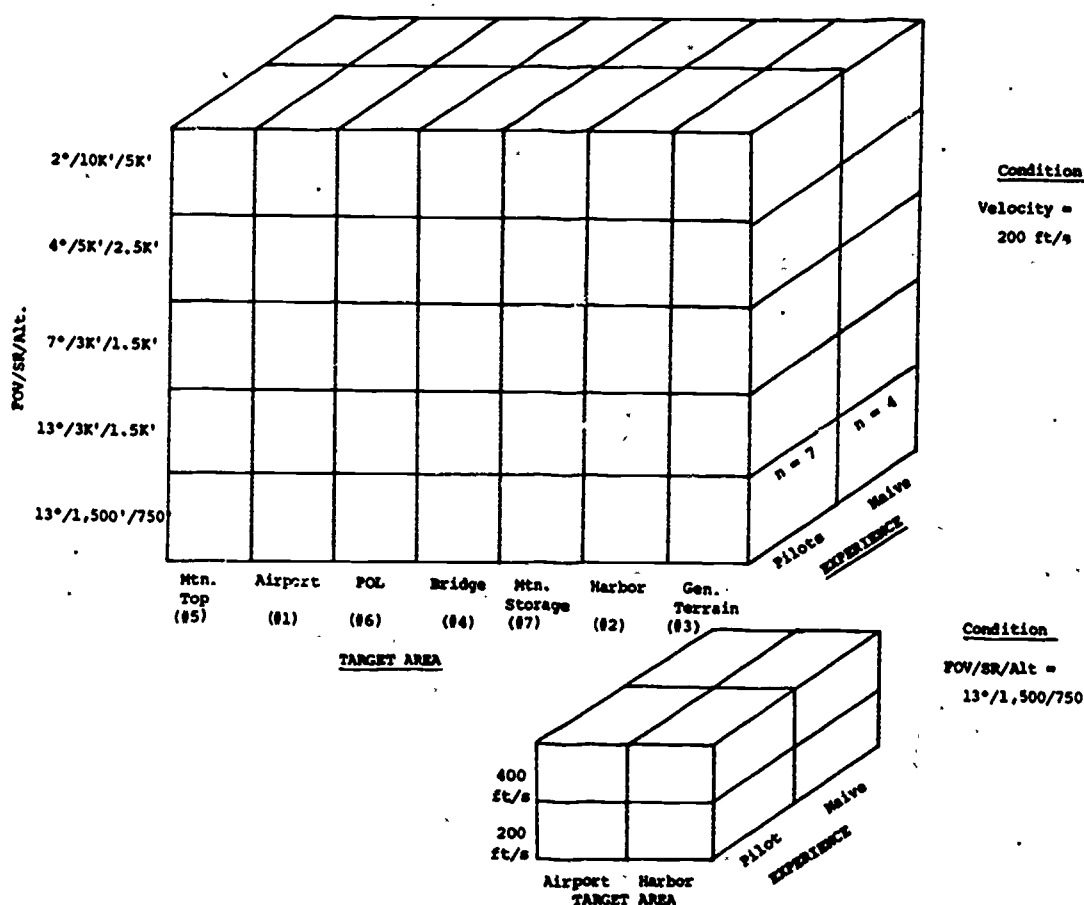


Figure 7. Complete Factorial Layout for Constant Altitude Test

3.2 BEHAVIORAL TEST PROCEDURES. The test facilities were identical to those described in Section 2.2 except that since subject responses were not time-critical, it was not necessary to use an audio recorder for this purpose.

3.2.1 Stimulus Presentation Sequence. The stimulus video tapes were dubbed from a master tape and were again arranged in an irregular sequence, with the restriction that no area was allowed to immediately

follow itself. Different combinations of the seven areas were offered in the first seven trials to provide a means of reshowing those runs at the end of the test to elicit subjective comments from the subjects. The presentation sequence is given in Table 7 of Appendix F.

3.2.2 Data Recording. The subjects responded at the end of each run by stating either "2D", "3D", or "Don't Know". The responses were recorded by the test conductor. At the end of each complete test, the subjects were reshowed each area and asked to describe what particular features offered them clues to the dimensionality of the image source. These comments were recorded for later comparison with performance.

SECTION III

DISCUSSION OF RESULTS

1. DIVE APPROACH TESTS.

Results of the analysis of variance (AOV) performed using both slant range (Table 1) and average correct response (Table 2) showed that subjects were unable to distinguish between the 2-D and 3-D presentation. The performance of the experienced pilot group was not significantly different from that of the naive college sophomores. Average slant range from the targets was about 2,800 feet when response was made (Figure 8), and even at this close range (termination was at 1,500 feet) the subjects' judgments were only approximately 50 percent correct. Figure 9 illustrates this correct response percentage as a function of target area.

TABLE 1. ANALYSIS OF VARIANCE SUMMARY FOR DIVE APPROACH TEST FOR THE SLANT RANGE DEPENDENT VARIABLE

Source	df*	SS	MS	F	Significant Level
Target Area (A)	3	3.176	1.058	1.36	N.S.
Velocity (V)	1	4.274	4.274	5.49	0.05
Experience (E)	1	0.005	0.005	< 1	N.S.
A x V	3	0.926	0.309	< 1	N.S.
A x E	3	2.023	0.674	< 1	N.S.
V x E	1	0.055	0.055	< 1	N.S.
A x V x E	3	1.734	0.578	< 1	N.S.
Error	96	74.716	0.778	--	

Total 111 86.91

1.1 TARGET AREA. While the target effect was not significant overall, there was a significant difference between the slant ranges at which responses were obtained for the Industrial and Airport areas compared to the Mountain Storage and Bridge areas (Figure 8). That is, the subjects responded to the

* Tables 1 and 2 summarize the AOV results for the selected combination of two approach velocities and four target areas. A complete factorial analysis also was performed using all five areas (including the Mountain Storage Facility) at the single velocity of 650 feet per second. Again, the target area factor was not significant.

NAVTRAEQUIPCEN 70-C-0238-1

TABLE 2. ANALYSIS OF VARIANCE SUMMARY FOR DIVE APPROACH TEST FOR THE AVERAGE CORRECT RESPONSE DEPENDENT VARIABLE

Source	df*	SS	MS	F	Significant Level
Area (A)	3	0.124	0.041	< 1	N.S.
Velocity (V)	1	0.0169	0.0169	< 1	N.S.
Experience (E)	1	0.031	0.031	< 1	N.S.
A x V	3	0.113	0.038	< 1	N.S.
A x E	3	0.119	0.040	< 1	N.S.
V x E	1	0.007	0.007	< 1	N.S.
A x V x E	3	0.076	0.025	< 1	N.S.
Error	96	5.075	0.053	< 1	N.S.
Total	111	5.563			

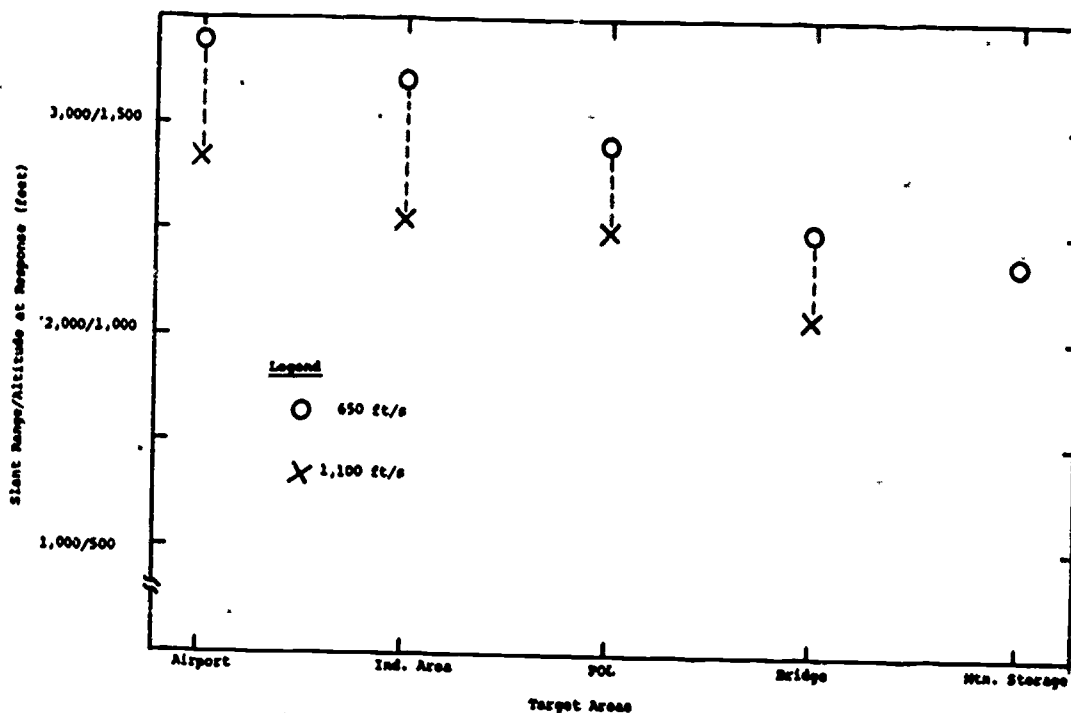


Figure 8. Slant Range/Altitude at Response as a Function of Target Area for 650 and 1,100 Feet per Second Velocities for Pilot Subjects: Dive Approach Test

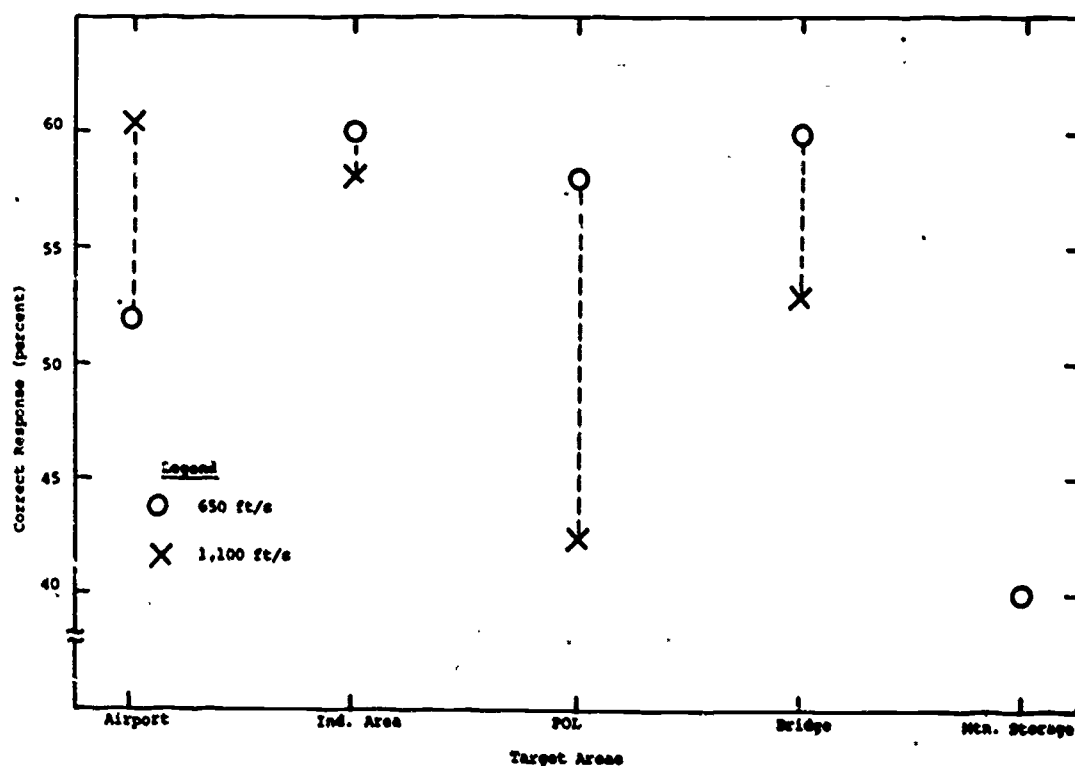


Figure 9. Percent Correct Response as a Function of Target Area for 650 and 1,100 Feet per Second Velocities for Pilot Subjects: Dive Approach Tests

Industrial and Airport areas at a significantly greater range than they did for the Mountain Storage area or the Bridge area (3,200 plus feet versus 2,300 feet for the latter area). This does indicate a trend in the subjects' responses (although still only chance statistically) which can be related to the target characteristics and relative sizes. While the subjects were able to respond at a greater slant range, their answers were not significantly different from their responses at the closer ranges. This is illustrated in Figure 9 which shows the percent correct response as a function of area. The target area characteristics for both the Dive and Constant Altitude approaches are discussed in detail in Appendix D.

1.2 VELOCITY. The effect of velocity was significant at the 0.05 level for the slant range variable (Table 1). The essentially constant differences in response ranges at the two velocities can probably be accounted for on the basis of simple reaction and/or decision time. That is, the subjects probably perceived target dimensionality at the same slant range for both velocities, but with an essentially constant response time, the higher approach speed resulted in a shorter slant range at the time of response. This appears to be the most likely explanation for the observed effect, since the time spans involved are consistent with this hypothesis. However, it is also possible that the different velocities may have had an effect not explainable within the context of this study. While the evidence is not conclusive, it appears that the differences in approach velocity, although they resulted in different response ranges, did not affect the discriminability of dimensionality under the conditions of this experiment.

NAVTRAEQUIPCEN 70-C-0238-1

1.3 SHADOW VERSUS NONSHADOW EFFECTS. Two areas, the POL Facility and the Airport were presented under both shadow and nonshadow conditions. This variable was not significant. While the nonshadowed imagery was consistently responded to at a greater distance than its shadowed counterpart, the differences in response distance were not statistically significant.

1.4 DISPLAY VIEWING DISTANCE. Two display viewing distances were used: 20 inches and 59 inches. There was no measurable difference in performance between the two. This indicates that the fidelity of the image displayed via TV was the limiting factor in both cases.

1.5 SUBJECTIVE RESPONSES: At the end of each test, the subjects were asked what aspects of the target areas aided them in making their decisions. For the most part the subjects were unable to identify the specific target characteristics responsible for their decisions. However, the control tower/operations building complex and the doorway of one hangar appeared to offer the most useful clues.

2. CONSTANT ALTITUDE TESTS

Complete factorial analyses of variance (AOV) of this experiment (layout is shown in Figure 7) were performed, and the summary of results is shown in Table 3. Both target areas and FOV/SR/Alt values were significant at the 0.01 level along with the interaction of experience and FOV/SR/Alt. The experience factor, i.e., pilots versus female secretarial help was significant at the 0.05 level indicating a difference in responses to the stimuli between the two groups. Two target areas were tested at two velocities and while there was a difference in performance with area there was no difference attributable to the increased approach velocity. Each factor is discussed in detail in the following sections.

TABLE 3. ANALYSIS OF VARIANCE SUMMARY FOR CONSTANT ALTITUDE TEST

Source	df	SS	MS	F	Significant Level
Area (A)	6	5415.4	902.6	10.00	0.01
Experience (E)	1	646.1	646.1	7.17	0.05
FOV/SR (F)	4	4974.2	1243.6	13.83	0.01
A x E	6	1064.0	177.3	1.97	N.S.
A x F	24	3616.0	150.7	1.67	N.S.
E x F	4	1004.2	251.1	2.79	0.01
Residual	24	2155.7	89.8		
Total	69	18,875.6			

2.1 TARGET AREA. Figure 10 depicts the percentage of responses in which the source material was correctly identified as being 3-D. The data for both groups of subjects are represented, the divisions on each bar showing the percent correct at several selected slant ranges. From this illustration it can be seen that Mountain Area (#5) and Airport (#1) were identified as 3-D approximately 95 percent of the time at the 1,500/750 foot SR/Alt by the pilots and only 75 percent and 50 percent, respectively, by the naive subjects. In the 3,000/1,500 foot SR/Alt case, experienced subjects got 85 percent correct for the Mountain Area and only 73 percent correct for the Airport. In the same tests the naive subjects correctly identified the source dimensionality on only 73 percent and 50 percent of the trials, respectively. The most difficult target to perceive as 3-D was the General Terrain Area (#3) which elicited only 28 and 25 percent correct responses for the experienced and naive subjects, respectively, at the closest (1,500/750 foot SR/Alt) distance.

An example of how the ability to perceive motion-dependent dimensionality cues changes as a function of the range/altitude combination is shown in Figure 11. At the closest range the POL Target Area (#6) was judged as 3-D at a response level similar to that of the Mountain Area (#5) which had the highest percentage of 3-D judgments. However, at the greater ranges the response level for Area 6 was statistically similar to Area 3 (General Terrain), the area receiving the lowest average percentage of 3-D judgments. Thus, somewhere between the closest approach (1,500/750) and the 3,000/1,500 condition, the ability to perceive motion-dependent dimensionality cues diminished appreciably. This decrement is evidently related to the specific characteristics of the target area involved. The reason for this abrupt change in performance on Target Area #6 is not clear. The tentative conclusion is that there must be some unusual cognitive process or some form of attention focusing involved in this case. Thus, on Area #3 there is a decided lack of target structure on which to focus attention. On the other hand, Area #6 contains a very conspicuous POL complex. Apparently, whatever cues exist are easier to discriminate on Target #6 than on the other two areas. This is probably because the subject's attention is focused on the structural details of the manmade objects for a proportionally longer time during an approach to such a conspicuous target.

Figure 12 shows the variability or range of responses across FOV/SR/Alt combinations. Responses ranged from a low of 28 percent judged correct at the closest SR/Alt for the General Terrain Area to 96 percent for both the Airport and Mountain Areas (#1 and #5). At the 10,000/5,000 foot distance, less than 4 percent were judged as 3-D for Areas #2 and #4 (Harbor and Bridge Areas) up to 45 percent judged 3-D for the Mountain Area (#5). The single wide FOV condition at the 3,000/1,500 foot distance resulted in an increase in the percentage judged to be 3-D for some of the target areas, notably Areas #4 (Bridge), #6 (POL), and #7 (Mountain Storage Area). The most dramatic increase was for the Mountain Storage Area which went from 42 percent judged 3-D at the 7 degree FOV at 3,000/1,500 feet to 88 percent when a 13 degree FOV was used. The other two areas were not as dramatic in their changes but were statistically significant at the 0.05 level of confidence. Analysis of the content of these areas revealed that in the wide FOV, new

NAVTRAEQUIPCEN 70-C-0238-1

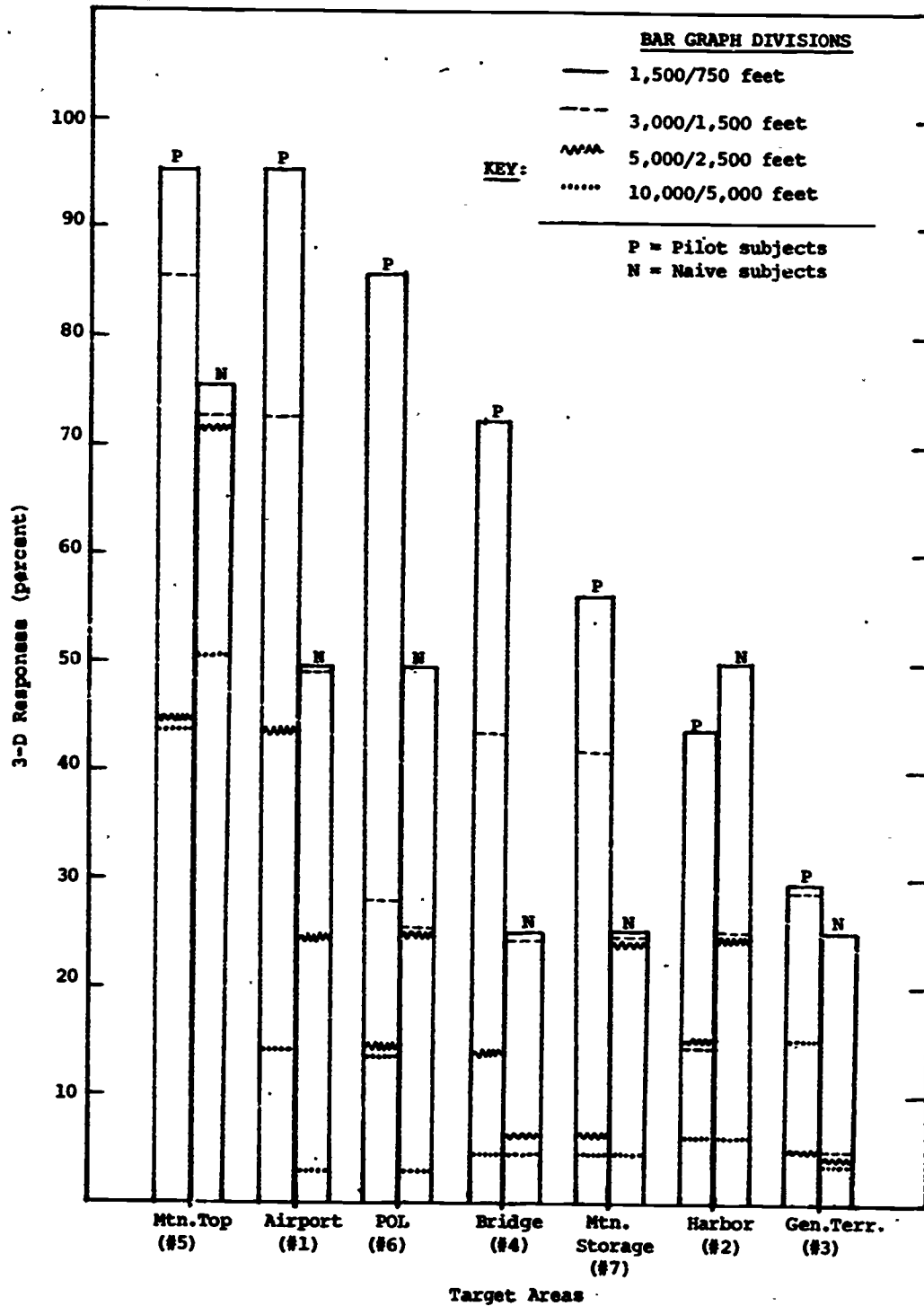


Figure 10. . Percent Judged 3-D as a Function of Target Area with SR/Alt Noted as Bar Graph Divisions (for Both Pilot and Naive Subjects) - Constant Altitude Test

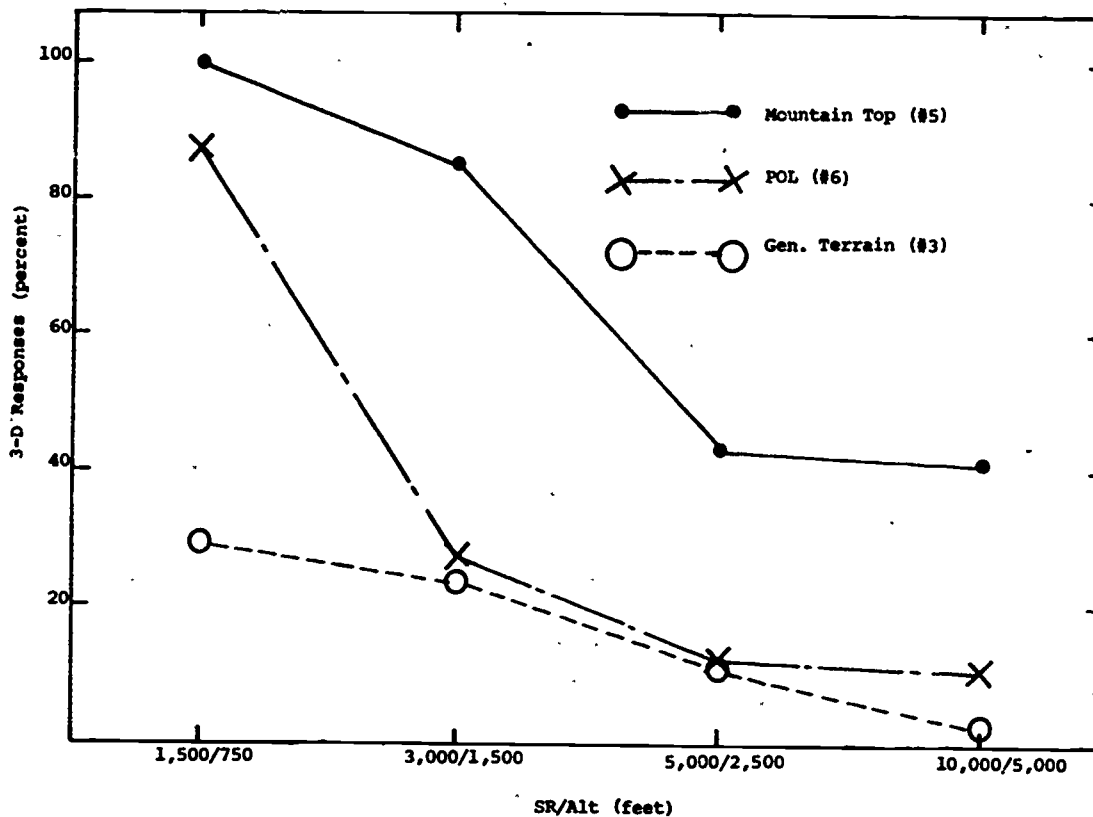


Figure 11. Interaction of Target Areas as a Function of Range/Altitude for Areas 5, 6 and 3 - Constant Altitude Test

areas of terrain containing higher vertical elevations were available to be seen as compared with the smaller FOV. This increase in the terrain within the FOV (containing additional and more prominent cues to dimensionality) more than offset the effects of increased range/altitude. This can best be seen by reference to Area #7. For the narrower FOV (7 degrees), the steep slope of a mountain side directly adjacent to the buildings was not visible. All judgments had to be made primarily on the basis of the buildings themselves which, although they were the most prominent features in the area, were relatively small and separated so that few cues could be derived from them. For the wide FOV, however, the total mountain side was visible and the subjects now had a completely different (and expanded) set of cues on which to base their judgments. Their scores were identical to those obtained on the Mountain Area (#5) at both 7 and 13 degree FOV's. For Area #5, the primary cue - the mountain side - was visible in both FOV presentations and the cues to dimensionality were so far above threshold that there was no difference between the two conditions.

Figure 13 shows the effects of altitude on the perception of source dimensionality. In the Constant Altitude Approach tests, FOV was systematically varied as a function of altitude in order to maintain the same

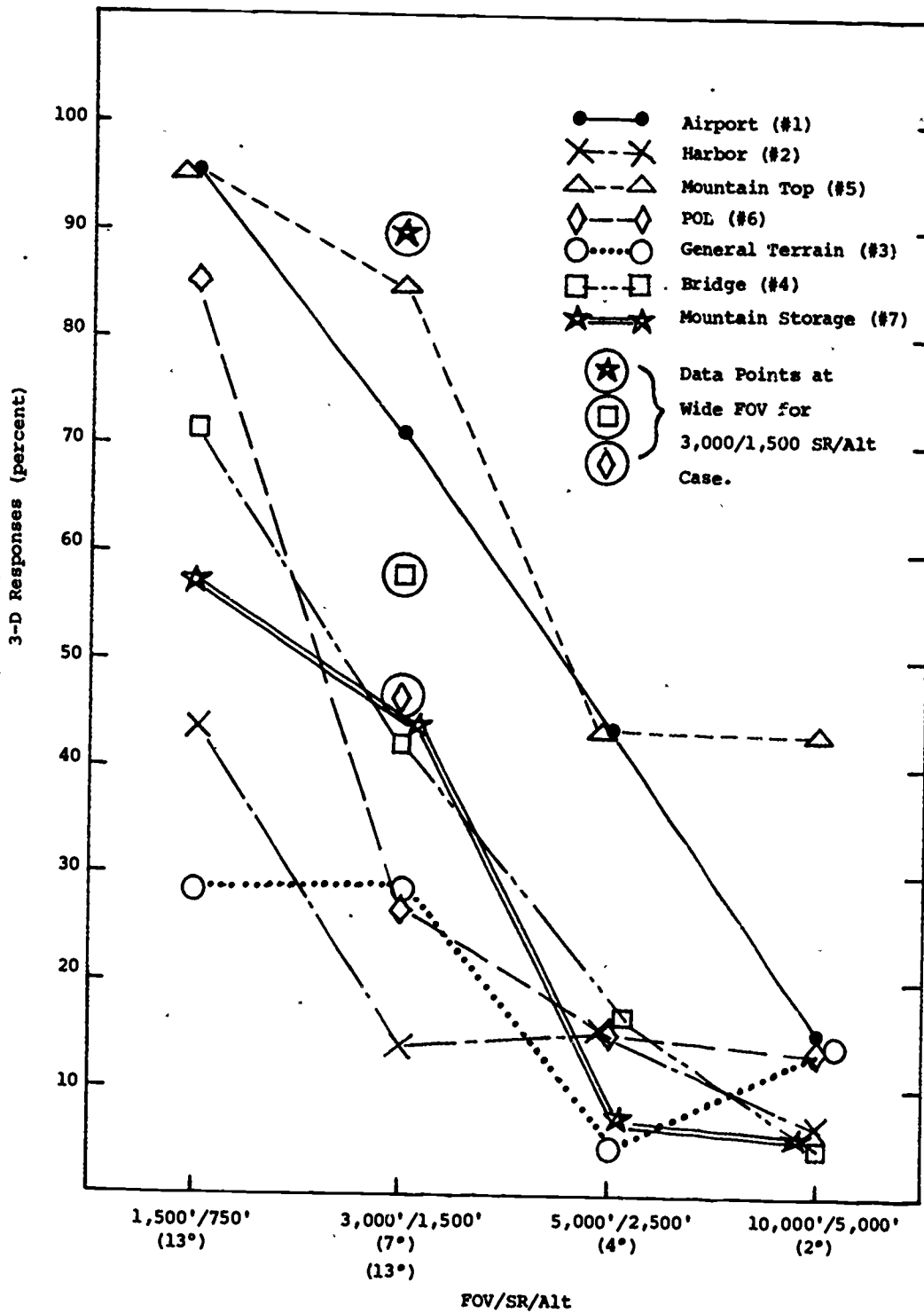


Figure 12. Percent Judged 3-D for Pilot Subjects: Performance on each area as a Function of FOV/SR/Alt - Constant Altitude Test

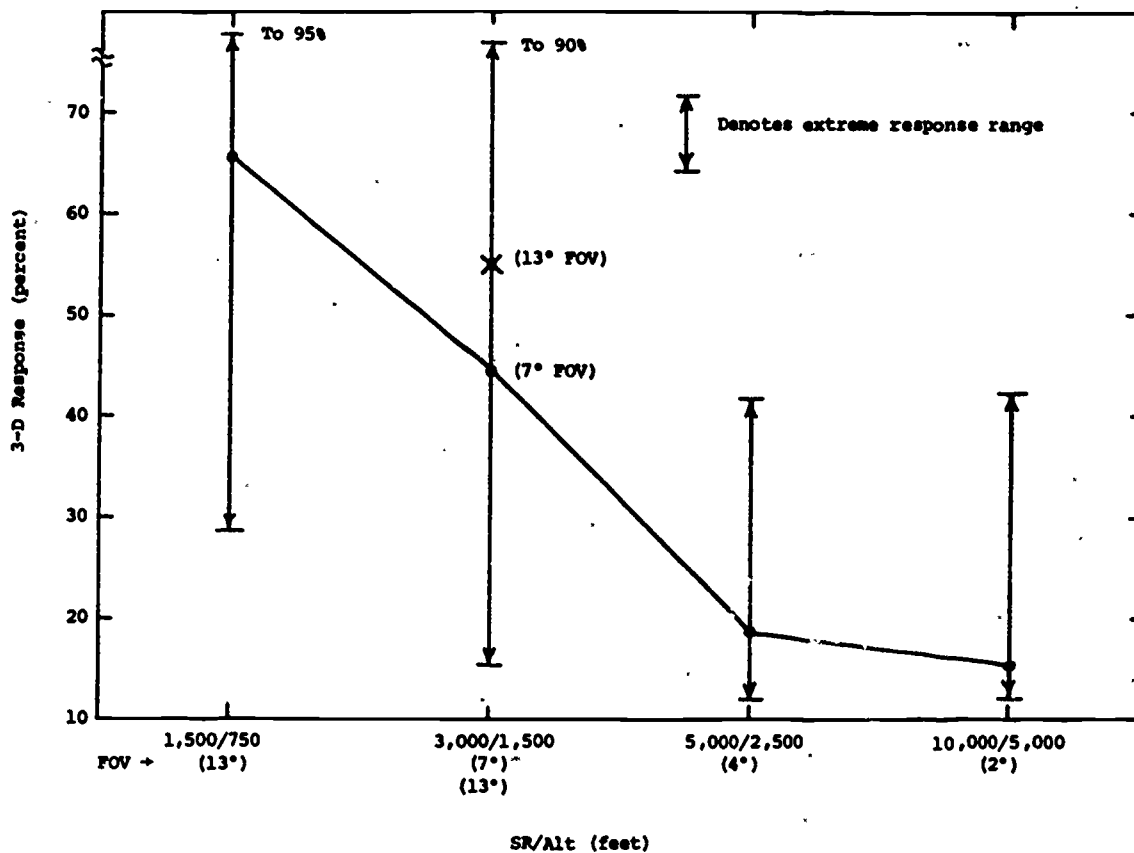


Figure 13. Percent Judged 3-D for Pilot Subjects: Averaged Over Areas as a Function of SR/Alt for the Constant Altitude Test

lateral coverage. Therefore, the FOV's shown in this figure vary from 13 to 2 degrees. As the figure shows, with the same lateral terrain coverage, the percentage of trials judged to be 3-D decreased systematically with increasing altitude. The data points on this curve are the averaged values for all target areas at each altitude, and the range of values obtained as a function of target area is shown by brackets. The effect of FOV per se at one selected slant range/altitude combination (3,000/1,500 feet) is also shown on this same figure for the purpose of comparison. The high percentage of 3-D judgments obtained at the wide FOV (13 degrees) reflects the high values obtained on target areas 4, 6, and 7. These areas included more 3-D cues when viewed with the 13 degree FOV than when viewed with the 7 degree FOV. It was, therefore, concluded that performance was not affected by the increased FOV unless additional cues to dimensionality are made available by the increase in area coverage.

2.2 FOV/SR/ALT. As shown in the previous section, FOV is not a significant factor in this series of tests. Therefore, performance will be considered in terms of SR/Alt conditions only.

NAVTRAEQUIPCEN 70-C-0238-1

Above 5,000 feet subjects were unable to consistently identify dimensionality of source material even for conspicuous, well defined manmade objects such as an airport, a harbor, or a bridge. Over flat natural terrain (Areas #2 and #3), performance was poor (an average of 35 percent) at 1,500/750 feet SR/Alt and dropped off from that point to a low of approximately 7 percent at 10,000/5,000 feet SR/Alt.

2.3 EXPERIENCE. As in the Dive Approach tests, both experienced and naive subjects were employed. Results of the analysis of variance showed that the experience factor was significant at the 0.05 level. There was, in addition, an interaction between this variable and the FOV/SR/Alt variable (see Table 3). This interaction is shown graphically in Figure 14. T-tests performed at each level show that at the 1,500/750 and 3,000/1,500 SR/Alt combinations, the performance of the pilot subjects was consistently better than that of the inexperienced subjects. There was, however, no difference in performance between the two groups at the 5,000/2,500 and 10,000/5,000 foot distances. At one representative SR/Alt combination (3,000/1,500 feet) additional data was acquired at a FOV almost twice as large (13 degrees) as that required to maintain constant lateral coverage (7 degrees). As mentioned previously, the performance of the experienced subjects was significantly better ($p < .05$) than that of the naive subjects at the 7 degree FOV. At the larger FOV the differences between the

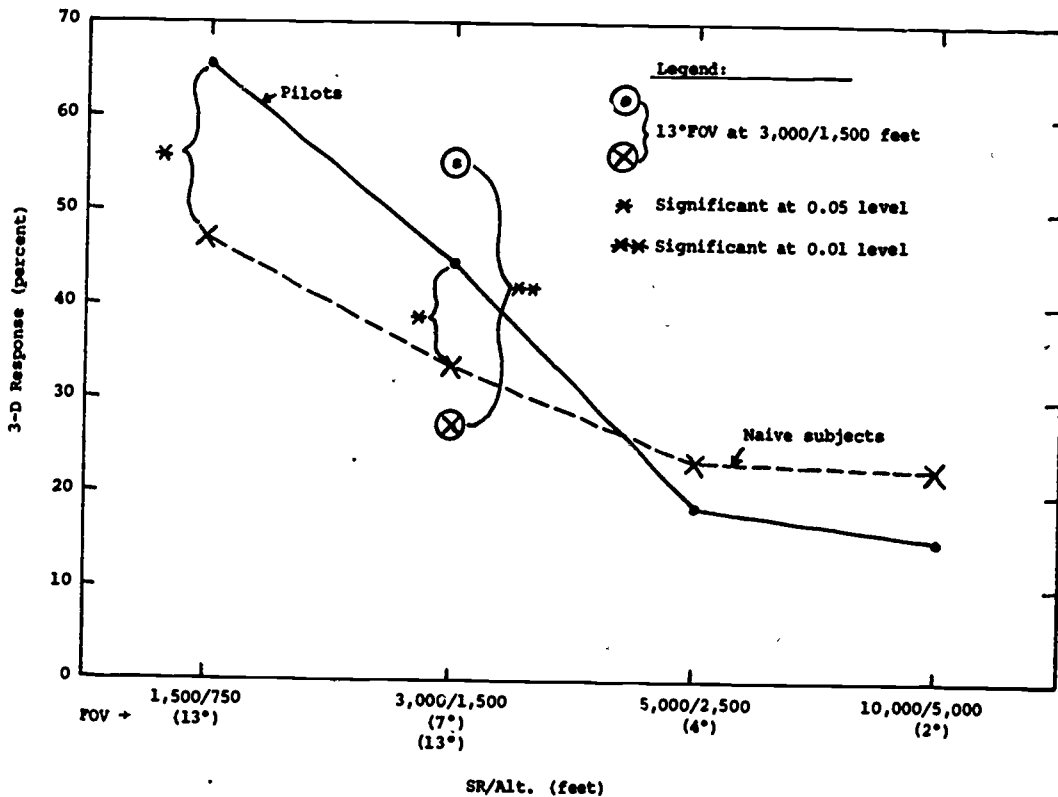


Figure 14. Pilot-Naive Subject Interaction as a Function of FOV/SR/Alt Averaged Over All Areas for Constant Altitude Test

NAVTRAEQUIPCEN 70-C-0238-1

two groups were even more marked ($p < .01$). Evidently, the experienced pilots made more (or better) use of the additional information available to them in the wider fields than did the naive subjects.

The results of this test show that the ability to perceive the dimensionality of the source material is closely related to piloting experience at the lower values of slant range/altitude. At SR/Alt values in excess of 3,000/1,500 feet, however, the differences in performance attributable to piloting experience are insignificant.

2.4 VELOCITY. Two simulated airspeeds were used on Areas #1 and #2 (Airport and Harbor). These velocities were 200 and 400 ft/s, scaled to the 250-to-1 ratio used in this study. As previously stated, these relatively slow speeds were a compromise based on the need to (1) maximize the viewing time available on each target run, and (2) minimize image smear on the TV monitor. These velocities (120 and 240 knots) allowed the subjects ample search time. An AOV was performed and the effect of velocity was determined to be not significant.

3. RELATED ANALYSES

The two series of tests outlined above were primarily concerned with the ability of observers to detect the nature of the image storage device used in the generation of simulated target imagery. However, the Dive Approach and Constant Altitude tests employed several common target areas to facilitate direct comparison of data differing only in respect to viewing conditions. Significant differences were obtained between the two viewing modes which are discussed in detail in paragraph 3.1. In addition, an attempt was made to relate the results of this study to the basic data available in the psychophysical literature. Unfortunately, because of numerous differences in experimental conditions, objectives, etc., direct comparisons were not meaningful in the context of this analysis. Problems encountered in this attempt are discussed in paragraph 3.2.

3.1 COMPARISONS BETWEEN THE DIVE APPROACH AND CONSTANT ALTITUDE TESTS. As previously stated, significant differences were observed between responses to identical targets in the Dive Approach and Constant Altitude Approach tests. Attempts to account for these differences in terms of measurable aspects of the displayed imagery were only partially successful. For example, it was expected that the observed behavioral differences would be reflected in angular displacement of the target images as a function of altitude. However, comparison of angular image displacement values calculated for targets common to both series of tests failed to confirm this (see Appendix G, Figures 43 and 46).

Target image movement was also compared. This was accomplished by determining the percentage of the total field which was obscured or displaced as the target image moved across the display. At the lowest altitude the total displacement in the Constant Altitude tests - 2 to 6 percent - was approximately twice that for the Dive Approach tests - 1 to 3 percent - (see Appendix G).

NAVTRAEQUIPCEN 70-C-0238-1

Finally, the relative rate of change of the displayed target/background images was calculated for both viewing conditions. Direct comparisons are very difficult to interpret since the data are based on essentially different perceptual conditions.

Failure to account for the observed behavioral differences in quantitative terms can be attributed to the confounding effects of two factors which are inherent in the applied nature of the study. The first of these is concerned with unavoidable differences in the dynamic relationships between targets and backgrounds in the two series of tests. In the Dive Approach tests the effects of motion parallax increase radially at a nonlinear rate from the TV camera's aim point at the center of the display. On the other hand, in the Constant Altitude Approach tests, the same effects appear parallel to the line of flight and at a nearly constant magnitude for any given height. Thus, the observer is faced with two perceptual tasks which differ in one very important aspect, i.e., the temporal characteristics of the motion parallax cues available to him. Although both sets of imagery were acquired under very carefully controlled conditions to ensure that the principal dynamic cue to depth was restricted to motion parallax, there are basic differences in the rates of change of this cue as a function of approach geometry.

From the observer's standpoint one of the principal differences between the two approaches is in the amount of time available to detect and respond to whatever cues are present. For example in the Constant Altitude Approach tests the target progresses from top to bottom of the display. Since the rate of change of angular displacement is essentially constant for a given altitude, the entire time that the target is within the FOV can be devoted to establishing the presence or absence of the cue. On the other hand, in the Dive Approach tests, although the target appears centered on the screen throughout each trial, the motion parallax cues (if they are present at all) can exceed the observer's threshold only for a very brief period at the end of each run. This constraint on the observer's detection and response time in the Dive Approach tests tends to exaggerate the problem of determining the instantaneous altitude at which a response was made.

Another factor which tended to obscure the basis for the observed behavioral differences was the inability to determine what specific features of a target an individual subject was attending to at any given time in the run. In both series of tests a wide variety of motion parallax cues were available depending primarily on the particular aspect of the target area which was fixated.

In summary, it was found that the differences in response to identical targets in the DA and CAA tests could not be satisfactorily explained in terms of either angular image displacement, per se, or the rate of change of angular image displacement.

However, consideration of the approach geometries involved shows that the two series of tests presented the observer with two essentially different perceptual tasks - not in terms of the cues available but in terms of their

temporal characteristics. When the implications of these temporal differences are taken into account the observed behavioral performance becomes more understandable at least on a semiquantitative level. For a given target and altitude combination the Constant Altitude Approach produced considerably greater image movement than the Dive Approach. This additional image movement combined with the additional time available to detect and respond to whatever differential movement existed is probably responsible for the superior performance in the CAA tests.

3.2. COMPARISONS WITH OTHER PSYCHOPHYSICAL DATA. Earlier work by many scientists (Reference 1) has shown that threshold values for the perception of movement parallax can be obtained as low as 1 to 2 arc minutes per second. The corresponding data from this study is well above this range (4.5 to 10 arc minutes per second), but in view of the problems inherent in applying basic laboratory findings to real world problems, the observed differences are not unreasonable. There are, of course, many sources of variability in the applied data which can be precisely controlled in the laboratory. In this case, one of the most important sources of uncertainty is in determining whether or not any individual subject was attending to the critical portions of the displayed imagery at the proper time, i.e., the time (measured in fractions of a second) at which the most prominent motion-dependent cues to dimensionality were available to him. Another factor which tends to degrade the obtained threshold values relative to those reported in the basic literature is the limitation imposed by the TV system. In effect, the TV system constitutes a spatial filter which limits the image detail available to the subject.

3.3 NOTES ON PERSPECTIVE CHANGE. Perspective change (principally foreshortening of vertical height) is another motion-dependent cue to dimensionality. It apparently plays a relatively minor role in the perception of apparent depth, however. In debriefings following both the DA and CAA tests, the subjects consistently indicated that they did not find that perspective change provided a major clue to dimensionality. Calculations presented in Appendix G support these observations. Here, it is shown that for a given target viewing geometry, target/background movement parallax displacements were approximately four times as great as the corresponding perspective shift values.

SECTION IV

CONCLUSIONS

For the Dive Approach (DA) tests the dimensionality of the original source material could not be reliably determined from a TV displayed image even at the minimum combination of scaled slant range/altitude (i.e., 1,500/750 feet).

With the same target/background conditions, the same altitudes, and a TV sensor depression angle equal to the dive angle used above, the Constant Altitude Approach (CAA) provides motion parallax cues approximately twice as large as the maximum achievable in the Dive Approach (DA) test. However, even in the CAA tests, subjects were unable to correctly identify dimensionality of the image source in more than 45 percent of the trials until altitude was reduced to 750 feet, the minimum used in this study (Figure 14).

Motion parallax (relative target image-to-background displacement) was the most important cue to dimensionality. Although some target perspective change (vertical foreshortening) undoubtedly occurred in the runs, the effect was minor and was masked by the much larger effect of movement parallax.

In both the DA and the CAA tests, several variables considered potentially important in the perception of image source dimensionality via TV were shown to have no significant effect. These include:

a. Display viewing distance - Viewing distance was not an important parameter, apparently because the TV display system was performance-limited under the conditions of this experiment.

b. Displayed target/background contrast - A wide range of inherent contrasts was included (estimated 15 to 70 percent, and much higher with shadow conditions).

c. Video signal-to-noise ratio (SNR) - SNR levels ranged from an estimated 35 dB to 20 dB.

d. Shadow effects - No apparent enhancement resulted from the use of shadows.

The effect of approach velocity was anomalous and requires some explanation based on the specific conditions of the tests. The effect of the difference in velocities used in the CAA tests - 200 to 400 feet/second - was clearly not significant. On the other hand, the effect attributed to the approach velocities used in the DA tests - 650 and 1,100 feet/second - was significant at the .05 level. In spite of this, it was concluded that approach velocity itself did not affect the discriminability of dimensionality. The basis for this conclusion lies in the special nature of the DA tests. In these tests two performance measures were unavoidably confounded; i.e., the verbal response which specified source dimensionality; and the slant range at the instant this

response was made. An essentially constant difference in response range was obtained with the two velocities for all targets. The most likely explanation for this observed effect is based on simple reaction and/or decision time. Thus, it is assumed that target dimensionality was perceived at the same slant range for both velocities. However, since the subject's response time is essentially constant, the higher approach velocity results in a shorter slant range at the instant of recording. In this case, therefore, the observed differences, while they are statistically significant, are considered to be an artifact attributable to the interaction of velocity and human information processing requirements rather than velocity per se.

Although the flight geometries are defined in terms of slant range/altitude combinations, the factor primarily responsible for the amount of movement parallax displayed on the monitor is the altitude of the sensor. This is true for both the Dive Approach and the Constant Altitude Approach tests. That is, motion parallax varies inversely with altitude, and for a given altitude, is not greatly affected by slant range.

Only in the case of pronounced target or terrain heights, as in the mountainous region on the GDC terrain model, is the subject capable of perceiving dimensionality at a reasonably high altitude, i.e., 85 percent correct judgments at 3,000/1,500 feet. However, even in these extreme areas, accuracy falls below the 50 percent correct level when the altitude is increased to 2,500 feet.

The sensor FOV has only a minor influence on movement parallax cues derivable from a given target/background complex. Although the total scene viewed by the sensor will increase with increasing FOV, the image is compressed within the fixed limits of the TV monitor, resulting in the same percent target image shift. That is, the image size decreases as the FOV increases, essentially negating the effect of increased viewing angle. This, of course, would not be true in a direct viewing case. An exception to the above occurs when there is a major change in the nature of the total scene with changing FOV. If a wider FOV encompasses target areas having more prominent cues (e.g., taller building or greater terrain elevations), then the new target area can considerably alter the ability of the subjects to perceive the dimensionality of the image source.

If movement parallax is described in terms of displayed image angular shifts, the resulting values can be misleading since the display near-viewing distance (20 inches) was somewhat arbitrary. That is, it was selected primarily to achieve adequate eye accommodation. In the course of the CAA tests, it was observed that the ability to perceive displayed image shifts was not significantly affected by viewing distance (at least up to approximately 60 inches, a factor of 3). This indicates that a TV display-limited condition existed in these tests; that is, visual acuity was not a primary factor in the perception of dimensionality. The essential point is that the computed angles are useful primarily as a relative performance measure (e.g., comparing the CAA and the DA results). A more generalized performance measure is the percent image shift relative to the total viewed field (from which the displayed angle values are computed - see Appendix G).

NAVTRAEQUIPCEN 70-C-0238-1

SECTION V

RECOMMENDATIONS

For training problems which require simulation of TV navigation and/or targeting imagery, serious consideration should be given to the use of relatively inexpensive 2-dimensional image storage devices for missions at altitudes in excess of 750 feet.

REFERENCES

- 1 Stevens, S. S., "Handbook of Experimental Psychology," Wiley and Sons, 1951
- 2 Federer, W. T., "Experimental Designs," The Macmillan Company, 1963
- 3 Hays, W. L., "Statistics for Psychologists," Holt, Rinehart and Winston, Inc., 1963

APPENDIX A

STATISTICAL ANALYSIS

The analysis of variance (AOV) was the principal statistical technique used in this study. To further analyze data points shown to be significant by the AOV, the t test and the Scheffé test were employed. For readers unfamiliar with these techniques, a brief description of each is outlined in paragraphs 3 through 5.

1. DIVE APPROACH TEST

This group was analyzed as a 2x2x2x4 complete factorial with two modes of dimensionality, two velocities, two levels of experience, and four target areas*. Seven subjects were used in each cell. A smaller complete factorial AOV was performed on those levels of data containing the shadow and nonshadow conditions. This test was a 2x2x2 containing two levels each of dimensionality, illumination conditions (shadow and nonshadow) and target areas (POL and Airport). These were conducted using seven subjects at the 650 feet per second velocity.

2. CONSTANT ALTITUDE TEST

This group was analyzed as a 2x5x7 complete factorial with two levels of subject experience, five FOV/SR/Alt combinations, and seven target areas. For the primary analysis, four subjects per cell were employed. For the experienced group, seven pilots were actually used. All data from these seven were subsequently used in a complete factorial containing one level of experience which was then a 5x7 factorial with five FOV/SR/Alt combinations, and seven target areas. Both of these tests were conducted at the 200 foot per second velocity. A subtest was used to determine the effects of velocity. This was a 2x2x2 with four subjects per cell, and two levels each of velocities, experience, and target area.

3. ANALYSIS OF VARIANCE

This technique is used to make simultaneous comparisons of the means of the several treatments and combinations of these treatments employed in these experiments, to determine whether some statistical relationships exist between the independent (experimental) and dependent (obtained visual angle) variables. The AOV tests for significance at some confidence level, the variance introduced by each of a number of variables against the variance of the entire experimental data set.

To determine these relationships, the total variance must first be determined. This is done by computing the variance (from the scores of the dependent variable) of all the subjects on all trials, and ignoring

* As noted in Section III, a 2x2x5 complete factorial analysis also was performed using the five target areas at a single velocity.

the fact that these scores were obtained under several experimental conditions. This total variance may then be partitioned into parts for analysis (viz., analysis of variance). The two major divisions become the variance "between groups" and that "within groups." The between groups variance may be thought of approximately as the extent to which the means of the groups differ. The between groups variance may itself be partitioned into smaller groups which represent the individual variance of the main experimental effects and the interactions of those effects with each other.

The within groups variance, commonly referred to as the error term, is determined by the extent to which the subjects (and their answers) in each group differ. If the subject responses in a group differ widely, then that within groups variance will be large. If the within groups variance for most of the treatment groups is large, the total error variance will be large.

To determine the statistical relationships between these groups, the individual between group variances are compared to the error variance (within groups) term. The larger the between groups variance and the smaller the within groups variance, the more likely it is that the groups will differ significantly. Figures 15 and 16 illustrate the concepts of between and within group variance about population means. In Figure 15, the within groups variance is large and between group variance is small,

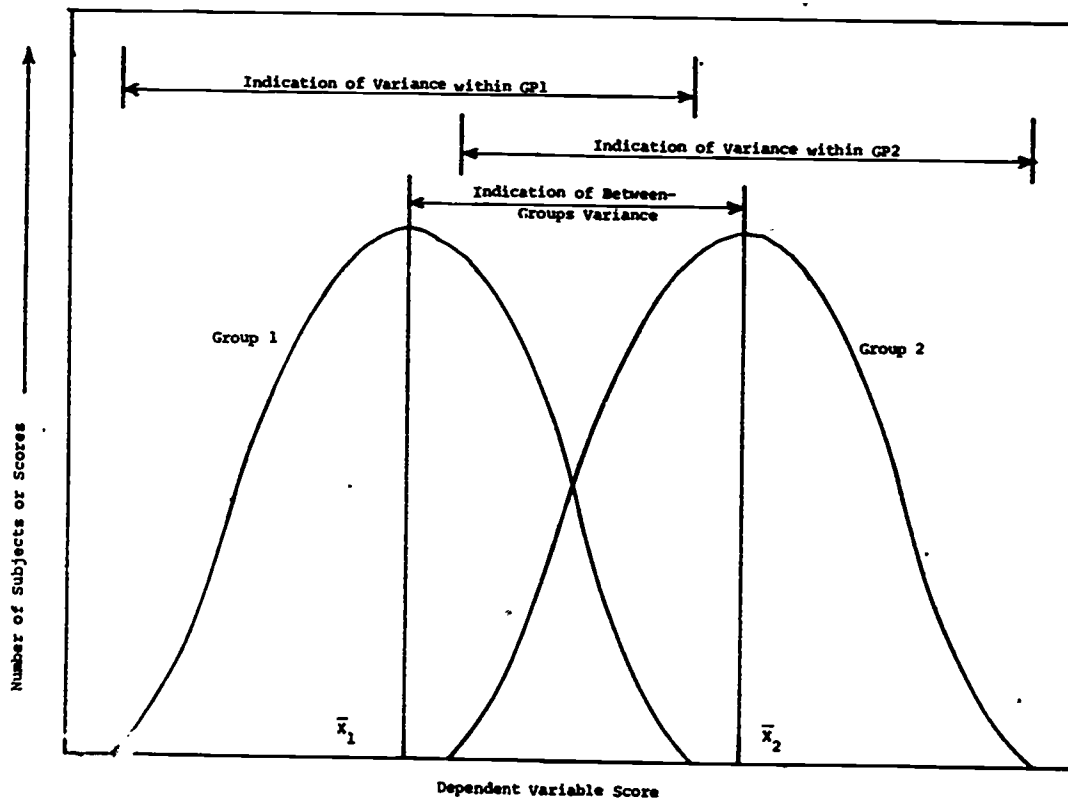


Figure 15. Indication of Large Within- and Small Between-Groups Variance

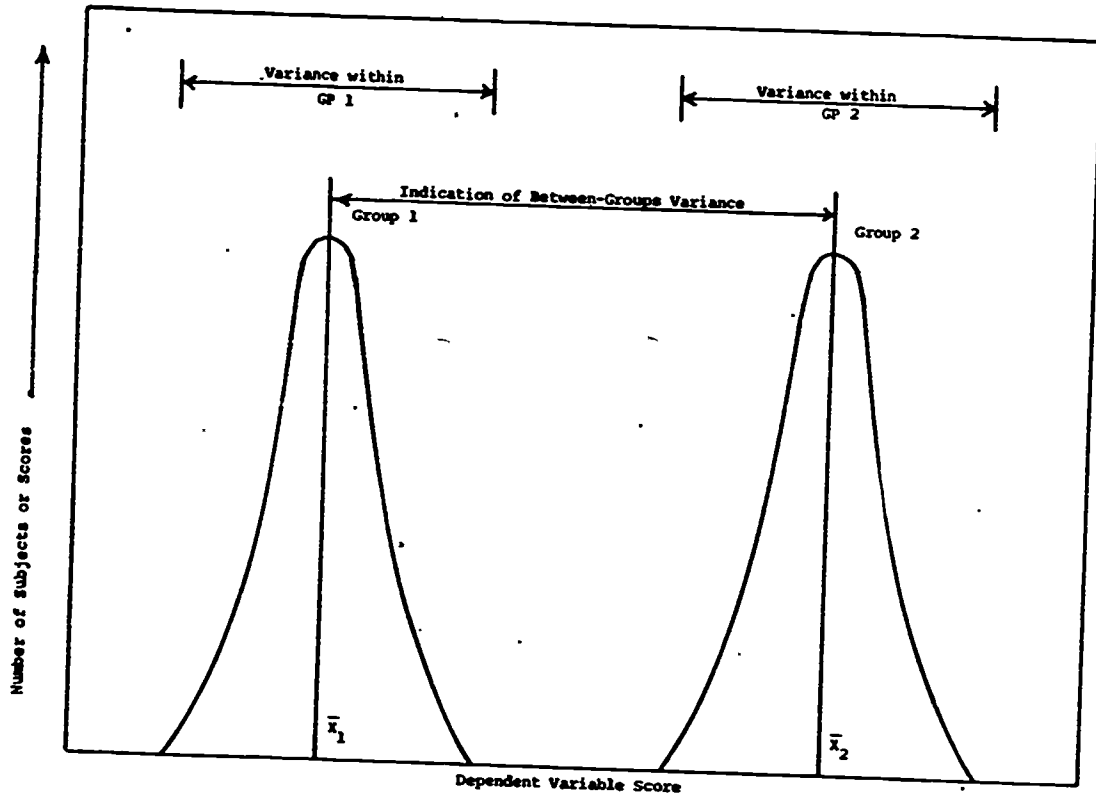


Figure 16. Indication of Small Within- and Large Between-Groups Variance

both of which help to make statistical inferences about the means unclear. In Figure 16, however, the within variance is small and the between variance large allowing a more precise prediction of the statistical relationships.

For practical analysis, there is no need to deal in variances but rather in the actual dependent parameter scores which have been transformed into certain sums of squares (SS). To follow through with the simplified explanation of the AOV, the total SS is first obtained and then its parts analyzed.

$$\text{Total SS} = (\sum X_1^2 + \sum X_2^2 + \dots + \sum X_r^2) - \frac{(\sum X_1 + \sum X_2 + \dots + \sum X_r)^2}{N}$$

where r indicates that we continue to add the values indicated (the sum of X squares, and the sum of X, respectively), for as many groups as there are in the experiment. N is the total number of measurements and X is the percent judged 3-D value. The SS is then analyzed into components: the between SS and the within SS.

$$\text{Between SS} = \frac{(\sum X_1)^2}{n_1} + \frac{(\sum X_2)^2}{n_2} + \dots + \frac{(\sum X_r)^2}{n_r} - \frac{(\sum X_1 + \sum X_2 + \dots + \sum X_r)^2}{N}$$

NAVTRAEQUIPCEN 70-C-0238-1

where n equals the number of measurements within each group.

Then

$$\text{Within SS} = \text{Total SS} - \text{Between SS}.$$

If there are more than two groups, as there are in this case, the between SS is then computed separately for each group by obtaining the $\sum X$ and $\sum X^2$ separately for each group. The subscripts above then indicate, e.g., X_1 , the sum of the dependent variable scores for group 1.

To obtain the variances of each effect now to be compared, the particular SS is divided by its degree of freedom (df). This term is then known as the mean square (MS) term.

The concept of degrees of freedom is seen by realizing that the sum of deviations or variances about a mean must be zero. Then if N equals a certain number of those deviations, and possible values can be guessed, the last guess or value of N is completely determined by the $N - 1$ earlier choices. Therefore, the degrees of freedom for a sample variance equals $N - 1$. In the AOV, each and every degree of freedom associated with the treatment effects corresponds to some possible comparison of those means.

The MS terms (of the partitioned between MS) are now individually compared to the error MS. To determine if the difference between the two are statistically significant, the F statistic is used:

$$F = \frac{\text{MS between-groups}}{\text{MS within-groups (error term)}}$$

The obtained values for these ratios are then looked up in appropriate tables for the levels of significance.

The AOV tables previously discussed for each test in the results section are a summarization of the steps outlined above.

When a variable is determined to be significant, e.g., the contrast effect, it may then be necessary to make further statistical inquiries at specific data points. This procedure is then termed a comparison or multiple comparison of data points and for this study was performed using either t test (for two point comparisons) or the Scheffé for more than two points. These are briefly explained below.

4. THE t TEST

This test is almost identical to the AOV for a two-group comparison. The t test compares the deviations between two means and again by using a table enables the experimenter to determine whether a statistically significant relationship exists.

5. SCHEFFE TEST

The Scheffé test is a procedure for testing comparisons between several means. It is a post hoc comparison used after a significant F has been found for the relevant factor. The comparison can be decided upon prior to the test or after test results are analyzed. It is suitable for groups of unequal size and is suitable for any comparison. The multiplier is obtained from the F table and is equal to:

$(v-1)F_{\alpha}(v-1, fdf) = S$, where v = number of means in the experiment, α = significance level, and f = degrees of freedom associated with the error variance. Additional discussion may be found in References 2 and 3.

APPENDIX B

GENERATION OF TWO-DIMENSIONAL DIVE APPROACH RUNS BY USING AN
OPTICAL ZOOM TECHNIQUE

1. BACKGROUND

The most straightforward method of generating 2-D video tape replicas of the selected 3-D target convergence runs would be to produce photographs of these areas at the correct scale factors and then physically move the TV camera toward the photographs at the proper scaled velocities. This approach was considered initially, but careful evaluation of the techniques required to produce accurate photographic target replicas at the desired scale factors revealed the following potential problem areas:

a. Photographs (if used) would have to have the same scale factor as the 3-D target model to permit the use of the same approach geometry and techniques as in the 3-D runs. This would require photographic prints approximately 4 feet wide at the maximum range.

Continuous target convergence over the 40-to-6 foot range extremes (a 6.7 to 1 ratio) would require that the resolution of the photographs be high enough that the subject could not detect photographic grain or general edge fuzziness at the closest approach. This level of image quality would present a difficult problem within the scope of this program.

It was therefore concluded that a single photograph would not satisfy the requirements. The alternative of providing two or more photographs at successive stages along the Dive Approach was considered. This would have alleviated the resolution problem by decreasing the required range ratio (and thus object magnification ratio) for a single photograph. This would, however, make it necessary to interrupt a given Dive Approach run; that is, break it into shorter segments. It would, in turn, be necessary to make equivalent interruptions of the 3-D runs to minimize differences between these two viewing modes. This approach was not considered desirable.

b. The relatively large width of the photographs would require use of a photomosaic technique to produce the desired size.

c. The 3-D terrain model has areas of high target/background contrast, particularly when shadows are employed. In this case, the TV system dynamic range would limit the contrast of displayed imagery. If photographs of the model were used, the dynamic range and grey scale characteristics of the photographs themselves would have to be carefully controlled to produce displayed images commensurate with their 3-D counterparts in terms of brightness relationships.

d. Special techniques would be necessary to minimize surface reflectances which could reveal that the source was photographic. A non-glossy, matte type finish would be a necessity, and special provisions would be required to keep the photographic surface quite flat, again to minimize surface reflectances.

2. OPTICAL ZOOM SIMULATED 2-D DIVE APPROACH

The problems outlined above stimulated the search for a better technique to generate the 2-D convergence runs. The prime considerations were that:

- a. No cues specific to a 3-D source (movement parallax and/or perspective changes in projected vertical dimension of target) would be present.
- b. Each run would exhibit, within the perceptual tolerance of the subjects, the same dynamic image growth and image fidelity (resolution, grey scale, dynamic range, video SNR) as its 3-D based counterparts.
- c. No artifacts sufficiently obvious to identify the source as 2-D would be present.

The technique which was selected employs an optical zoom lens coupled to a TV camera to simulate 2-D dynamic target convergence. This technique is described in the following section.

2.1 GENERAL DESCRIPTION OF 2-D ZOOM TECHNIQUE. The zoom technique for simulating 2-D target approaches can be explained by reference to Figure 17. The upper portion of this illustration shows the normal 3-D Dive Approach geometry in plan view. Here, the TV camera with a fixed field of view (FOV) approaches targets identified as elements A and B. These targets are separated in the longitudinal direction and offset from the approach path. From the start to the end of the run, the TV camera coverage decreases from width W_i to W_f , and the line of sight (LOS) to elements A and B undergoes a shift (element A LOS shifts from the light portion of element B to the shaded portion). This angular shift is termed movement parallax, and it is the primary cue (perspective shift being secondary) which permits a subject viewing a TV display of this imagery to perceive the source material as 3-D. The lower diagram of this figure shows the TV camera FOV as it is zoomed over the focal length range which provides the same change in viewed widths, W_i to W_f . In this case, the image is magnified and the general effect is similar to physical closure on the targets. The significant difference between the two conditions, however, is that the TV LOS to target element A relative to element B remains fixed throughout the simulated convergence run. Therefore, no movement parallax or perspective change occur. To produce equivalent dynamic closure effects (same apparent image growth rates) it is necessary to control the zoom focal length as a function of run time. This was accomplished by analog computer control as described in Appendix E.

2.2 EFFECTS PECULIAR TO ZOOM TECHNIQUE. It was known at the outset of this program that the zoom approach was not without problems. Therefore, preliminary tests were carried out to determine whether the undesired dimensionality clues associated with zoom convergence were perceptible under the conditions employed in the behavioral tests. The major effects which were evaluated are summarized below:

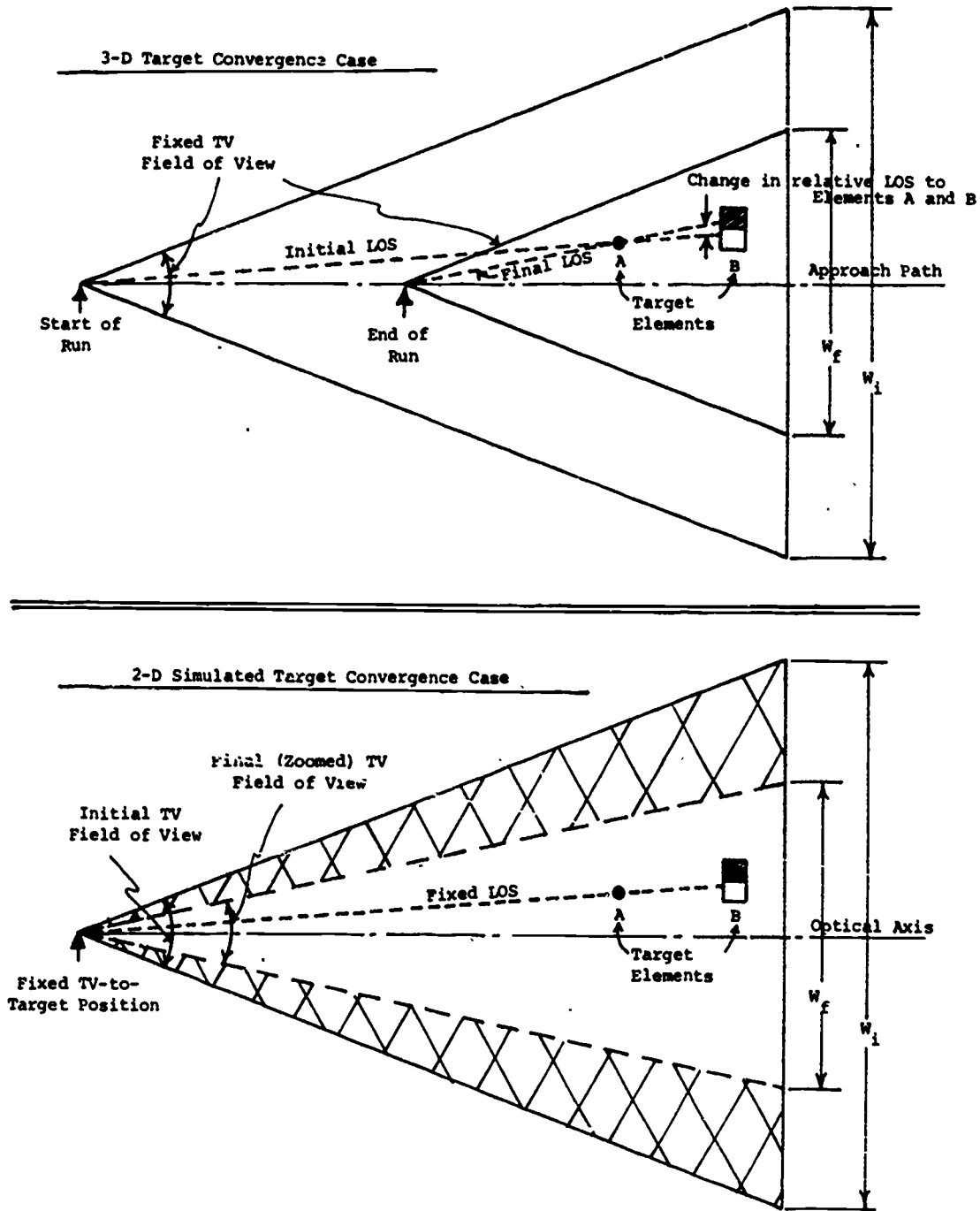


Figure 17. Comparison of 2-D and 3-D Target Convergence Geometries (Vertical View)

NAVTRAEQUIPCEN 70-C-0238-1

a. When zoom magnification is employed, the image expands from the center of the FOV (the optical axis) at equal radial velocities. This is, of course, not true in the 3-D runs. Since the Dive Approach angle was 30 degrees, the near-field image expands faster than the far-field in the 3-D runs. Therefore, a preliminary test was necessary to determine whether this difference between 2-D and 3-D radial growth rates was apparent to the subjects; it was not.

b. The longitudinal areas seen by the fixed 3-D and the zoom 2-D FOV's were not precisely matched. Figure 3 in Section II, paragraph 2.1.1.4 depicts this mismatch at the beginning of the 3-D dive approach. Calculations showed that the maximum near-field difference was 10 percent (dimension viewed by fixed FOV was greater than zoom FOV) and the maximum far-field difference was 16 percent (dimension viewed by fixed FOV less than zoom FOV).

It was expected that this mismatch in longitudinal area might provide an undesired clue to the dimensionality of the stored (video taped) imagery. However, preliminary studies showed that the area mismatch did not provide noticeable cues to image dimensionality.

c. Another study was concerned with the effect of differences in target perspective. As previously noted, some change in perspective is experienced when physically moving toward a target (3-D), while in the zoom approach (2-D), the perspective is fixed. Preliminary studies showed, however, that the perspective change in the 3-D approach was below threshold.

d. Finally, the minimum zoom rate (minimum simulated closing velocity) at which the lens could be operated was determined. This minimum rate was a function of the stiction effects associated with driving the zoom lens elements which control focal length.

At low zoom rates, a discontinuous image expansion was observed. A preliminary study was run to demonstrate that at the simulated velocities used in these studies, this effect was not perceptible.

APPENDIX C

TEST FACILITIES AND EQUIPMENT

The 2-D and 3-D target stimulus material (video tapes) were produced at the Martin Marietta Guidance Development Center. Behavioral tests (excluding preliminary runs made in the GDC) were performed in a separate room in the Engineering Research laboratory area. A summary of facility and equipment items employed in those two phases of the experiment is presented in the following sections.

1. TARGET STIMULUS GENERATION

Items used to generate the video taped stimulus runs for the Dive Approach and Constant Altitude tests consisted of (1) the GDC optical simulation facility, (2) TV camera and display subsystem, (3) video recording equipment, and (4) a precision spot photometer. These items are discussed below.

1.1 GDC FACILITY. The elements of this facility which were utilized in this experiment are shown in Figure 18. They consist of the terrain model (including the new 250 to 1 scale targets described in Appendix D), the computer-controlled precision movement subsystem within which the TV camera was mounted, and the computer laboratory.

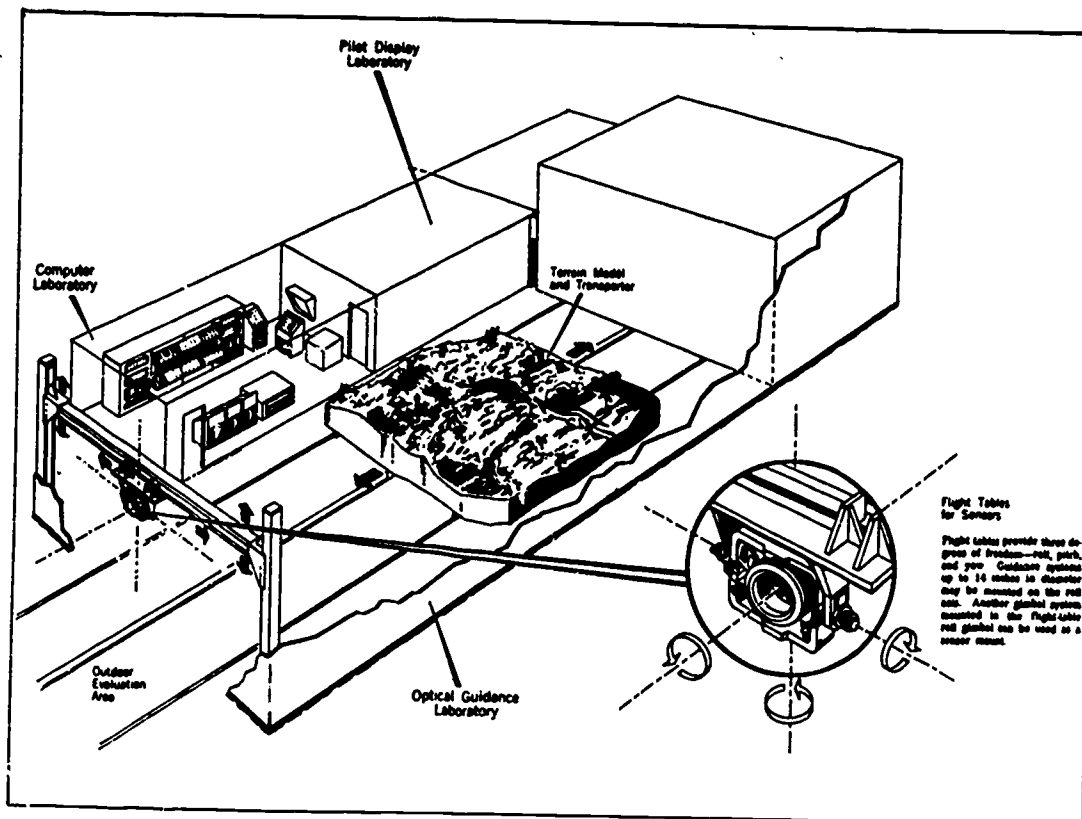


Figure 18. Martin Marietta's Guidance Development Center

1.1.1 Terrain Model. A photograph of the overall terrain model is shown in Figure 6 of Section II in the main body of the report. This photograph shows the model in the outdoor test area which permits use of natural illumination. This particular view is from an elevated position corresponding roughly to that at which the TV camera was located at the start of a 3-D run.

The model is 40 feet on a side and it contains a wide range of topographical features together with a variety of manmade targets. The basic scale factor is 600 to 1; however, by substituting the new 250 to 1 scale targets at selected areas on the model, those areas were redesignated as 250 to 1 scale areas for purposes of these tests (see Appendix D for a description of the selected target areas and a discussion of scale factor change).

The model is driven longitudinally on rails and its position and velocity are accurately controlled by an analog computer. The drive system is capable of providing a wide range of velocities up to a maximum of 10 feet per second. As implemented in the Dive Approach tests, model movement provided one component of dive convergence (see Appendix E). At the 250 to 1 scale factor used, the maximum rate required was approximately 3.8 feet per second.

1.1.2 TV Camera Precision Movement Subsystem. Three elements of the GDC comprised the TV camera precision movement subsystem. The TV camera and zoom lens were rigidly mounted in the inner (roll) gimbal of the three-axis flight table as shown in Figure 19. The fixed 30 degree depression angle was provided by the pitch gimbal. The roll and yaw gimbals were maintained in their nominal zero positions since these particular degrees of freedom were not required.

Horizontal positioning of the TV sensor was accomplished by the transverse carriage assembly which was aligned on a selected target area prior to each run.

A vertically moving I-beam provided the necessary freedom in the TV camera's vertical translation. Accurate positioning of the I-beam in height, together with longitudinal positioning of the terrain model, produced correct initial slant ranges to the targets in the Dive Approach tests. Then, under computer control, this assembly moved down to provide the vertical component of the dive convergence. The longitudinal component was provided by the movement of the model.

1.1.3 Analog Computer Laboratory. The analog computational equipment used in this study consists of a EAI 231 R-V console. This was programmed to provide precision control of the simulated flight paths for both the Dive Approach and Constant Altitude runs. The zoom lens focus and focal length servo drives were also operated under computer control in the 3-D Dive Approach runs to provide correct simulated convergence rates and continuous optimum optical focus.

L.



Figure 19. TV Camera Mounted in GDC Gimbal Assembly

1.2 TV CAMERA AND DISPLAY SUBSYSTEM. The TV equipment used in these tests was a composite of two Martin Marietta TV systems; (1) the standard GDC 1-inch vidicon camera and camera control¹, and (2) the gamma control unit and high quality 8-inch TV display², which are elements of the Variable Parameter Research TV system. These latter items were needed to

1 Cohu Model 2004 camera and Model 3952 camera control.

2 Conrac Model CZB-8. This display incorporates a "keyed clamp" type dc restorer to maintain accurate black level control independent of changing scene content.

NAVTRAEQUIPCEN 70-C-0238-1

achieve and maintain a nominal unity gamma characteristic (system brightness transfer function) and thus provide an approximately one-to-one transfer of scene contrasts to displayed image contrast (within the dynamic range capability of the display - approximately 20 to 1*).

A remotely controlled Angenieux 10 to 1 zoom lens, incorporating Martin Marietta designed servo drive refinements, was used with the above TV camera. The range of camera FOV's employed in this program required use of a standard 2X extender lens which provided a maximum zoom focal length range from 30 to 300 mm (with a useful range slightly less - to avoid hitting the limits at each end).

Table 4 provides a summary of the composite TV system operating characteristics (including the zoom lens, gamma control, and display performance). It should be noted, however, that the image degradation resulting from the sequential video recording/duplicating process used in producing the final stimulus tapes is not included in this table. Appendix F includes data on the characteristics of the tapes used in the behavioral tests.

TABLE 4. TV SYSTEM OPERATING CHARACTERISTICS SUMMARY

Characteristic	Performance
Horizontal scan rate	525 lines per frame, 2 to 1 interlace
Vertical scan rate	30 frames/60 fields per second
Limiting horizontal resolution (center)	600 TV lines (nominal) using EIA type wedge pattern
Video signal-to-noise (SNR)	>40 dB nominal peak video/RMS noise (estimated)
System gamma	Nominal value of unity
Grey scale response	9 shades of grey discernible using $\sqrt{2}$ type grey scale test pattern input

* By this means, the effects of target/background contrast on subjects' dimensionality perception could be more accurately assessed.

NAVTRAEQUIPCEN 70-C-0738-1

1.3 VIDEO RECORDING EQUIPMENT. The video recording, editing, and dubbing techniques employed to produce behavioral test stimuli for the Dive Approach and the Constant Altitude runs are described in Appendix F. This section identifies the equipment used and summarizes the pertinent operating characteristics.

All runs on the GDC terrain model were recorded on a SONY helical scan type video tape recorder (VTR), Model PV-120U. The unit uses a 2 inch wide magnetic tape. This ensures high resolution reproduction together with a high video SNR. Its rated characteristics of special interest are:

- SNR
 - (1) Video 42 dB
 - (2) Audio 40 dB (two audio channels available)
- Video response 3 dB down at 3.3 MHz
- Horizontal resolution (limiting) Nominal 330 TV lines (using EIA standard chart signal input)

An irregular sequence of runs was used on the tapes employed in the behavioral tests for both the Dive Approach and Constant Altitude phases. Reordering of the basic VTR runs and rerecording (duplicating) them to form a master tape for each of the above tests required a second video recorder having an electronic edit capability. The electronic edit feature permits insertion of selected portions of external composite video signals (in this case the basic runs recorded on the PV-120U VTR) onto a second tape in any desired sequence, and ensures that the dubbed video sequences are recorded with the proper time relationships to avoid interruption of the vertical sync pulses. In this manner, smooth transitions are made from one run to the next without picture roll-over at the monitor.

A SONY 1 inch helical scan VTR, Model EV-320 was used for the above purpose. A summary of its rated performance characteristics is given below:

- SNR
 - (1) Video 43 dB
 - (2) Audio 40 dB (two audio channels available)
- Horizontal resolution (limiting) Nominal 300 TV lines (using EIA standard chart signal input)

1.4 SPOT PHOTOMETER. A Spectra Pritchard spot photometer was used to measure target and background brightness values. Appendix D includes computed contrast data derived from these photometric measurements.

2. SUBJECTIVE TEST FACILITIES AND EQUIPMENT

A separate room in the Engineering Research Laboratory was used for the behavioral tests. This room was equipped with controllable lighting to provide proper and consistent TV viewing conditions.

Equipment used in this portion of the experiment consisted of the 8 inch (diagonal) Conrac display, the PV-120U SONY video recorder, and an Ampex audio recorder. The video recorder was used to play back a reproduction of the master video tape. The Ampex was used to record pertinent audio information derived from both the video tapes and the subjects' verbal responses.

APPENDIX D

TARGET PREPARATION AND TARGET CHARACTERISTICS

1. GENERAL DISCUSSION

The areas selected for study provide a wide range of typical military targets and natural terrain features. Knowledge of the target characteristics and the approach geometries employed permitted responses to be quantified by calculating corresponding target/background relative displacements and angular velocities.

Precise control of target/background contrast was not attempted; however, target paints (shades of grey) were selected to produce a fairly wide range of basic contrasts as subsequently discussed. Under shadowed conditions, substantial increases in contrast were observed. Responses were obtained under both shadow (direct sunlight) and no-shadow (diffuse outdoor lighting) conditions to evaluate the effect of information derived from shadows on the perception of dimensionality. A Spectra Pritchard spot photometer was used to measure the absolute brightness levels of the various key target and background areas, from which brightness contrast* values were calculated. These key features and their associated contrasts are included in the general descriptions of each target area included below.

The ground tracks of four of the Constant Altitude runs were made to pass over targets used in the Dive Approach tests to provide a basis for comparing responses between the two approach geometries.

2. SCALE FACTOR

To provide the desired minimum slant range/ altitude values (1,500/750 feet), it was necessary to alter the GDC terrain model scale factor from 600:1 to 250:1. This was dictated by requirements for maintaining physical clearance and adequate depth of field. The scale factor was changed by making new targets at the 250:1 scale and locating them in areas on the model where they were compatible with existing manmade and natural features within the TV field of view.** For example, an unused portion of the airport runway complex was selected and the specially

* Brightness contrast as used in this study is defined as:

$$C(\%) = \frac{B_H - B_L}{B_H} \times 100, \text{ where } B_H = \text{Highlight brightness and}$$

$$B_L = \text{Lowlight brightness}$$

**At maximum range in the Dive Approach runs, viewed longitudinal distance, D_D , on the model equalled approximately 6 feet and lateral distance, D_C , was approximately 4 feet. For the Constant Altitude runs, values of D_D and D_C were approximately 50 percent of the above values and were essentially constant.

constructed hangars, buildings and aircraft were placed on the model. At the larger slant ranges, some of the 600:1 buildings were visible. The more prominent of these were covered by placing 250:1 scale building shells over them. For the Constant Altitude test runs, where the flight path covered additional 600:1 structures, a preliminary test indicated that the larger 250:1 models were by far the most distinguishable targets. The tendency of the subjects was to focus on these larger 250:1 models in attempting to determine dimensionality.

Where the Constant Altitude flights covered natural terrain with few manmade objects, no attempt was made to alter the models. Rather, by definition, they assumed a 250:1 scale, thereby making them smaller in simulated size by the factor of 250/600.

3. DIVE APPROACH TARGET AREAS

The following paragraphs describe the targets used for the Dive Approach tests. The descriptions include data on target/background contrast, target dimensions and separations, nominal TV camera aim points, and other pertinent details. A total of six areas were used in this series of tests, including an unaltered area of the GDC model which contains relatively tall structures providing good motion parallax cues (in the 3-D operating mode). The subjects used this area for familiarization and for practice runs.

3.1 AIRPORT. Figure 20 depicts the airport area. The aim point for this test was slightly below the F-4 aircraft facing to the left, as shown by the small dot. The tallest elements of the targets remaining in the television FOV during the terminal phase of the run offered the most prominent clues to dimensionality. These included the quonset-type hangar doorway and the roof of the operations building. Basic target-to-background contrasts in these areas were in the neighborhood of 25 percent*.

Representative sizes and spacings of objects within the central target area (expressed in simulated feet) were as follows: the roof of the operations building was 40 feet tall, with the tower making the total height 73 feet. Its width was 90 feet and longitudinal separation from the nearest hangar was 90 feet. The two large hangars were each 57 feet high by 165 feet long with doorway heights of 25 feet. The runways, instead of being scaled to 600:1 assumed a 250:1 scale. They were approximately 80 feet wide, which was commensurate with the sizes of the fighter aircraft on and near the runways.

3.2 TRUSS BRIDGE. Figure 21 depicts the truss bridge target which was constructed to overlay an existing, smaller bridge spanning the riverbed. Aim point on this test run, as denoted by the dot, was near the second-from-right bridge piling. Contrast values ranged from 30 percent between

* Shadowed conditions substantially increased these contrast values up to levels ranging from approximately 50 to 90 percent.

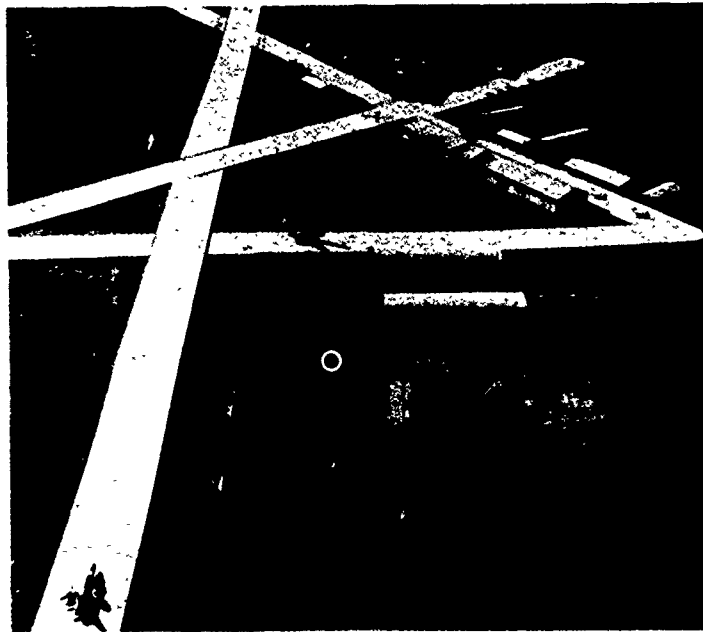


Figure 20. Airport Target Area



Figure 21. Truss Bridge Target Area

the surfaces of the truss structure and the riverbed background, to 70 percent between the riverbed and the bottom vertical side surface of the bridge.

The bridge roadbed was 165 feet long by 20 feet wide, and truss element structures were each 20 feet by 20 feet. The maximum height of the bridge structure above the riverbed was 40 feet.

3.3 INDUSTRIAL AREA. Figure 22 shows the complex of buildings and other structures which comprised the Industrial Area. The aim point was near the upper right hand corner of the five-sided building, as shown by the dot. The largest centrally located buildings in this target area were 25 feet tall and about 100 feet wide. Separation between these buildings ranged from 5 feet to 25 feet. Nominal contrast between the tallest building and its background reached a value of 60 percent.

3.4 POL STORAGE FACILITY. The aim point for this target area, shown in Figure 23, was near the bottom of the right spherical tank. Contrasts between the upper surfaces of the tanks and their respective backgrounds ranged from 65 to 75 percent.

The scaled sizes of the cylindrical tanks were 25 feet high and 60 feet in diameter. The longitudinal separation of these tanks was 40 feet. The spherical tanks were 45 feet in diameter and 50 feet tall.

3.5 MOUNTAIN STORAGE FACILITY. This target, along with the Industrial Area, offered the fewest clues to dimensionality of the five selected targets.* Contrasts ranged from 20 percent for the roof of the larger building relative to its background to 75 percent for the top of the oil tank relative to its background.

Aim point for this target area was slightly to the right of the oil storage tank, as shown in Figure 24. The simulated size of the oil tank was 25 feet high and 40 feet in diameter. The larger building measured 35 feet in height and 45 feet in length. The total complex was small and uncomplicated in nature and also had relatively large separations between the structures.

3.6 TEST AREA. This area, which included unaltered models of a bridge and tall central city type structures, contained the greatest amount of verticality and was used for 2-D and 3-D trial runs for this reason. The aim point was at the lower right hand corner of the large building facing the water, as shown in Figure 25. Contrast measurements for this area were high for those certain elements offering prominent cues to dimensionality. For example, the bridge tower and roadway background had a contrast of 90 percent. Contrasts between the streets and building sides was in the neighborhood of 60 percent.

* The smaller heights of target elements within the FOV during the critical terminal flight phase is considered the principal reason for fewer dimensionality clues in these two target areas.



Figure 22. Industrial Complex Target Area



Figure 23. POL Storage Facility Target Area

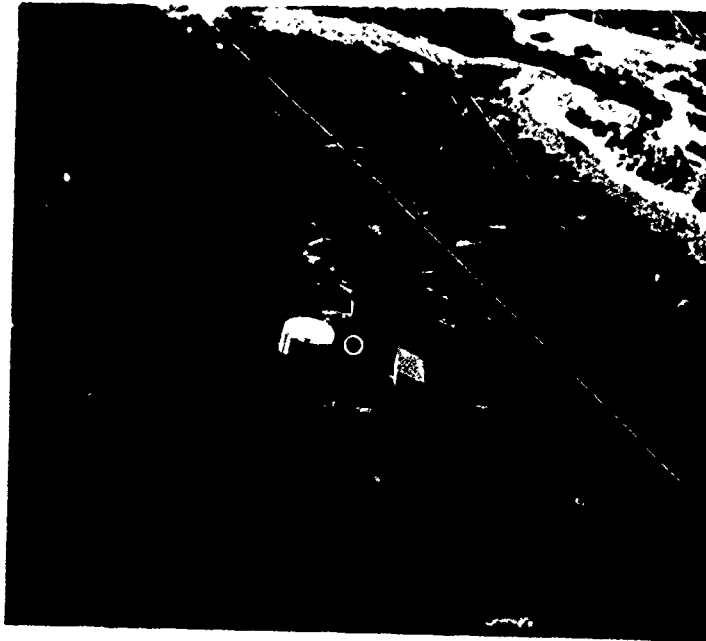


Figure 24. Mountain Storage Facility Target Area

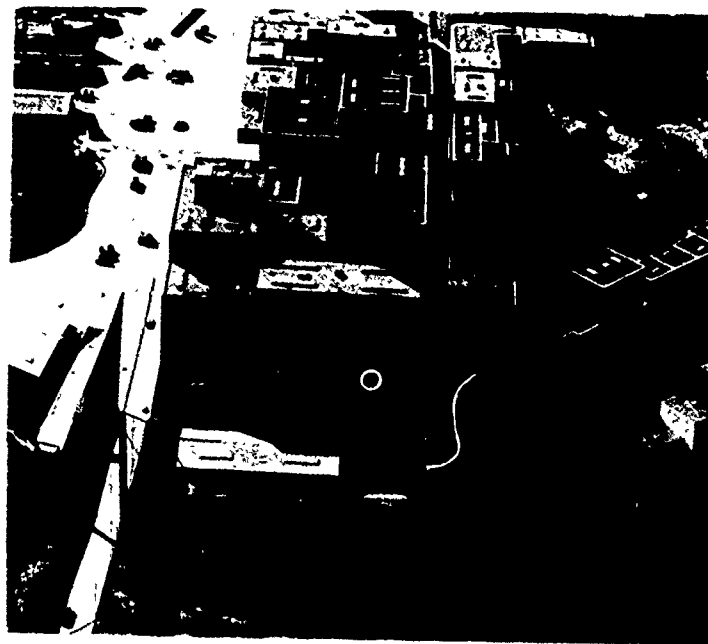


Figure 25. Test Target Area

NAVTRAEQUIPCEN 70-C-0238-1

The bridge towers, which provided the most obvious movement parallax cue, had heights of 80 feet relative to the roadway, and the distance between the two towers was 245 feet. The large building facing the water was 90 feet tall and 52 feet in depth. Some relative movement could be perceived between the upper right side of this building and the adjacent street background.

4. CONSTANT ALTITUDE AREAS

A total of eight target runs, including the practice run, were used in the Constant Altitude tests (see Figure 6). The imagery for each of the Constant Altitude approaches covered a long, narrow strip of terrain in which the target of interest appeared. Four of the runs used for data collection included targets which were also used in the Dive Approach tests. Brief descriptions are given below for each Constant Altitude run. Where the run includes a previously described Dive Approach target area, it is identified by this target area name.

4.1 AIRPORT - RUN NO. 1. This flight path passed directly over the airport. The flight duration was 14 and 7 seconds for the 200 ft/s and 400 ft/s velocities, respectively. Objects that offered the more prominent dimensionality clues were the top of the lower roof of the operations shack relative to the ground. The height of the building was 40 feet.

4.2 HARBOR - RUN NO. 2. This area was a continuation of the airport flight path consisting of the area directly south of the airport, as shown in Figure 6. The area was characterized by few manmade structures. There was a cluster of small buildings north of the harbor, but these were not significant in terms of dimensional cues. A highway bridge in this area appeared to be one of the prominent clues as did the bow of the tanker situated at the left of the harbor. The simulated height of the bow was 20 feet above the water line. The height of the bridge was a simulated 16 feet above the railroad track. The length of this run was also 14 seconds for the 200 and 7 seconds for the 400 ft/s velocities, respectively.

4.3 GENERAL TERRAIN - RUN NO. 3. This flight path was selected because it was relatively devoid of manmade structures and consisted of flat undistinguished terrain with a minimum of elevation gradients. The most prominent feature was a stand of trees located on the north (near) side of the shore of the reservoir. The maximum height of the trees above the surface of the reservoir was approximately 35 feet. Duration of flight over the general terrain area was 20 seconds at the 200 ft/s velocity.

4.4 TRUSS BRIDGE - RUN NO. 4. The truss bridge was the most prominent feature along this total flight path. The maximum height of this structure was a simulated 40 feet from the top bridge railing to the surface of the river. Duration of flight over this path was 11 seconds at the 200 ft/s rate.

NAVTRAEQUIPCEN 70-C-0238-1

4.5 MOUNTAIN TOP - RUN NO. 5. This area was selected because it contained a high elevation with a steep gradient. The maximum height of the mountain top above the plateau was more than 330 feet. There were no prominent man-made structures in this imagery, which was 15 seconds in duration at 200 ft/s velocity.

4.6 POL STORAGE FACILITY - RUN NO. 6. This flight path was a continuation of the flight path used in the Mountain Top target run directly to the north. It began past the river as shown in Figure 6, and the POL target complex offered the primary dimensionality clues. The top rear edge of the nearer cylindrical tank (which was 25 feet high and spaced 40 feet from the rear tank) could be observed to shift with respect to the forward vertical side of the rear tank providing the most prominent motion parallax cue. The duration of this run was 11 seconds at 200 ft/s velocity.

4.7 MOUNTAIN STORAGE FACILITY - RUN NO. 7. This flight included the same three structures described in the Dive Approach paragraph 3.5 (Figure 24). The most prominent cue in this area was the shift in position of the peak of the rearmost shed with respect to the terrain directly behind it. This shed was approximately 30 feet in height. Duration of this run was 12 seconds at the 200 ft/s velocity.

4.8 PRACTICE AREA - RUN NO. 8. This run included the same practice area that was used in the Dive Approach test. Other manmade structures were exposed to the subject during the flight, including a freeway interchange system, but subjective comments revealed that these additional cues were not utilized. Total duration of flight was 16 seconds at the 200 ft/s velocity. The bridge towers again provided the most obvious movement parallax cue. The top of the bridge towers were 80 feet above the roadway and the distance between towers was 245 feet. Significant movements could be observed between buildings as they appeared to cover or uncover each other. The large building facing the water was 90 feet tall and 52 feet long. The building directly behind it was 122 feet tall and 115 feet long.

APPENDIX E

APPROACH GEOMETRIES

This appendix describes the approach geometries used in both the Dive Approach and Constant Altitude Approach runs. Technical factors which influenced the selection of these conditions are also discussed.

1. DIVE APPROACH RUNS

Since this study was intended to yield applied data for use in the design of training equipment, representative real world conditions in terms of ground imagery, sensor viewing geometry, and flight dynamics were employed. The Dive Approach series of tests were therefore designed to produce target imagery characteristic of data transmitted from a TV guided missile during the terminal phase of its flight. The TV FOV was 4.5 by 6 degrees, which is typical of air-to-surface missiles. Two simulated approach velocities were used - 1,100 and 650 feet/second - in order to evaluate the effects of terminal velocity on the perception of source dimensionality. The critical factor involved is the rate of displayed image growth and thus the time available to the observer to detect and respond to the presence or absence of the movement parallax cue.

Preliminary analysis showed that slant range at the termination of the Dive Approach runs should not exceed 1,500 feet. This requirement was achieved by redefining the terrain model's basic scale factor and modifying certain critical target areas. This resulted in a minimum camera-to-terrain surface distance of 6 feet.

1.1 DIVE APPROACH GEOMETRY. A profile of the 3-D and 2-D dive approach geometries is shown in Figure 26. The more important characteristics are discussed in the following subsections.

1.1.1 Determination of 3-D Dive Approach Characteristics. The above section described rationales for the initial conditions shown in Figure 26, including the TV camera fixed FOV, α_{FV} and α_{FH} (4.5 by 6 degrees), the minimum slant range, R_{min} , and approach velocities V_1 and V_2 (1,100 and 600 feet/second). Determination of dive angle, θ , involved several factors. First, a relatively low dive angle was necessary to provide realistic approach imagery. Second, limitations imposed by the depth of field had to be considered; that is, the lower the dive angle, the greater the depth of field required to maintain acceptable optical focus. Third, the dive angle had to provide an approach which would maintain sufficient vertical clearance between the bottom of the GDC gimbal assembly (housing the TV camera and zoom lens) and the highest GDC terrain model features.

On the basis of the above considerations, an angle of 30 degrees was selected. Figure 27 shows a plot of lateral and longitudinal distance (i.e., viewed object plane dimensions) as a function of slant range for the selected fixed FOV. Dive angle is used as a parameter in this figure. Lateral values remain constant (independent of dive angle) for a fixed slant

NAVTRAEQUIPCEN 70-C-0238-1

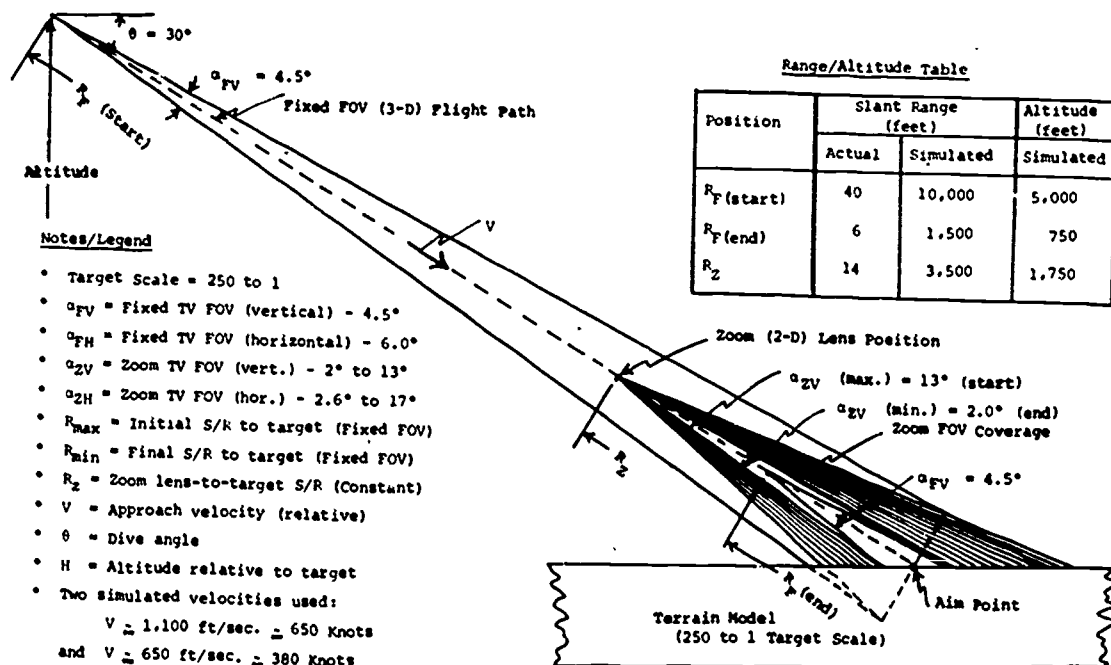


Figure 26. Profile of Basic 2-D 3-D Dive Approach Geometry

range; however, longitudinal distance, and therefore depth-of-field*, increases substantially (and at an increasing rate) as the dive angle is reduced. With θ equal to 30 degrees, the total longitudinal distance is approximately 1 foot at the minimum slant range, R_{min} of 6 feet. Measurements showed that the TV camera/zoom lens (with the 2X extender) provided acceptable near and far-field focus under these conditions with lens f/stop settings compatible with the reflected brightness levels of the terrain model under natural illumination.

With a 30 degree dive angle, the camera lens height, H , equals one-half the corresponding slant range, R (i.e., $H = R \sin 30^\circ$). Since R_{min} equals 6 feet, H_{min} equals 3 feet, or a 750 foot simulated altitude. This distance was large enough to assure proper clearance.

Maximum range, R_{max} , was determined by the maximum operating height of the vertical movement I-beam on which the TV sensor was mounted. With H_{max} equal to 20 feet, maximum slant range R_{max} was 40 feet which represents a simulated 10,000 feet.

* Depth of field, F_D , (required) approximately equals the product of longitudinal distance, D , from the center to edge of the FOV and the cosine of dive angle, or: $F_D \approx D \cos \theta$.

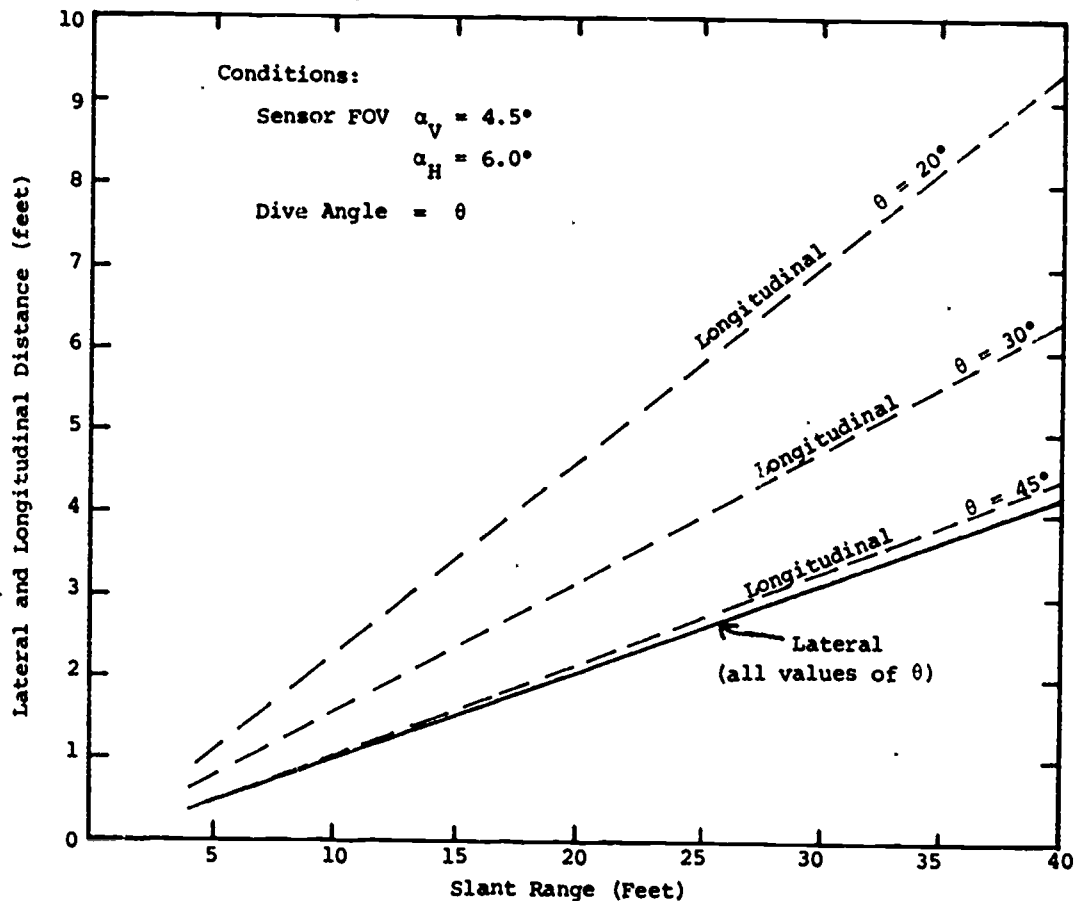


Figure 27. Lateral and Longitudinal Distances Viewed by Sensor with Fixed FOV

1.1.2 3-D Dive Approach Implementation. The sensor movement system consisting of the three-axis flight table, transverse carriage assembly, and vertical movement I-beam is designed to provide, in conjunction with the longitudinally driven terrain model, movement with 6 degrees of freedom under analog computer control. The terrain model can be operated either in a horizontal position or tilted at 25 degrees. For this series of tests, the model was used in the horizontal position to obtain natural shadow conditions in direct sunlight.

Closure on a selected target along a constant dive approach was accomplished by simultaneous movement of the I-beam and the terrain model under computer control. With the camera at depression angle, θ (30 degrees) and with approach velocity, V_R , the vertical velocity component, V_V , of the I-beam equals $V_R \sin 30^\circ = 0.5 V_R$. The corresponding horizontal velocity component, V_H , provided by terrain model movement, equals $V_R \cos 30^\circ = 0.866 V_R$. Thus, for a simulated approach velocity of 1,100 feet per second (or $1,100/250 = 4.4$ feet per second actual), corresponding vertical and horizontal drive rates are

$$V_V = \frac{4.4}{2} = 2.2 \text{ feet per second}$$

$$V_H = 0.866 V_R = 3.8 \text{ feet per second.}$$

The above values are the maximum rates used in this series of tests.

1.1.3 Determination of 2-D Dive Approach Geometries. This section discusses the derivation of the techniques used to produce the 2-D runs equivalent to their 3-D counterparts. Referring again to Figure 26, which shows profiles of both 2-D and 3-D geometries, the operating conditions which must be defined for the 2-D series of tests are: (1) zoom lens-to-target slant range, R_Z (a constant value for the 2-D Dive Approach runs), and (2) minimum and maximum values for both the vertical and horizontal FOV's (α_{ZV} and α_{ZH}) throughout the zoom range of the lens. In addition, it was necessary to determine the rate at which the zoom FOV had to be varied to simulate a constant velocity approach.

The key relationship between the 3-D and 2-D geometries is shown in plan view in Figure 28. In the 3-D case, as the TV camera with a fixed FOV approaches the target plane at constant velocity, the lateral dimension in the target plane decreases linearly with range. In other words, distance (A to A') - (B to B') = (B to B') - (C to C') = (C to C') - (D to D'), etc. Also, lateral values vary inversely with run time, as shown in this illustration. Run time is normalized here for clarity. To simulate

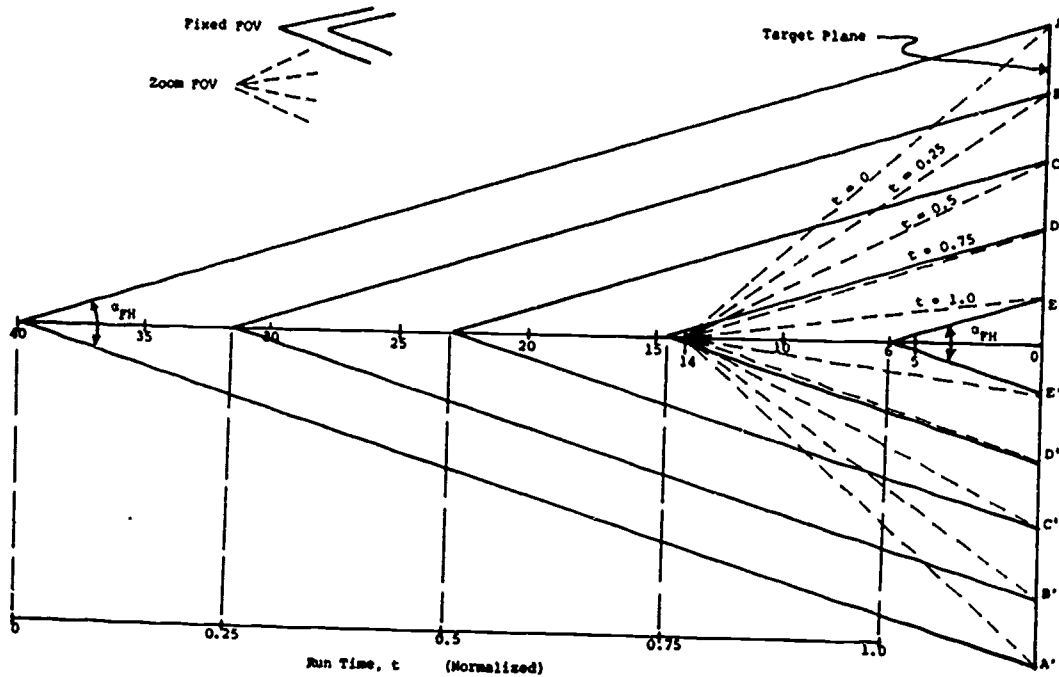
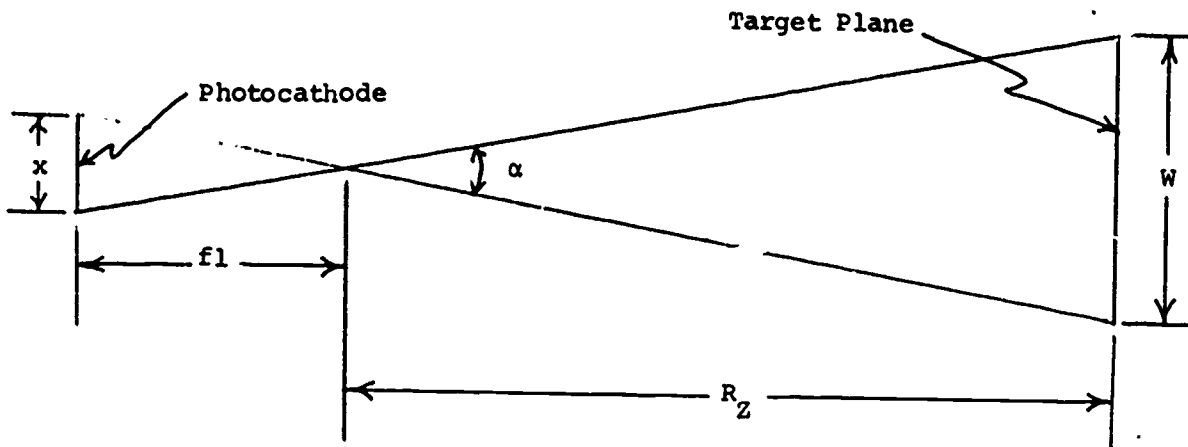


Figure 28. 2-D and 3-D Run Geometry Relationships

the same apparent closure rates (image expansion rates) in the 2-D runs, the TV camera zoom FOV must be adjusted as a function of run time, starting with the widest FOV at time t_0 to match the corresponding lateral dimension seen in the 3-D convergence runs.

A simple relationship exists between focal length, slant range, lateral coverage, and vidicon sensor photocathode width, as shown in the sketch below.



Here,

x = Vidicon photocathode active width = 0.5 inch

fl = Lens focal length

R_z = Lens-to-target plane slant range

W = Total viewed lateral distance in target plane

It may be seen that:

$$\frac{x}{fl} = \frac{W}{R_z}$$

$$R_z \text{ (inches)} = 2 fl \text{ (inches)} \cdot W \text{ (inches)}$$

$$\text{and } W \text{ (inches)} = \frac{R_z \text{ (inches)}}{2 fl \text{ (inches)}}$$

To simulate a 2-D image source, the zoom lens was placed approximately midway between the maximum and minimum slant range values used in the 3-D runs. This provided a fixed perspective which represented an average of

the changing perspectives obtained in the 3-D runs.* The maximum zoom lens focal length, fl_Z (maximum), corresponding to the minimum zoom horizontal field of view, α_{ZH} , determined the location of the TV camera in slant range. This condition occurs at the end of the run (at normalized time, $t=1.0$) where the camera with a fixed FOV, α_{FH} , as used in the 3-D run covers the lateral distance (E to E') as shown in Figure 28. This final lateral distance is designated as W_f . For a one inch vidicon camera, the angle α_{FH} can be converted into its equivalent focal length, fl_F , by the expression:

$$fl_F \text{ (inches)} = \frac{0.25}{\tan\left(\frac{\alpha_{FH}}{2}\right)}$$

$$\text{and } fl_F \text{ (mm)} = \frac{6.35}{\tan\left(\frac{\alpha_{FH}}{2}\right)}$$

Since $\alpha_F = 6$ degrees

$$fl_F \text{ (mm)} = \frac{6.35}{\tan 3^\circ} = \frac{6.35}{.0524} = 120 \text{ mm}$$

Then, based on the previously defined relationship,

$$W_f = \frac{R \text{ min (inches)}}{2 fl_F}$$

As indicated above, at the end point in the run, the lateral distance W_Z (min) viewed by the minimum zoom FOV should match the final FOV lateral distance, W_f .

Therefore:

$$W_Z \text{ (min)} = \frac{R_Z}{2 fl_Z \text{ (max)}}$$

$$\text{and } W_f = \frac{R \text{ (min)}}{2 fl_F}$$

Since $W_Z \text{ (min)} = W_f$ at this point,

* As discussed in Appendix B, paragraph 2.2, pilot tests showed that the differences in perspective between the 2-D and 3-D viewing modes were below threshold for all subjects.

$$\frac{R_Z}{2 \text{ fl}_Z (\text{max})} = \frac{R (\text{min})}{2 \text{ fl}_F}$$

and $R_Z = \frac{\text{fl}_Z (\text{max}) \cdot R (\text{min})}{\text{fl}_F}$

Using a 2X zoom lens extender, the maximum useful zoom focal length was 280 mm.

With: $\text{fl}_{Z(\text{max})} = 280 \text{ mm}$

$\text{fl}_F = 120 \text{ mm}$

$R_{\text{min}} = 6 \text{ feet}$

then $R_Z = \frac{280 \times 6}{120} = 14 \text{ feet}$

This calculation therefore determined the fixed position of the zoom lens for the 2-D runs.

As previously noted, the criterion for controlling the zoom lens FOV was to maintain lateral coverage equal to the 3-D viewed dimensions at corresponding times in the runs. Figure 28 depicts this time relationship for the two operating modes. The actual zoom focal length, fl_Z , values corresponding to physical 3-D range, were computed from the previous expression, rearranged to make fl_Z the dependent variable. Thus,

$$\text{fl}_Z = \text{fl}_F \times \frac{R_Z}{R} = \frac{14 \text{ fl}_F}{R (\text{feet})}$$

$$\text{fl}_Z (\text{mm}) = \frac{14 \times 120}{R (\text{feet})} = \frac{1,680}{R (\text{feet})}$$

Table 5 lists required values of fl_Z and FOV's for several values of physical range, R. These ranges are based on the established, fixed values of 3-D field of view and 2-D zoom lens-to-target range.

A plot of the above zoom focal length values is shown in Figure 29, with 3-D slant range and run time (normalized) shown on the abscissa. Function generators in the GDC analog computer were set up on the basis of the fl versus time curve. Focal length values were converted to corresponding zoom lens drive voltage levels.

1.1.4 2-D Simulated Approach Implementation. As noted above, the zoom lens was operated under analog computer control to produce the desired target convergence rates. Both the 1,100 and 600 foot per second 3-D approach velocities were simulated in the 2-D runs by varying the time base.

NAVTRAEQUIPCEN 70-C-0238-1

TABLE 5. ZOOM FOCAL LENGTHS AND FOV CORRESPONDING TO 3-D RANGES

3-D Range (Feet)	Zoom Focal Length f_{LZ} (mm)	Zoom FOVs (Degrees)	
		Horizontal α_{ZH}	Vertical α_{ZV}
40.0	42	17.2	12.9
31.5	53	13.7	10.3
23.0	73	9.9	7.4
14.5	116	6.3	4.7
6.0	280	2.6	1.95

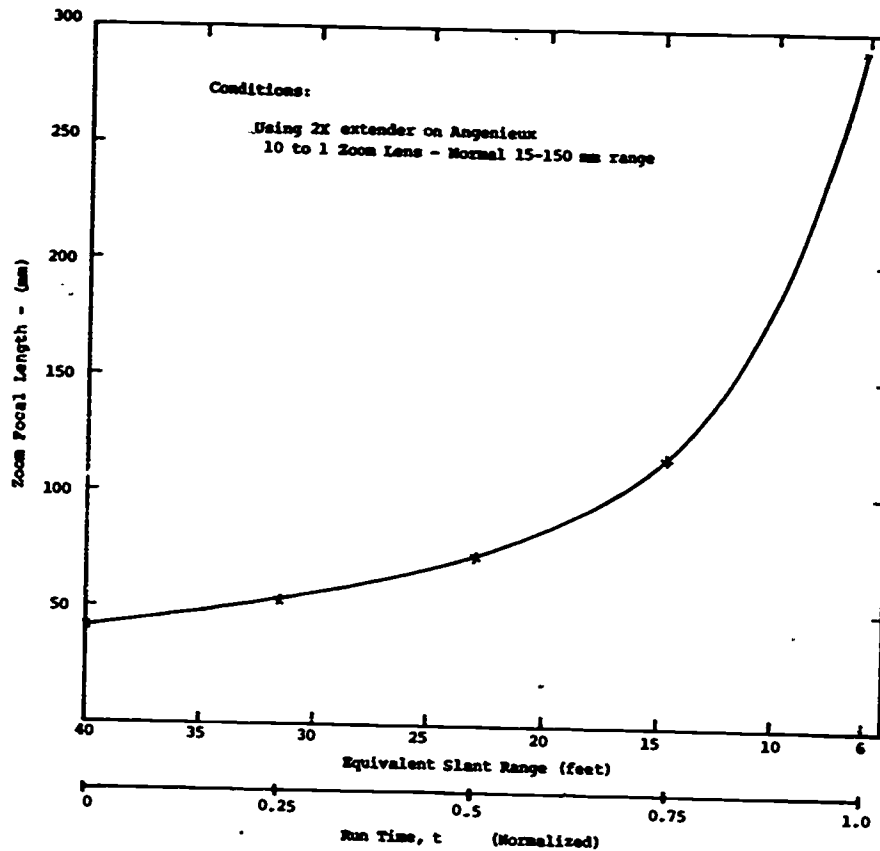


Figure 29. Zoom Focal Length Required as a Function of Slant Range and Normalized Time

Since a fixed range was used, there was no requirement to adjust the vertical movement I-beam. Initial alignment of the camera LOS on the target aim points used in the 3-D runs was accomplished by accurate, manual control of the transverse carriage assembly and the terrain model. Also, the focus of the TV camera lens was set manually and remained fixed throughout each 2-D run.

2. CONSTANT ALTITUDE APPROACH RUNS

The conditions employed in this series of tests were dictated in part by a desire to maintain certain commonalities between the Dive Approach and Constant Altitude Approach tests, and in part by equipment characteristics. These considerations are discussed in the following sections.

2.1 CONSTANT ALTITUDE APPROACH GEOMETRY. A profile view of the approach geometry employed is shown in Figure 30. Comparison of Figures 26 and 30 shows that both series of tests utilize the same sensor depression angle and the same maximum and minimum slant range/altitude values. Also, as discussed in Appendix D, four target areas on the GDC terrain were common to both tests.

In addition to the difference in target approach paths - dive versus constant altitude - there was a second difference between these stimulus generation modes. In the dive case, equivalent 2-D runs were in fact made, whereas in the constant altitude case, all runs were actually 3-D; that is, there was movement of the TV camera LOS relative to the targets and their backgrounds. Based on the experience gained in the Dive Approach series,

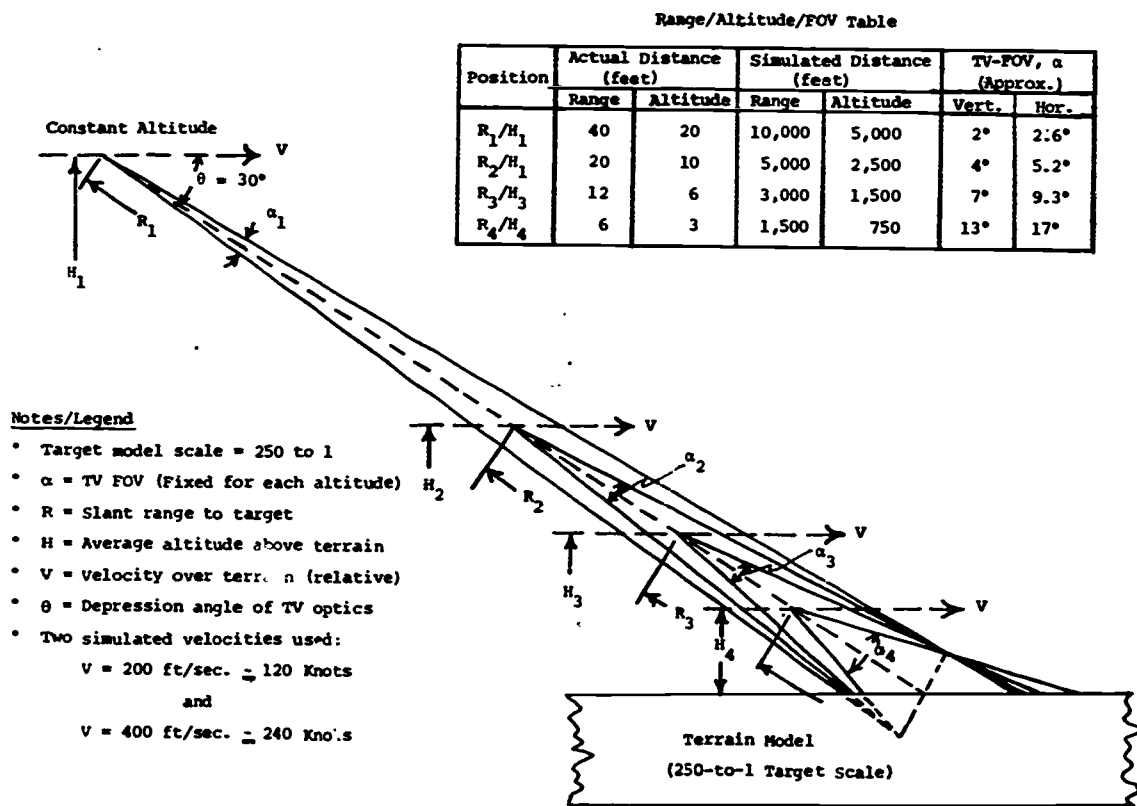
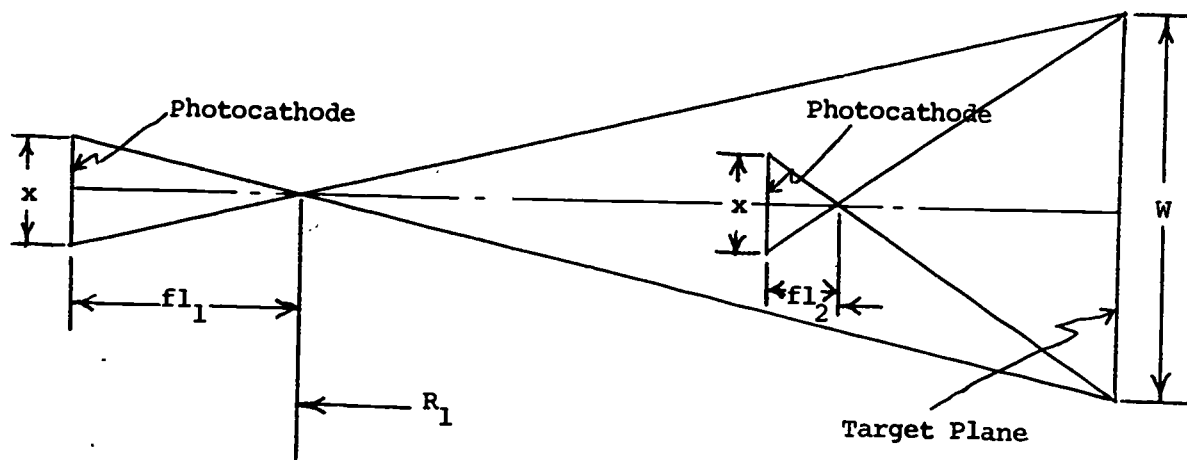


Figure 30. Profile of the Constant Altitude Approach Geometry

however, it was known that at the greater range/altitude combinations (40 feet/20 feet, or 10,000/5,000 feet simulated), the degree of motion parallax and perspective change was generally below threshold. Therefore, 2-D conditions were effectively achieved by use of these extended distances.

To provide dynamic imagery as similar to the 3-D runs as possible at the various range/altitude values the width of the viewed terrain area was held constant for each run. This was accomplished by adjusting the sensor focal length to produce the required FOV for each condition. The sketch and calculations below show the basic geometry and the relationship between slant range and focal length used to calculate the necessary compensation in FOV.



In the above sketch:

x = Vidicon photocathode active width = 0.5 inch

fl_1 = Lens focal length (initial)

fl_2 = Lens focal length (final)

R_1 = Slant range (initial)

R_2 = Slant range (final)

W = Viewed terrain width (constant value)

Here,

$$\frac{x}{fl_1} = \frac{W}{R_1}$$

and

$$\frac{x}{fl_2} = \frac{W}{R_2}$$

Therefore

$$\frac{x \cdot R_1}{fl_1} = \frac{x \cdot R_2}{fl_2}$$

$$fl_2 = fl_1 \times \frac{R_2}{R_1}$$

The next decision involved selection of the desired values of fl_1 and fl_2 , corresponding to minimum and maximum FOV's, respectively (the ratio fl_1/fl_2 was already established at 6.7 to 1 since R_1/R_2 was known). Pilot tests were run in the GDC to obtain a preliminary assessment of different FOV ratios. It was determined that at the lowest range/altitude, the TV sensor vertical FOV should be limited to about 10 to 15 degrees to minimize the difference in near and far field target image magnifications. At larger FOV's it became increasingly evident that the run was made at a low altitude because of this magnification difference. Since the greater range/altitude runs were performed using smaller FOV's (to maintain equal viewed terrain widths) the near and far field magnifications were essentially equal. The maximum vertical FOV, α_v , selected on the above basis was approximately 13 degrees. This established the minimum sensor focal length of 42 mm. Based on the relationship stated above, the focal length corresponding to the maximum range/altitude values of 40/20 feet (10,000/5,000 feet simulated) was computed as follows:

$$fl_{(max)} = fl_{(min)} \times \frac{R_{(max)}}{R_{(min)}}$$

$$fl_{(max)} = 42 \times \frac{40}{6} = 280 \text{ mm}$$

Two intermediate range/altitude values were also necessary to achieve reasonably small incremental changes. Values of 12/6 feet and 20/10 feet were selected on the basis of pilot tests. The table included in Figure 30 shows the required focal lengths and FOV's corresponding to the four range/altitude conditions.

Approach velocity was also investigated in a pilot study. Two values were finally chosen, viz., 0.8 feet/second and 1.6 feet/second (200 and 400 feet/second simulated). The higher velocity represents the maximum value which did not result in objectionable image smearing.

APPENDIX F

STIMULUS TAPE GENERATION

1. INTRODUCTION

This appendix describes the procedures used to acquire the basic imagery and produce the video tapes used in the behavioral analyses.

The experimental designs and behavioral test procedures for both the Dive Approach and the Constant Altitude Approach tests were discussed in the main body of this report. Appendices B, C, D, and E describe the geometrical relationships, test facilities, target area characteristics, test procedures, and typical pilot runs leading to acquisition of the basic 3-D and 2-D imagery.

Video tape recording (VTR) permitted portions of the basic imagery to be arranged into irregularly ordered sequences for the behavioral analyses. In addition, the necessary range-to-go data and run identifications (voice inputs) could be dubbed onto the audio channel(s) of the video tapes.

2. DATA GENERATION AND RECORDING

For initial TV system setup, a half-black/half-white card was placed flat on the terrain model, and using the viewing geometry to be employed in the actual data runs, the TV camera lens iris* was adjusted to produce a nominal peak-to-peak level of 1.5 volts video into the gamma corrector. This established the desired operating range of the gamma corrector unit, which then added horizontal and vertical sync to produce approximately 1.0 volt video plus 0.5 volt sync at its output (input to the SONY 2 inch VTR). The TV camera then was accurately aligned on the selected target area and the camera iris was adjusted (along with minor adjustment of camera control video gain) to produce the desired video level from the gamma corrector. The VTR recording level then was adjusted, while observing the video recording level meter, to the optimum recording level. The selected run was recorded on the 2 inch SONY VTR.

Electronic editing was used to produce a semi-random order of target runs on the Final Stimulus Tapes. The procedure was to prepare a random listing of runs (see Tables 6 and 7) which included the various combinations of target area, dimensionality, shadow condition, approach velocity, and in the Constant Altitude case, the slant range/altitude/FOV condition. Composite video from the 2 inch machine was fed to a second VTR - a 1 inch type SONY - which incorporated the electronic editing capability. This permitted these basic runs to be duplicated on the 1 inch tape in the desired sequence while maintaining vertical synchronization (to prevent picture

* The Angenieux zoom lens (with 2X extender) was typically set between f/16 and f/5.6, depending on natural illumination conditions.

NAVTRAEQUIPCEN 70-C-0238-1

roll-over when switching from one run to another in the duplicating process). Using this procedure, Master Stimulus Tapes were prepared (including dubbed audio data) for both of the behavioral tests.

Final Stimulus Tapes used in the behavioral tests were then prepared from these master tapes. This was done by direct duplication of the 1 inch tape data on 2 inch tapes.

3. FIDELITY OF FINAL STIMULUS IMAGERY

There was some initial concern regarding the image fidelity which could be expected from third generation video tapes. Preliminary tests indicated that acceptable image quality should be achievable since reasonably high levels of performance were obtained with both the 1 and 2 inch SONY recorders. To verify this, however, image quality was assessed at several stages in the recording/duplicating process by use of a resolution/grey scale signal obtained from the TV camera viewing a RETMA type test chart. The results of this evaluation are summarized in Table 8.

TABLE 6. DIVE APPROACH STIMULUS PRESENTATION SEQUENCE

<u>Trial No.</u>	<u>Target Area</u>	<u>Dimensionality</u>	<u>Condition*</u>	<u>Simulated Velocity (ft/s)</u>
(Practice Trials)				
1	Power Plant	3-D	S	650
2	Power Plant	3-D	S	650
3	Power Plant	3-D	S	1,100
4	Power Plant	2-D	S	650
5	Power Plant	2-D	S	650
6	Power Plant	2-D	S	1,100
(Test Runs)				
1	Ind. Area	2-D	S	650
2	POL	3-D	NS	650
3	Airport	2-D	S	1,100
4	Bridge	2-D	S	650
5	Bridge	3-D	S	1,100
6	Airport	3-D	S	650
7	POL	2-D	S	1,100
8	Ind. Area	2-D	S	1,100
9	Mtn. Storage	3-D	S	650
10	POL	3-D	S	1,100
11	Airport	3-D	NS	650
12	POL	2-D	S	650
13	Bridge	2-D	S	1,100

NAVTRAEQUIPCEN 70-C-0238-1

TABLE 6. DIVE APPROACH STIMULUS PRESENTATION SEQUENCE (CONT)

<u>Trial No.</u>	<u>Target Area</u>	<u>Dimensionality</u>	<u>Condition*</u>	<u>Simulated Velocity (ft/s)</u>
14	POL	2-D	NS	650
15	Ind. Area	3-D	S	1,100
16	Airport	2-D	S	650
17	Bridge	3-D	S	650
18	Mtn. Storage	2-D	S	650
19	Ind. Area	3-D	S	650
20	Airport	2-D	NS	650
21	POL	3-D	S	650
22	Airport	3-D	S	1,100
23	Bridge	3-D	S	650
24	POL	2-D	NS	650
25	Mtn. Storage	3-D	S	650
26	Airport	3-D	S	650
27	Airport	2-D	S	650
28	Bridge	3-D	S	1,100
29	Ind. Area	3-D	S	650
30	POL	3-D	S	650
31	Mtn. Storage	2-D	S	650
32	POL	2-D	S	1,100
33	Bridge	2-D	S	650
34	Airport	3-D	S	1,100
35	POL	3-D	S	1,100
36	Ind. Area	2-D	S	1,100
37	POL	3-D	NS	650
38	Ind. Area	2-D	S	650
39	Airport	2-D	S	1,100
40	Bridge	2-D	S	1,100
41	Airport	3-D	NS	650
42	POL	2-D	S	650
43	Ind. Area	3-D	S	1,100
44	Airport	2-D	NS	650

*S - Shadowed

NS - Non-shadowed

NAVTRAEQUIPCEN 70-C-0238-1

TABLE 7. CONSTANT ALTITUDE STIMULUS PRESENTATION SEQUENCE

<u>Trial No.</u>	<u>Area</u>	<u>FOV/SR (deg-ft)</u>	<u>Simulated Velocity (ft/s)</u>
(Practice Trials)			
1	8	13/6	200
2	8	2/40	200
(Test Runs)			
1	1	13/6	400
2	2	4/20	200
3	3	2/40	200
4	4	13/12	200
5	5	7/12	200
6	6	13/6	200
7	7	7/12	200
8	5	2/40	200
9	3	7/12	200
10	2	13/6	400
11	1	13/12	200
12	4	4/20	200
13	3	4/20	200
14	5	13/6	200
15	7	4/20	200
16	6	13/12	200
17	7	13/12	200
18	4	7/12	200
19	1	7/12	200
20	2	2/40	200
21	3	13/12	200
22	1	2/40	200
23	4	13/6	200
24	1	13/6	200
25	5	13/12	200
26	7	13/6	200
27	2	13/6	200
28	5	4/20	200
29	6	2/40	200
30	4	2/40	200
31	6	4/20	200
32	3	13/6	200
33	2	7/12	200
34	1	4/20	200
35	2	13/12	200
36	6	7/12	200
37	7	2/40	200

NAVTRAEQUIPCEN 70-C-0238-1

TABLE 8. COMPARISON OF VTR STIMULUS MATERIAL FIDELITIES

Displayed Image Characteristic	Signal Source			
	Basic TV Camera Signal	Basic Data Tape (2 in. VTR)	Master Subjective Tape (1 in. VTR)	Final Stimulus Tape (2 in. VTR)
Limiting Horizontal Resolution (TV lines)	600	300 to 350	275 to 300	275
Limiting Vertical Resolution (TV lines)	350 to 400	350 to 400	350 to 400	350 to 400
Grey scale steps	8 to 9	8	8	8
SNR (Estimated)	> 40 dB	40 dB	37 dB	34 dB

The image fidelity obtained using the final stimulus tape is representative of the signal quality obtained from an airborne TV system.

NAVTRAEQUIPCEN 70-C-0238-1

APPENDIX G

MOVEMENT PARALLAX AND TARGET PERSPECTIVE CALCULATIONS

1. INTRODUCTION

This appendix presents the basic geometries and calculations related to movement parallax and target perspective changes. Initial equations use sensor viewing geometry as a reference, in which the above target image effects are defined in terms of percent change relative to the sensor FOV. Later equations translate these changes into image angular displacements and angular rates referred to the display viewing geometry. Critical factors associated with these dynamic image effects are discussed as they become apparent from consideration of these geometrical relationships.

Methods used to derive the target measurements necessary to compute the above image movements are also described.

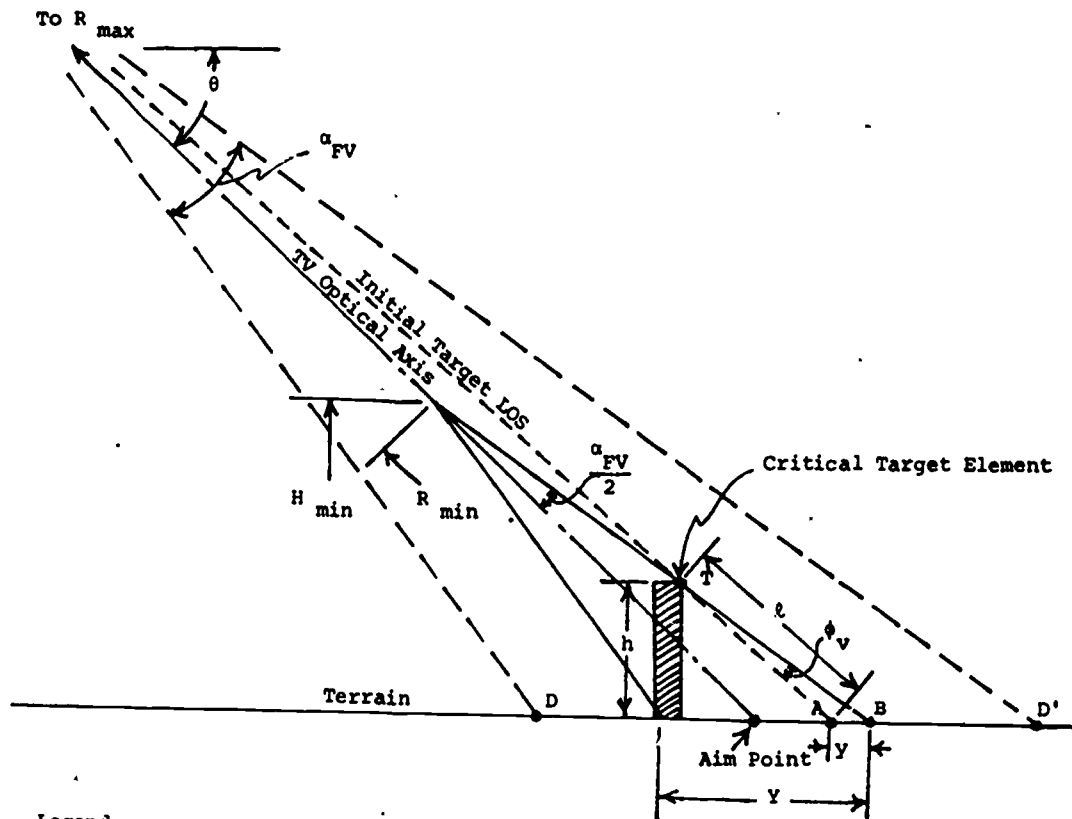
2. BASIC GEOMETRY AND RELATED EQUATIONS

Movement parallax and perspective change relationships relative to both sensor and to display viewing geometries are presented in this section.

2.1 MOVEMENT PARALLAX REFERENCED TO SENSOR GEOMETRY. Both Dive Approach and Constant Altitude Approach conditions are discussed below.

2.1.1 Dive Approach - Longitudinal Image Displacement. The basic sensor/target geometry is shown in Figure 31 in profile. The target is depicted as a simple, vertical object of height, h , above the terrain background. At the start of the run -- where slant range equals $R_{(max)}$ -- the sensor optical axis is aligned on the Aim Point and the sensor fixed vertical FOV, α_{FV} , covers a distance D to D' on the horizontal terrain surface. At this time, the initial LOS from the top of the target projected onto the terrain surface appears at point A. As the dive commences, this projected target LOS shifts with respect to the terrain surface at an increasing radial rate until at the termination of the run, this target LOS appears at point B. The total shift of the LOS relative to the terrain background is designated as distance, y . This represents the movement parallax effect for this particular geometry. Maximum parallax change will occur if the TV camera aim point is aligned such that the top edge of the target (identified as the critical target element, T)* appears at the top of the camera FOV at the end of the run.

* That portion of the target providing the largest movement parallax effect.



Legend

- θ = Dive angle $\approx 30^\circ$
- α_{FV} = Fixed TV FCV = 4.5° (vertical)
- R_{max} = Initial slant range to target = 40 ft.
- R_{min} = Final slant range to target = 6 ft.
- h = Target height above terrain background
- l = Projected slant distance, target to background, along initial LOS
- H_{min} = Final TV sensor altitude above the terrain
- ϕ_v = Total angular displacement of projected target LOS from start to finish of run
- y = Total longitudinal displacement of projected target LOS from start to finish of run
- Y = Longitudinal distance (total) viewed by sensor at R_{min} .

Figure 31. Dive Approach - Longitudinal Image Displacement Geometry (Full Image Displacement) - Profile View

Based on this geometry, the following relationships are established*:

$$\phi_V = \frac{\alpha_{FV}}{2}$$

$$\text{and } y = \frac{l \cdot \phi_V}{\sin\theta} \approx K \cdot l \cdot \phi_V \approx \frac{K \cdot l \cdot \alpha_{FV}}{2}$$

where

$$K = \frac{1}{\sin\theta}$$

Similarly, $Y \approx K \cdot R_{\min} \cdot \alpha_{FV}$

Let d_V = percent target vertical shift relative to sensor vertical FOV

$$d(\%) = \frac{Y}{Y} \cdot 100 = \frac{K \cdot l \cdot \alpha_{FV}}{2 K \cdot R_{\min} \cdot \alpha_{FV}} \cdot 100$$

$$d(\%) = \frac{l}{2 R_{\min}} \cdot 100 \quad (1)$$

Since $l \approx \frac{h}{\sin\theta}$ and $R_{\min} \approx \frac{H_{\min}}{\sin\theta}$

$$d(\%) \approx \frac{h}{2 \sin\theta} \cdot \frac{\sin\theta}{H_{\min}} \cdot 100 \approx \frac{h}{2 H_{\min}} \cdot 100 \quad (2)$$

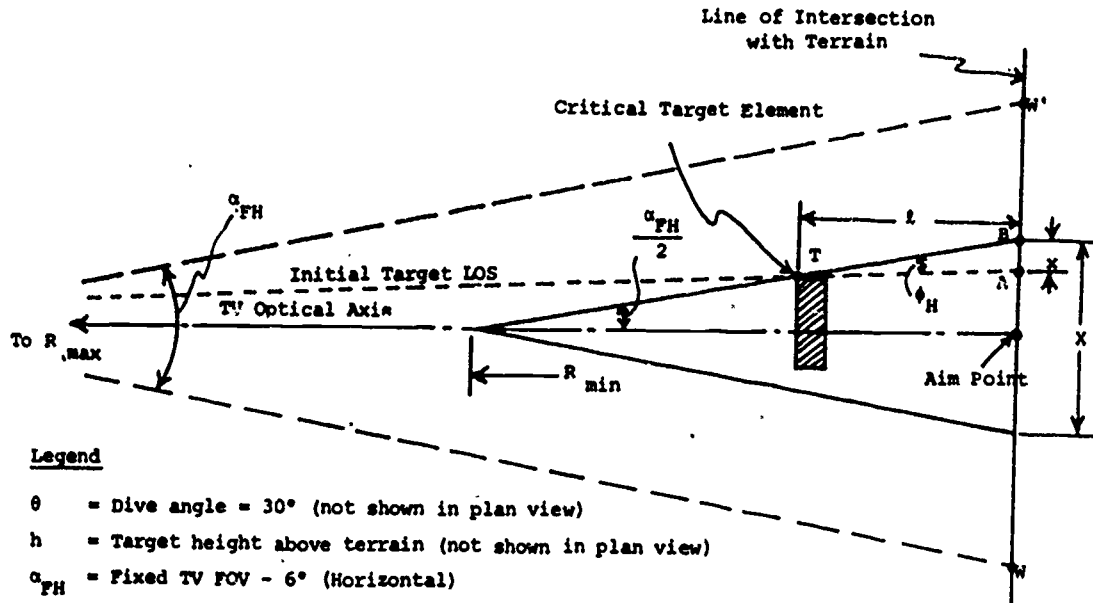
Equation (2) shows that movement parallax, expressed as a percent vertical image shift relative to the total sensor FOV, is directly proportional to the height of the target within the vertical FOV and inversely proportional to altitude, over a reasonable range of dive angles. As would be expected then, the maximum parallax effect will occur on the tallest targets at the lowest altitudes. Also, it can be seen that $d(\%)$ is essentially independent of the actual sensor FOV within certain limits (paragraph 2.4.2).

* One assumption is made to simplify the expressions; namely, that the initial target LOS is parallel to the TV optical axis. This assumption introduces a maximum error of approximately 15 percent in the computed value of displacement, y . However, the same assumption is applied to all dive approach target geometries; therefore, it acts as a small bias having a minimum effect on overall results.

NAVTRAEQUIPCEN 70-C-0238-1

If, as was the case in certain of the runs made in this program, the camera aim point is positioned such that the top of the target does not extend to the edge of the FOV at the end of the run, the expression for displacement, d , is modified. (See paragraph 2.3.2 and Figure 37 for a discussion of this effect.) In summary, the percent displacement varies in direct proportion to the relative location of the critical target element within the vertical FOV half-angle. That is, if the aim point coincides with the top of the target, no vertical image displacement relative to the background takes place during convergence. Therefore, major parallax effects should be (and were observed to be) at the edges of the camera FOV.

2.1.2 Dive Approach - Lateral Image Displacement. The basic sensor/target geometry is shown in Figure 32 in plan view. Only the top of the target is seen in this view and the critical element, T, is at its top corner. This figure represents a plane containing the camera optical axis (oriented along the dive line) which passes through point T and intersects the terrain background along line W-W'. The distance W to W' is the lateral dimension covered by the camera FOV at maximum range. The aim point, also along this line, is selected to produce the maximum movement parallax effect; that is, at the end of the run, point T will be at the edge of the camera FOV (in line with point B). At the start of the run, the projection of the target element onto the terrain background is designated as point A. Thus, the total shift of the target LOS relative to the background is the distance between points A and B, designated as x .



Legend

- θ = Dive angle = 30° (not shown in plan view)
- h = Target height above terrain (not shown in plan view)
- α_{FH} = Fixed TV FOV - 6° (Horizontal)
- R_{max} = Initial slant range to target = 40 feet
- R_{min} = Final slant range to target = 6 feet
- l = Projected slant distance, target-to-background, along LOS dive angle
- ϕ_H = Total angular displacement of projected target LOS from start to finish of run
- x = Total lateral displacement of projected target LOS from start to finish of run
- X = Lateral distance viewed by sensor at range R_{min}

Figure 32. Dive Approach - Lateral Image Displacement Geometry (Full Image Displacement) - Plan View

It should be noted that as in the previous longitudinal displacement case, target height, h , is a critical factor in producing relative image shifts. This is because the projected slant distance, ℓ , from the target to the background is a direct function of target height, and the value of ℓ , in turn, is a major factor in determining target horizontal image displacement. This will be evident from the derived relationship presented below:

$$\phi_H \cong \frac{\alpha_{FH}}{2} \quad (\text{Based on the same assumption discussed in paragraph 2.1.1})$$

$$\text{and } x = \ell \cdot \phi_H \cong \frac{\ell \cdot \alpha_{FH}}{2}$$

$$\text{Similarly, } X = R_{(\min)} \cdot \alpha_{FH}$$

Let d_H = Percent target horizontal shift relative to sensor horizontal FOV.

$$d(\%) = \frac{x}{X} \cdot 100 = \frac{\ell \cdot \alpha_{FH}}{2 R_{\min} \cdot \alpha_{FH}} \cdot 100$$

$$d(\%) = \frac{\ell}{2 R_{\min}} \cdot 100 \quad (3)$$

$$\text{Since } \ell \cong \frac{h}{\sin\theta} \quad \text{and } R_{\min} \cong \frac{H_{\min}^*}{\sin\theta}$$

$$d(\%) \cong \frac{h}{2 \sin\theta} \cdot \frac{\sin\theta}{H_{\min}} \cdot 100 \cong \frac{h}{2 H_{\min}} \cdot 100 \quad (4)$$

Comparison of Equation (2) for percent vertical displacement with Equation (4) for percent horizontal displacement reveals that they are the same. It should be noted, however, that the values of h in these two equations are not necessarily equal. In the single target case presented here, they would be; but in the case of a complex target, the critical target elements producing maximum vertical and horizontal image shifts may not be one and the same, in which case the corresponding values of h could differ.

Equation (4) shows that movement parallax, expressed as percent horizontal image shift relative to the total sensor FOV, is directly proportional to the height of the target within the horizontal FOV and is inversely proportional to altitude over a reasonable range of dive angles. Also, $d(\%)$ is independent of the actual sensor FOV (see paragraph 2.4.2).

* H_{\min} equals final TV sensor altitude, as in the previous example.

A condition may be experienced similar to that discussed in the previous section, where the camera aim point is positioned such that the side of the target (the critical point) does not extend to the edge of the FOV at the end of the run. The result would be similar to that portrayed for the vertical (longitudinal) case; that is, the percent displacement varies in direct proportion to the relative location of the critical target element within the horizontal FOV half-angle (being zero if the aim point is in line with the critical element).

2.1.3 Constant Altitude Approach - Flat Terrain. Figure 33 shows the sensor/target geometry in profile. A fixed sensor depression angle is used on these runs and sensor FOV is constant for a given altitude; therefore, the longitudinal distance viewed by the sensor is a constant value. However, due to horizontal movement of the sensor, the actual viewed terrain is constantly changing. This fixed longitudinal distance is designated as F in this figure.

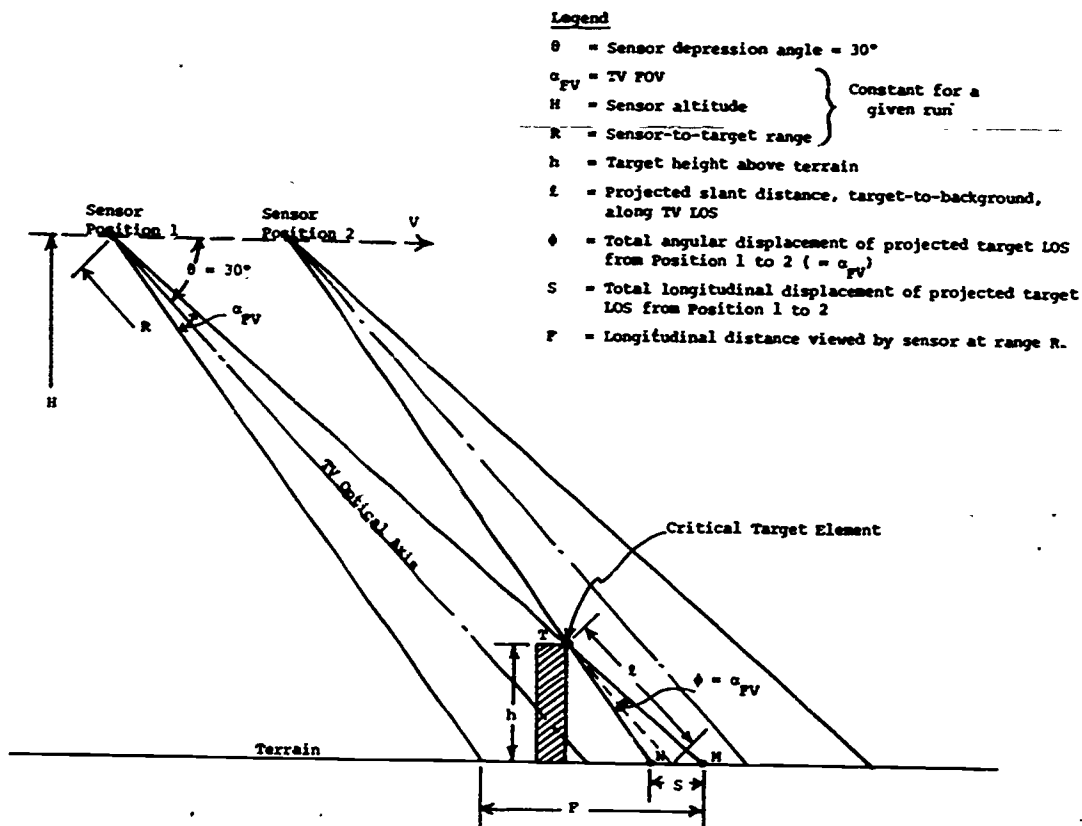


Figure 33. Constant Altitude Approach Geometry - Flat Terrain Case

As the upper edge of the FOV intersects the critical target element, T, at sensor Position 1, the corresponding target projection on the terrain is at point M. This projected target LOS shifts toward point N as the FOV traverses the target and background area, finally reaching point N (at Position 2) as the bottom edge of the FOV intersects target element, T. It can be seen from Figure 33 that the total angular shift, ϕ , of this projected target LOS relative to the background is equal to the sensor FOV angle, α_{FV} . The corresponding longitudinal displacement distance is designated as s.

The following relationships are obtained from this geometry:

$$s = \frac{l \cdot \phi}{\sin\theta} = \frac{l \cdot \alpha_{FV}}{\sin\theta} = K \cdot l \cdot \alpha_{FV}$$

where $K = \frac{1}{\sin\theta}$

Similarly, $F \cong K \cdot R \cdot \alpha_{FV}$

Then, $\frac{s}{F} = \frac{K \cdot l \cdot \alpha_{FV}}{K \cdot R \cdot \alpha_{FV}} = \frac{l}{R}$ (5)

Let d = Percent target vertical shift relative to sensor vertical FOV.

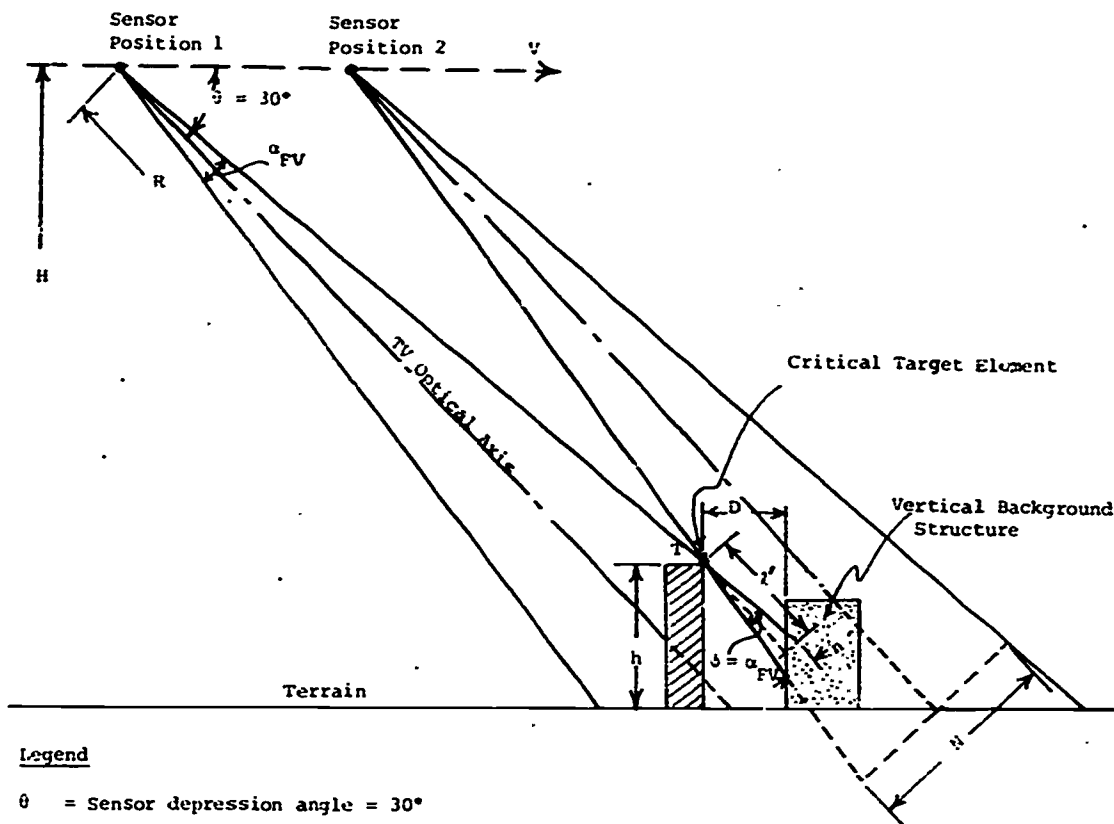
$$d(\%) = \frac{s}{F} \cdot 100 = \frac{l}{R} \cdot 100$$

Since $l \cong \frac{h}{\sin\theta}$ and $R \cong \frac{H}{\sin\theta}$

$$d(\%) \cong \frac{h}{\sin\theta} \cdot \frac{\sin\theta}{H} \cdot 100 = \frac{h}{H} \cdot 100$$
 (6)

Comparison of Equation (6) with Equations (2) and (4) reveals that for a given target height and sensor altitude, the value of total percent displacement, d, is twice as large for the constant altitude geometry as for the dive approach geometry. Also, as in the dive approach cases, it will be noted that the value of d(%), is essentially independent of the actual value of sensor FOV (paragraph 2.4.2). As discussed in detail in paragraph 2.4.1, sensor altitude is the major parameter controlling the value of d(%).

2.1.4 Constant Altitude Approach - Vertical Background. The geometry and the critical factors associated with this case are shown in Figure 34. The major difference between this and the previous constant altitude case is that the projected target LOS moves down the vertical background surface rather than along a longitudinal horizontal path as the sensor goes from Position 1 to Position 2. The cases are similar in that the total angular displacement of the projected target LOS, designated ϕ , is equal to the TV sensor FOV angle, α_{FV} . Also this angle multiplied by the range, R , defines the total projected longitudinal distance, N , viewed by the sensor.



Legend

- θ = Sensor depression angle = 30°
- α_{FV} = Sensor FOV
- H = Sensor Altitude
- R = Slant range
- h = Height of critical target element above the terrain
- l' = Projected slant distance, target-to-vertical background along sensor LOS
- ϕ = Total angular displacement of projected target LOS from Position 1 to Position 2 ($= \alpha_{FV}$)
- n = Displacement of projected target LOS (normal to TV LOS) on vertical background from Position 1 to Position 2
- N = Total projected longitudinal distance (normal to TV LOS) viewed by the sensor at range R .
- D = Longitudinal separation of critical target element to the vertical background.

Figure 34. Constant Altitude Approach Geometry - Vertical Background Case

The important new factor identified in Figure 34 is D, the longitudinal separation between the critical target element and the vertical background. The significance of the value of D may be seen from the following relationships:

$$\text{Here } \ell' = \frac{D}{\cos \theta}$$

since $\theta = 30^\circ$,

$$\ell' = \frac{D}{.866} = 1.155 D$$

$$\text{and } n = \ell' \cdot \phi = \ell' \cdot \alpha_{FV}$$

$$\text{also, } N = R \cdot \alpha_{FV}$$

$$\text{then, } \frac{n}{N} = \frac{\ell' \cdot \alpha_{FV}}{R \cdot \alpha_{FV}} \quad (7)$$

Let d = Percent target vertical shift relative to sensor vertical FOV.

$$d(\%) = \frac{n}{N} \cdot 100$$

$$\text{Finally, } d(\%) = \frac{1.155 D}{R} = .100 \quad (8)$$

The interesting point about Equation (8) is that percent displacement, d, is shown to be controlled by the longitudinal separation between the target and the vertical background and not by the target height, as in previous cases. Also, altitude, H, (as defined by the slant range and depression angle values) is the second controlling factor. As in previous cases, the actual sensor FOV size is not a significant factor in determining the value of d(%) based on this single target geometry.

2.2 PERSPECTIVE CHANGE RELATIONSHIPS. An effect of changing target perspective was known to be present in the Dive Approach 3-D runs and in the Constant Altitude runs, but behavioral tests showed it was not a primary clue to dimensionality of the final stimulus tape sequences. As previously stated, the primary clue was the presence or absence of a detectable degree of movement parallax. To understand the reason for the differences in responses to these two types of dimensionality clues, perspective change relationships were derived to permit a quantitative comparison with calculated movement parallax values.

The perspective shift of interest in this study is foreshortening in the vertical plane. Perspective changes also occur in the horizontal plane, but generally similar changes would occur with either 3-D targets or a 2-D replica of these targets; therefore, they would not constitute clues to the dimensionality of the image source. For example, the flat roof of a 3-D

building would change shape as a function of viewing angle, but a photographic image of this same roof also would change shape with variation in viewing angle.

With regard to vertical perspective change, the Constant Altitude Approach inherently should produce the greater effect at a given altitude, since more translatory motion of the sensor FOV across the target occurs in this approach mode. This, therefore, is the particular geometry discussed in this section.

Figure 35 depicts the Constant Altitude perspective change geometry. As the target of height, h , enters the top of the sensor FOV, LOS 1, corresponding to this top edge intersects the tallest front-viewed target element, T. The line of sight to the bottom of the target, point B, is designated LOS 2. Due to the relatively small target height compared with slant range, R , LOS 2 is essentially parallel to LOS 1*. The separation of these two lines of sight, identified as distance h , represents the initial projected target height normal to the TV LOS. As the sensor moves along the constant altitude path and gets closer to the target, the projected height of the target continuously decreases. It assumes a minimum value when point B reaches the bottom edge (LOS 3) of the sensor FOV. Here, the line of sight to the top of the target, point T, is shown as LOS 4. Due to previously discussed reasons, these two lines of sight are essentially parallel. Here the geometry is purposely distorted as in the case of LOS 2 for illustrative purposes. The separation between LOS 3 and LOS 4, designated h_2 represents the minimum projected target height. The difference between h_1 and h_2 then is a measure of the change in target vertical perspective. The following formulas derived from this geometry include expressions for h_1 and h_2 . Their difference is then related to the total distance, N , viewed by the sensor vertical FOV to obtain a percent displacement expression which can be compared with the previously derived percent displacements produced by movement prallax effects.

From basic geometry:

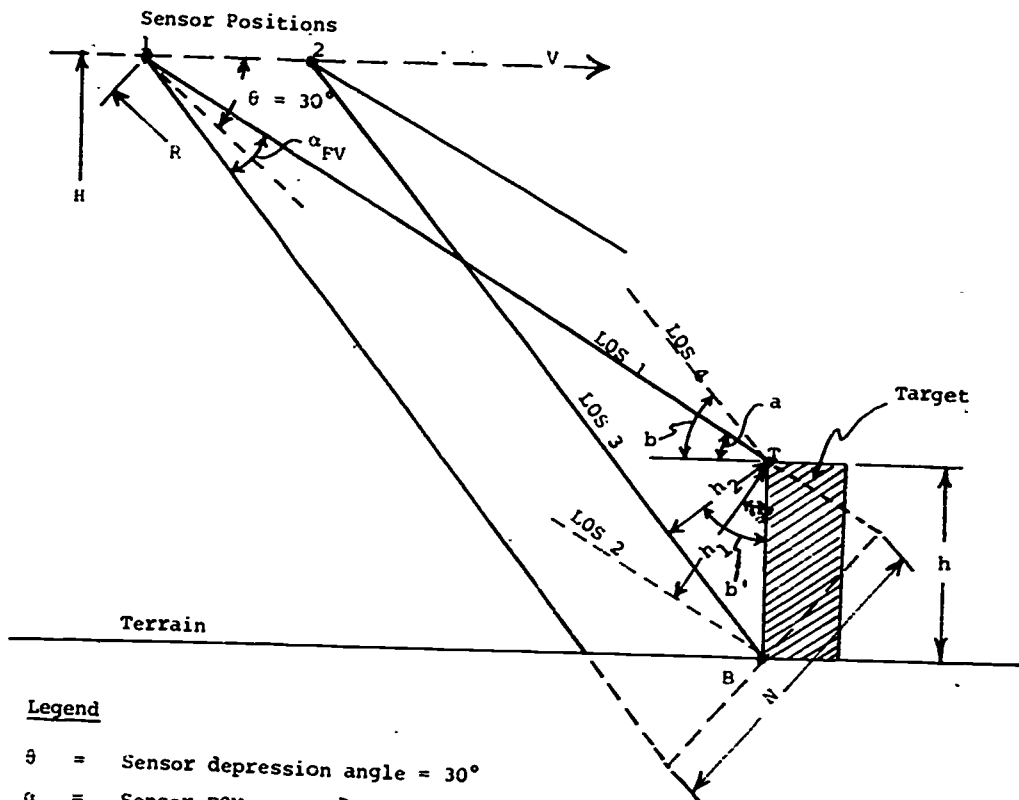
$$\text{Angle } a = \text{Angle } a'$$

$$\text{and angle } b = \text{angle } b'$$

$$\text{where Angle } a = \theta - \frac{\alpha_{FV}}{2}$$

$$\text{and angle } b = \theta + \frac{\alpha_{FV}}{2}$$

* This illustration is purposely distorted to magnify the vertical perspective change effect. In actuality, LOS 2 would intersect LOS 1 at the point shown as Sensor Position 1.



Legend

- θ = Sensor depression angle = 30°
- α_{FV} = Sensor FOV
- H = Sensor altitude
- R = Slant range
- h = Maximum height of viewed target surface above the terrain
- h_1 = Initial projected target height normal to TV LOS
- h_2 = Final projected target height normal to TV LOS
- N = Total projected longitudinal distance (normal to TV LOS) viewed by the sensor at range R
- LOS 1 } Line of sight to top and bottom of target parallel to top edge of TV FOV
- LOS 2 }
- LOS 3 } Line of sight to top and bottom of target parallel to bottom edge of TV FOV
- LOS 4 }

Figure 35. Perspective Change Geometry - Constant Altitude Approach

$$\text{Then, } h_1 = h \cdot \cos \left(\theta - \frac{\alpha_{FV}}{2} \right)$$

$$\text{and } h_2 = h \cdot \cos \left(\theta + \frac{\alpha_{FV}}{2} \right)$$

If vertical foreshortening (perspective change) is identified as Δh , then:

$$\Delta h = h_1 - h_2$$

$$\Delta h = h \left(\cos \theta - \frac{\alpha_{FV}}{2} \right) - \left(\cos \theta + \frac{\alpha_{FV}}{2} \right)$$

$$\text{Also, } N = R \cdot \alpha_{FV} \text{ (radians)}$$

Let p = Percent perspective change relative to sensor vertical FOV

$$p(\%) = \frac{\Delta h}{N} \cdot 100$$

$$p(\%) = \frac{h \left(\cos \theta - \frac{\alpha_{FV}}{2} \right) - \left(\cos \theta + \frac{\alpha_{FV}}{2} \right)}{R \cdot \alpha_{FV} \text{ (radians)}} \cdot 100 \quad (9)$$

Examination of Equation (9) reveals that percent perspective change, p , is directly proportional to target height* and inversely proportional to slant range. Other factors influence the value of p as well, including sensor depression angle and sensor FOV, but their effects on the value of p are not as evident. It can be shown that over a reasonable range of geometries, $p(\%)$ is not affected by the absolute size of the TV FOV. Also, p is found to vary directly with depression angle.

As previously noted, these perspective change relationships are more of academic rather than practical interest in this study, since they had only a minor influence on subject perceptual responses. Paragraph 3.3 does include a sample calculation to quantitatively verify that the available values of p were small compared to the available values of motion parallax, d , in this test series.

2.3 DISPLAY VIEWING GEOMETRY. This section initially discusses the basis for presenting image displacements both in terms of percentage of the sensor FOV and actual displayed visual angle. Then, the display viewing relationships are presented which provide the basis for displayed angular displacement and angular rate calculations included in paragraphs 3.2.1 and 3.2.2.

* This is true as long as target height subtends a small portion of the total vertical FOV of the sensor.

2.3.1 Introduction. Previous sections have presented 3-D target effects relative to the TV sensor FOV geometry. This has provided the basis for computing target/background movement parallax and target perspective changes in terms of percent shift of the affected lines-of-sight relative to the total sensor FOV. Defining these effects as a percentage of the sensor FOV has the advantage that the results are not specific to one TV display viewing geometry*. The percentage FOV displacements can be correlated with behavioral test results and then used to predict subjects' perceptual performance using other 3-D target configurations and viewing geometries.** However, it is also important to relate these LOS angular shifts to the specific display viewing geometry employed. This provides data on the magnitude of TV displayed angular image movements required to reach perceptual thresholds. The associated geometrical relationships are derived below.

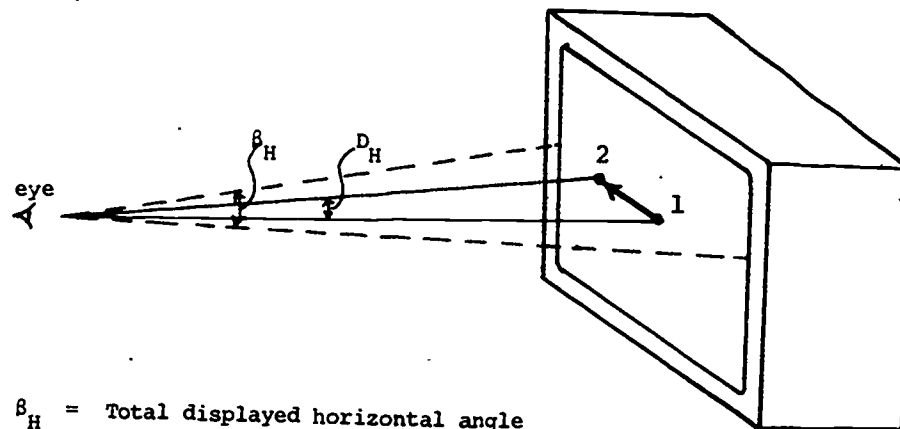
2.3.2 Display Image Displacement Geometrical Relationships. The primary display viewing distance used in the behavioral tests was 20 inches. This was selected to provide adequate eye accommodation while being sufficiently close to achieve a display limited viewing condition. At this distance, the active display raster size of 4-5/8 x 6-1/8 inches subtended total vertical and horizontal angles of 13.2 x 17.6 degrees. Relative to the fixed TV sensor FOV of 4.5 x 6.0 degrees used in the Dive Approach tests, this represented a display magnification*** of approximately three. A second nominal viewing distance of 60 inches (providing unity display magnification) also was used in the Dive Approach tests to determine if this degree of magnification affected image dimensionality perception. As previously discussed, there was no measurable difference between the two conditions, indicating that displayed image fidelity was the limiting factor rather than the subjects' visual perception. For this reason, all the Constant Altitude tests were performed at the 20 inch viewing distance and the computed displayed image displacements and rates were based on this viewing distance.

Figure 36 depicts the display viewing geometry. For the sake of clarity, the horizontal and vertical viewing parameters are shown in separate sketches.

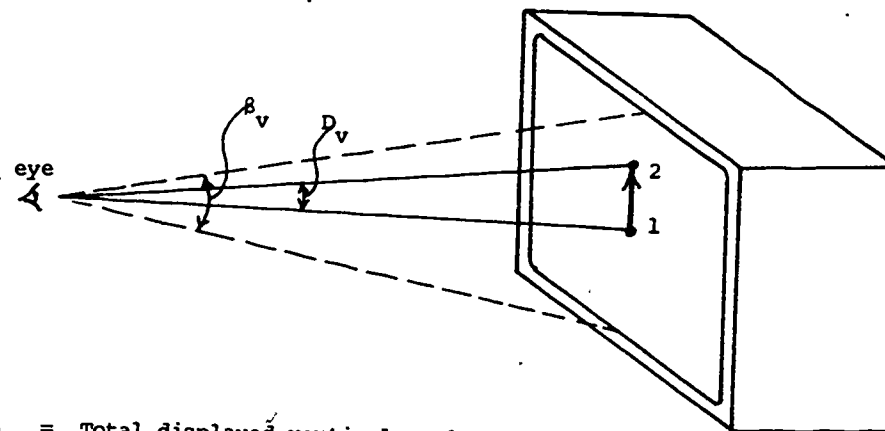
* This presumes TV mediated cases where the acuity of the eye does not significantly limit the fidelity of the perceived displayed imagery; that is, a TV performance-limited viewing condition exists, which was the case in this test program.

** These predictions, however, should be limited to cases in which the resolution and SNR performance of the image display system used approximates those of the TV system employed in this test program (see Appendix F, Paragraph 4, for a summary of resolution and SNR performance obtained from the video tapes on which the final stimulus data were stored).

*** Display magnification = $\frac{\text{Total display angle}}{\text{Sensor FOV}}$



β_H = Total displayed horizontal angle
 D_H = Displayed horizontal image displacement



β_V = Total displayed vertical angle
 D_V = Displayed vertical image displacement

Figure 36. Basic Display Viewing Geometry

The values of horizontal and vertical image displacements, D_H and D_V , are directly related to the percentage sensor FOV lateral and longitudinal image displacements, $d(\%)$, previously discussed. Figures 37 and 38 portray both sensor FOV geometry and the resulting displayed image effects for a Dive Approach run. Figure 37 shows the case in which maximum horizontal LOS displacement is produced (the critical target element is at the edge of the TV FOV at the end of the run). In this case, the target/background relative lines-of-sight have shifted from position A to position B, a distance designated as x . As previously described, the ratio $x/X \cdot 100 = d(\%)$, horizontal image shift. This sketch shows that both image points A and B move farther out from the center of the display as the range decreases, due to image growth effects; however, the target image shifts more rapidly - this differential shift being the movement parallax effect.

Legend

- α_{FH} = TV sensor fixed FOV
- x = Total displacement of projected target LOS from start to finish of run
- X = Total distance viewed by sensor at range R_{min} .

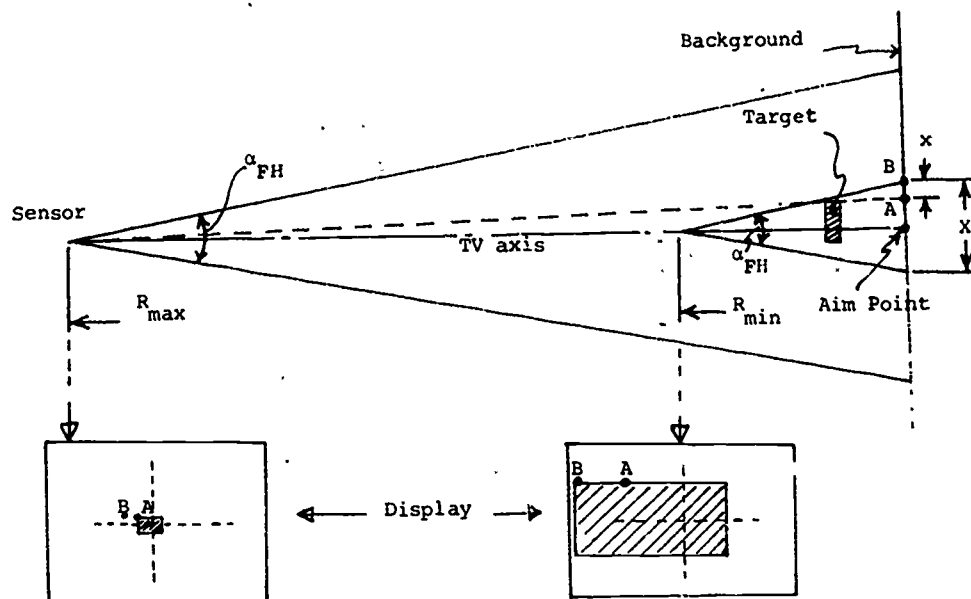


Figure 37. Sensor and TV Display Relationships for Maximum LOS Displacement Case in Dive Approach Runs

The following relationships can be derived from this illustration:

$$\frac{x}{X} = \frac{D_H}{\beta_H}$$

Since $\frac{x}{X}$ is the horizontal (lateral) image displacement ratio, termed d_H ,

$$D_H = d_H \cdot \beta_H \quad (10)$$

In similar fashion, the corresponding vertical (longitudinal) image shift,

$$d_V = \frac{Y}{Y}$$

and $\frac{Y}{Y} = \frac{D_V}{\beta_V}$

$$d_{H(a)} = d_H \cdot \frac{S_{PH}}{S_H} \quad (12)$$

Also, actual displayed image displacement becomes:

$$D_H = d_{H(a)} \cdot \beta_H \quad (13)$$

Similar relationships hold in the vertical (longitudinal) case, i.e.,

$$d_{V(a)} = d_V \cdot \frac{S_{PV}}{S_V} \quad (14)$$

$$\text{and } D_V = d_{V(a)} \cdot \beta_V \quad (15)$$

Also, from Figure 38, it can be seen that:

$$\frac{S_{PH}}{S_H} = \frac{S_{PHD}}{S_{HD}}$$

and

$$\frac{S_{PV}}{S_V} = \frac{S_{PVD}}{S_{VD}}$$

therefore, equations (12) and (14) can be rewritten as:

$$d_{H(a)} = d_H \cdot \frac{S_{PHD}}{S_{HD}} \quad (16)$$

Here, $\frac{S_{PHD}}{S_{HD}}$ is termed the horizontal displacement factor,

and

$$d_{V(a)} = d_V \cdot \frac{S_{PVD}}{S_{VD}} \quad (17)$$

Here, $\frac{S_{PVD}}{S_{VD}}$ is termed the vertical displacement factor.

Equations (16) and (17) were used (in paragraph 3.2.1.1) to compute LOS displacements relative to the sensor FOV (expressed as percent FOV), and equations (13) and (15) were used in the computation of displayed image angular displacements.

2.3.3 Displayed Image Angular Rate Relationships. Different types of displayed image rate effects were experienced with the two categories of target approach runs used (i.e., Dive and Constant Altitude). In the Dive Approach case, an increasing radial image growth rate exists over the entire scene, independent of movement parallax effects. This overall scene growth rate is defined herein as the absolute rate and it applies both to the target and background images. In addition, the movement parallax effect produced a relative rate (also radial) between the selected target and its background. In the case of the Constant Altitude runs, again two rates were involved. The absolute rate in this case was in a downward (near field) direction and resulted from translation of the sensor FOV along the selected terrain paths. The relative target/background LOS rate in this case, resulting from movement parallax, also was in the vertical direction.

In both the Dive and Constant Altitude runs, the absolute rates were substantially higher than the relative rates. However, in none of the cases did the rates appear to fall in a critical region where they would significantly affect perceptual performance. That is, performance remained essentially unchanged when the rates were varied over a two-to-one range. Still, it is of interest to know in quantitative terms what these rates were since this indicates a region of noncritical TV mediated dynamic viewing.

2.3.3.1 Dive Approach Rate Relationships. Absolute growth rates can be determined by use of expressions derived from sensor FOV geometry. Figure 39 shows the terminal phase of a dive approach, since the displayed image growth rate is the greatest at this point.

Referring to this illustration:

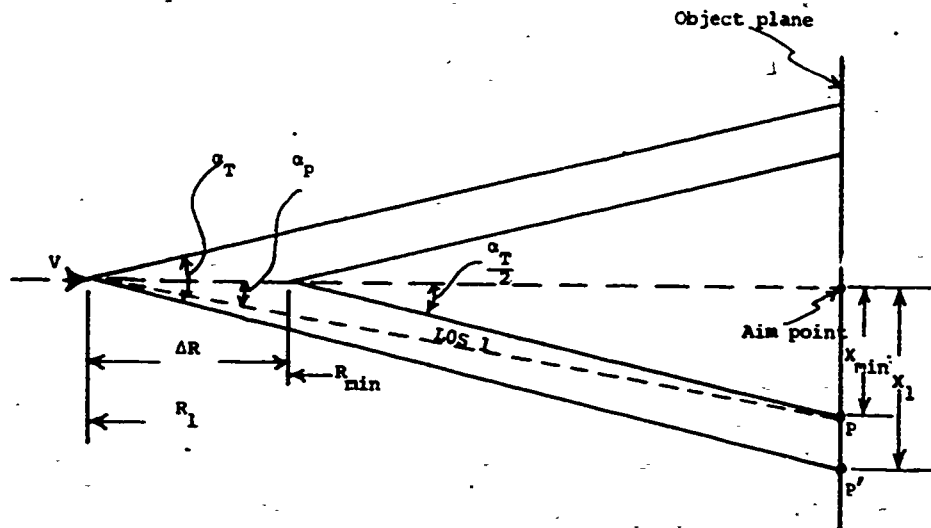
$$\frac{X_{\min}}{R_{\min}} = \frac{X_1}{R_1}$$

$$X_{\min} = \frac{X_1 \cdot R_{\min}}{R_1}$$

$$\text{and } \alpha_P = \frac{X_{\min}}{R_1} = \frac{X_1 \cdot R_{\min}}{R_1 \cdot R_1}$$

$$\text{Since } \frac{\alpha_T}{2} = \frac{X_1}{R_1}$$

$$\alpha_P = \frac{\alpha_T \cdot R_{\min}}{2 \cdot R_1}$$



Legend

V = Approach velocity

t = Final time increment prior to end of run

R_{min} = Minimum slant range

ΔR = Final slant range increment prior to end of run

$$(\Delta R = V \cdot t)$$

$$R_1 = R_{min} + \Delta R$$

α_T = Total sensor FOV

X_{min} = Object distance within one-half sensor FOV at R_{min}

X_1 = Object distance within one-half sensor FOV at R_1

α_P = Partial sensor half FOV angle required to cover distance X_{min} at range R_1

Figure 39. Sensor Geometry Related to Dive Approach Absolute Growth Rate

Since the image of point P will shift to position P' in time, t, the final absolute rate, $\dot{\alpha}_s$, of the sensor LOS 1 is:

$$\dot{\alpha}_s = \frac{\frac{\alpha_T}{2} - \alpha_P}{t} = \frac{\alpha_T - 2\alpha_P}{2t} \quad (18)$$

As previously discussed, at the 20 inch viewing distance, display magnification equals three; therefore, the displayed image rates will be three times the corresponding sensor LOS rate. The final absolute rate, $\dot{\beta}_D$, of the displayed image is:

$$\dot{\beta}_D = 3 \dot{\alpha}_S$$

$$\dot{\beta}_D = \frac{3}{2} \cdot \frac{(\alpha_T - 2\alpha_P)}{t} \quad (19)$$

NOTE: The above expressions are of a general form. If horizontal rates are desired, then α_T will assume a value equal to the sensor horizontal FOV, or a sensor vertical FOV value if vertical rates are desired.

The expressions for Dive Approach relative displayed rates can be derived by reference to paragraphs 2.1.1 and 2.1.2 of this appendix. There, equations (2) and (4) show that with a fixed dive angle and fixed target height, motion parallax-generated sensor LOS displacements are inversely proportional to slant range. Also, equations (10) and (11) in paragraph 2.3.2 show that displayed image shifts are proportional to sensor displacements.

Let:

V = approach velocity

R_{min} = minimum slant range

R_c = current slant range

d_{min} = total sensor LOS shift at R_{min}

d_c = total sensor LOS shift at R_c

D_{min} = total displayed image shift at R_{min}

D_c = total displayed image shift at R_c

ΔD = displayed image incremental shift between R_c and R_{min} ,

$$\text{thus } \Delta D = D_{min} - D_c$$

\dot{D} = displayed image relative rate

t = time (seconds) to travel the distance $(R_c - R_{min}) =$

$$\frac{R_c - R_{min}}{V}$$

From the above referenced equations:

$$d_{\min} = \frac{K}{R_{\min}}$$

$$\text{and } d_c = \frac{K}{R_c}$$

$$\frac{d_c}{d_{\min}} = \frac{R_{\min}}{R_c}$$

$$\text{Also, } D_{\min} = K \cdot d_{\min}$$

$$\text{and } D_c = K \cdot d_c$$

$$\frac{d_c}{d_{\min}} = \frac{D_c}{D_{\min}} = \frac{R_{\min}}{R_c}$$

$$D_c = D_{\min} \cdot \frac{R_{\min}}{R_c}$$

$$\text{Since } \Delta D = D_{\min} - D_c$$

$$\Delta D = D_{\min} - D_{\min} \cdot \frac{R_{\min}}{R_c}$$

$$\Delta D = D_{\min} \left(1 - \frac{R_{\min}}{R_c}\right)$$

Average displayed image rate, \dot{D} , is:

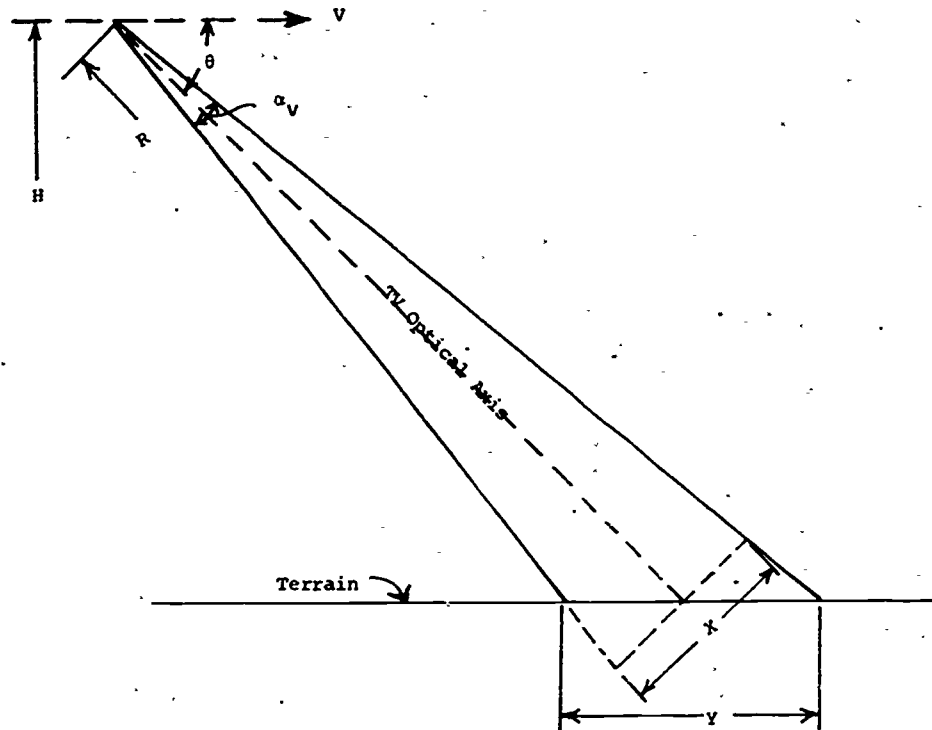
$$\dot{D} = \frac{\Delta D}{t}$$

$$\dot{D} = \frac{D_{\min} \left(1 - \frac{R_{\min}}{R_c}\right)}{t} \quad (20)$$

NOTE: The above expression is in a general form. Appropriate horizontal or vertical displayed image displacements substituted for D_{\min} will produce corresponding horizontal and vertical displayed image relative rates.

2.3.3.2 Constant Altitude Rate Relationships. The displayed rates of interest in this case are the average absolute and relative rates observed as the images move from top to bottom of the display. The values can be determined by computing the total time, t , required for a point entering the top of the displayed scene to move to the bottom, and then dividing this time into the appropriate angular displacement values.

Figure 40 presents the Constant Altitude flight geometry from which the required time may be computed, based on a simulated 200 ft/s. velocity. Since by design, the sensor FOV was adjusted as altitude was varied to



Legend

- R = Slant range, Sensor-to-target
- H = Altitude, Sensor-to-terrain
- θ = Sensor depression angle
- α_V = Sensor vertical FOV
- X = Total viewed longitudinal distance normal to TV optical axis
- Y = Total viewed longitudinal horizontal distance
- V = Relative sensor/terrain model velocity
(= 0.8 ft/sec. actual - 200 ft/sec. simulated)

Figure 40. Constant Altitude Geometry
(for use in Image Rate Computations)

maintain essentially a constant viewed terrain dimension, the time factor will be the same for all sensor FOV/altitude combinations. The maximum altitude case was used in the following computation.

For the maximum altitude (20 feet) case:

$$R = 40 \text{ feet}$$

$$\alpha_v = 2 \text{ degrees} = 0.035 \text{ radian}$$

$$\text{Here, } X = R \cdot \alpha_v$$

$$\text{and } Y = \frac{X}{\sin\theta} = \frac{X}{0.5} = 2X$$

$$\begin{aligned} Y &= 2 \cdot R \cdot \alpha_v \\ &= 2 \cdot 40 \cdot 0.035 \\ &= 2.8 \text{ feet} \end{aligned}$$

$$t = \frac{Y}{V}$$

For a velocity, $V = 0.8$ feet/second (actual),

$$t = \frac{2.8}{.8} = 3.5 \text{ seconds.}$$

Knowing the value of t , the average absolute displayed image rate, $\dot{\beta}_v$, is most simply determined by dividing the total display vertical angle, β_v by time, t .

$$\text{Thus, } \dot{\beta}_v = \frac{\beta_v}{t} = \frac{\beta_v}{3.5} \quad (21)$$

Finally, the expression for Constant Altitude relative target/background average displayed rates (produced by movement parallax) can be obtained by dividing the total relative displayed angle, D_v , for each target condition - see equation (11) - by the above computed time interval.

$$\text{Thus, } \dot{D}_v = \frac{D_v}{t} = \frac{D_v}{3.5} \quad (22)$$

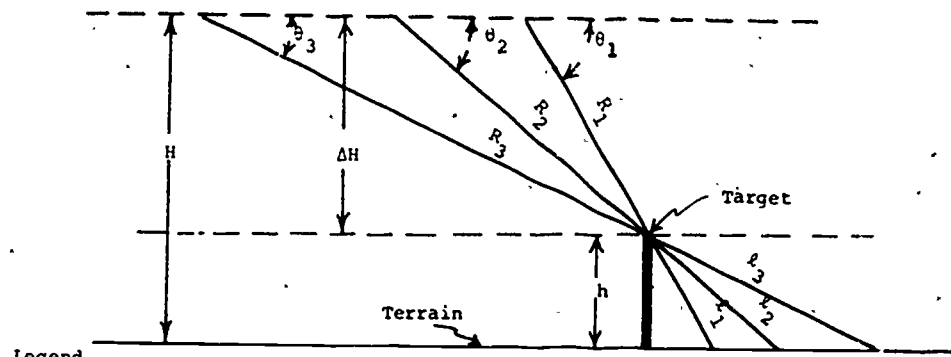
2.4 DISCUSSION OF SPECIAL MOVEMENT PARALLAX RELATIONSHIPS. Certain effects of special interest were noted in the course of the foregoing analyses. Although previously discussed in the context of a particular geometrical

approach, those relationships which have more general application are summarized below. They are: 1) altitude/depression angle/slant range effects, and 2) sensor FOV effects.

2.4.1 Altitude/Depression Angle/Slant Range Effects. Equations (1) and (3) for the DA and Equations (5) and (7) for the CAA geometries show that percent target displacement, d , relative to the sensor FOV, is inversely proportional to slant range, R . This would indicate that if the minimum value of R were doubled, the values of $d(\%)$ would decrease by one-half. This is true under the specific conditions of this test, in which dive angle, θ , is constant. In this case, target heights, h , and/or target-to-background separation, D , are related to target-to-background projected slant distance, ℓ , by a trigonometric function involving θ . Here, image displacements are related to the projected slant distances, ℓ , and the slant ranges, R . However, Figure 41 shows that for a fixed altitude, H , the slant range, R , and thus the dive angle, θ , can vary over wide limits while the ratio of ℓ/R remains constant. With a constant ℓ/R ratio, image displacement, d , or $d(\%)$, remains constant. This relationship applies not only to the CAA geometries but also to the DA cases. In other words, although slant range may be treated as the critical parameter for a given dive angle, in the general case the parameter is altitude. In summary, the image displacements resulting from movement parallax vary inversely with sensor altitude and are not significantly affected by dive angle and slant range changes over a relatively wide range of geometries.

2.4.2 Sensor FOV Effects. In the same series of equations the sensor FOV term, α , appears both in the numerator and the denominator of the sensor LOS percent displacement equations and is therefore cancelled out. This eliminates sensor FOV as a significant variable. That is, although the displacement of the target LOS relative to the background is larger in absolute terms with increases in FOV, the total angular image shifts seen on the TV display remain essentially unchanged. Therefore, if the dimensionality of the target source material is to be determined by displayed movement parallax cues, FOV changes would not affect the results.

An exception to this exists in some cases involving complex, extended targets. If the wider FOV encompasses new target areas having additional prominent features (e.g., taller structures or greater terrain elevations), then the increased area can considerably affect the perception of dimensionality.



Legend

- θ = Sensor depression angle
- H = Sensor altitude
- h = Target Height
- ΔH = $H - h = \text{constant}$
- R = Slant range to target
- l = Projected LOS from target to terrain background

Relationship

By similar triangle relationship,

$$\frac{R_1}{\Delta H} = \frac{l_1}{h} \quad \text{and} \quad \frac{l_1}{R_1} = \frac{h}{\Delta H}$$

$$\text{Also, } \frac{l_2}{R_2} = \frac{h}{\Delta H} \quad \text{and} \quad \frac{l_3}{R_3} = \frac{h}{\Delta H}$$

$$\text{Therefore, } \frac{l_1}{R_1} = \frac{l_2}{R_2} = \frac{l_3}{R_3} = \text{Constant ratio for fixed sensor altitude}$$

Figure 41. General Relationship Between Slant Ranges and Projected Target LOS Slant Distances to Terrain

3. IMAGE DISPLACEMENT AND RATE CALCULATIONS

Image displacements and image rates experienced in the DA and CAA tests are discussed below.

3.1 IDENTIFICATION AND MEASUREMENT OF CRITICAL TARGET ELEMENTS. This section describes the procedures used to identify the critical target elements associated with each of the DA and CAA runs and to translate this data into measurements suitable for use in the previously derived image displacement equations.

3.1.1 Dive Approach Tests. Appendix D, Section 3 describes the general configuration and sizes of representative elements within the five target areas used in these tests. Because of the difficulty in perceiving movement parallax with these targets, few critical elements were perceived with any degree of consistency by the subjects. However, through familiarity with the critical terminal phases of each target run, the investigators were able to identify the particular elements which exhibited the largest movement parallax effects. Subject comments were of course taken into account and were assigned a relatively heavy weighting. In addition to identifying the particular critical element in each displayed target area, its final verti-

NAVTRAEQUIPCEN 70-C-0238-1

cal and horizontal location relative to the center of the display (the sensor aim point) was also marked on a separate photograph of each target area.

These measurements provided the ratios S_{PHD}/S_{HD} and S_{PVD}/S_{VD} used to compute actual horizontal and vertical image displacements as discussed in paragraph 2.3.2 of this appendix.

The final target image position within the viewed field determined the actual percent relative image shift compared to the maximum possible shift which occurs if the target element is at the edge of the viewed area at the end of the run.

Table 9 lists the critical target elements in each area and summarizes the displacement factor values for the Dive Approach displayed imagery.

TABLE 9. CRITICAL DISPLAYED TARGET IMAGE MEASUREMENTS - DIVE APPROACH

Tape Run No.	Target Area	Critical Target Element	Displ. from Center of Display			
			Horizontal		Vertical	
			L/R	S_{PHD}/S_{HD}	U/D	S_{PVD}/S_{VD}
6	Airport	Quonset hut doorway	R	1.0	U	1.0
5	Truss Bridge	Far top bridge railing	R	1.0	U	1.0
15	Industrial Area	Building roof	L	0.9	U	0.6
10	POL Facility	Top of left spherical tank	L	1.0	U	0.75
9	Mt. Storage Facility	Top of tank	L	0.8	U	0.8

Having identified the critical target element for each run, individual annotated photographs of the target areas were used to determine the height of each critical target element. Actually, the true critical dimensions in these cases were the projected slant distances from the target elements to their backgrounds (see the analyses in Paragraph 2). Table 10 provides a summary of these measurements (actual and simulated values).

3.1.2 Constant Altitude Approach Tests. The seven target areas used in this test series are described in Appendix D, Paragraph 4. Although responses to dimensionality clues in this series of tests were superior to those in the DA tests, there was still very little consistency among the subjects concerning the particular target elements which enabled them to detect movement parallax along some of the flight paths. In the Mountain Top, the Airport, and to a lesser extent the POL areas, the target elements responsible for the perception of dimensionality were consistently identified by the subjects. In the remaining four areas, the critical target elements were determined in a way similar to that used in the DA case.

NAVTRAEQUIPCEN 70-C-0238-1

TABLE 10. HEIGHTS OF CRITICAL TARGET ELEMENTS - DIVE APPROACH

Target Area	Target Heights Above Terrain	
	Actual (inches)	Simulated (feet)
Airport	1.25	26
Truss Bridge	2.0	42
Industrial Area	1.25	26
POL Facility	2.25	47
Mt. Storage Facility	1.25	26

Table 11 lists the selected target areas and includes the measurements (actual and simulated) required for subsequent image displacement calculations.

TABLE 11. CRITICAL TARGET ELEMENT MEASUREMENTS - CONSTANT ALTITUDE APPROACH

Target Area No.	Target Area	Critical Target Element	Target Measurements			
			Target Height ⁽¹⁾		Target to Background Separation ⁽²⁾	
			Actual (inches)	Simul. (feet)	Actual (inches)	Simul. (feet)
1	Airport	Roof of Operations Building	2.0	42		
2	Harbor Area	Highway bridge over railroad tracks	0.75	16		
3	General Terrain	Trees on north bank of lake	1.75	36		
4	Truss Bridge	Far, top bridge railing	2.0	42		
5	Mountain Top	Mountain peak (to first plateau)	16.0	330		
6	POL Facility	Top of nearer cylindrical tank (to rear tank)			2.0	42
7	Mountain Storage Facility	Roof peak of far shed	1.5	31		

Notes: (1) For flat terrain background
 (2) For vertical background

3.2 MOVEMENT PARALLAX CALCULATIONS. This section includes a complete set of calculated image displacement data plus representative data on displayed image rates resulting from the simulated dynamic flight conditions.

3.2.1 Image Displacement Calculations. This section summarizes the movement parallax calculations based on the DA and CAA geometric relationships derived in Paragraph 2.1 and on the target measurements discussed in Paragraph 3.1. Tabulated relative target/background displacement values are given in terms of percent sensor FOV, d , and in terms of displayed angular shifts, D . Also, plots of these displacements for each target area are included.

3.2.1.1 Dive Approach Displacement Calculations. Depending on the sensor aim point, the maximum movement parallax potentially available from a given target configuration might not be attained in both the horizontal and vertical directions on a given dive approach. Therefore, the procedure used in calculating displacements was to first calculate the maximum percent sensor FOV values, d_H and d_V based on equations (2) and (4). Then these values and the target heights given in Table 10 were multiplied by the corresponding displacement factors given in Table 9 to obtain the actual percent image displacements, $d_{H(a)}$ and $d_{V(a)}$ -- see equations (16) and (17). The resulting values are shown in Table 12.

TABLE 12. PERCENT TARGET IMAGE DISPLACEMENTS RELATIVE TO SENSOR FOV - DIVE APPROACH

Target Area	Horiz. Displ (% FOV)		Vert. Displ (% FOV)	
	Max. %	Actual %	Max. %	Actual %
	d_H	$d_{H(a)}$	d_H	$d_{H(a)}$
Airport	1.7	1.7	1.7	1.7
Truss Bridge	2.8	2.8	2.8	2.8
Industrial Area	1.7	1.6	1.7	1.0
POL Facility	3.1	3.1	3.1	2.3
Mountain Storage Facility	1.7	1.4	1.7	1.4

Figure 42 shows values of obtained movement parallax (percent horizontal and vertical displacements) plotted as a function of target height. This provides a means of estimating the magnitude of the cues which can be derived from a given amount of vertical development.

Motion parallax effects are dependent on the position of the target image relative to the center of the FOV, with the maximum effect occurring at the edge of the FOV. To provide a uniform basis for comparing the magnitude of this effect available from each target, the actual target heights - measured directly on the terrain model - are multiplied by their displace-

d_H and d_V - Percent Target Image Horizontal and Vertical Displacement Relative to Total Viewed Field

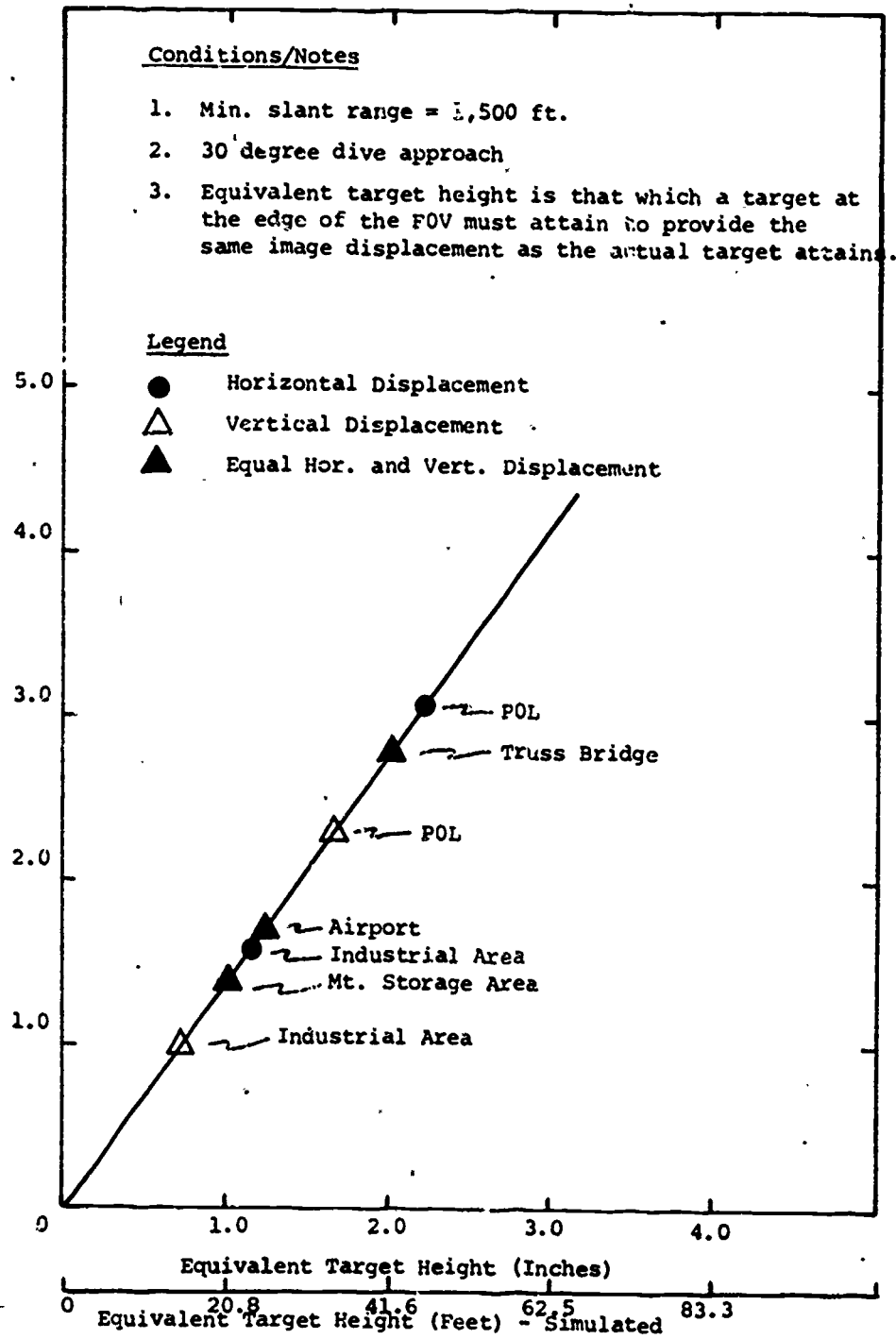


Figure 42. Percent Target Image Horizontal and Vertical Displacement versus Target Height - Dive Approach

NAVTRAEQUIPCEN 70-C-0238-1

ment factors (paragraph 2.3.2). This determines the target height required to produce an equivalent degree of motion parallax at maximum image displacement - the selected reference condition.

Displayed image angular displacement values were computed using equations (13) and (15). Table 13 lists these values and Figure 43 presents the same data in bar graph form. These calculations are based on the 20 inch viewing distance common to the DA and CAA test series.

TABLE 13. DISPLAYED IMAGE ANGULAR DISPLACEMENT - DIVE APPROACH

Target Area	Displayed Displacements (arc minutes)	
	D _H	D _V
Airport Area	17.8	13.4
Truss Bridge	29.3	22.1
Industrial Area	16.7	7.9
POL Facility	32.4	18.2
Mountain Storage Facility	14.6	11.0

3.2.1.2 Constant Altitude Displacement Calculations. The percent displacement values for these runs were computed using equations (6) and (8) as appropriate, and the target measurements given in Table 11. These percent displacement values are listed in Table 14 below for the seven target areas and the four sensor altitude conditions.

TABLE 14. PERCENT IMAGE DISPLACEMENTS RELATIVE TO SENSOR FOV - CONSTANT ALTITUDE APPROACH

Target Area No.	Target Area	Vertical Displacement, d _v (% FOV)			
		Altitude (feet)			
		Actual/Simul 20/5,000	Actual/Simul 10/2,500	Actual/Simul 6/1,500	Actual/Simul 3/750
1	Airport	0.8	1.7	2.8	5.6
2	Harbor Area	0.3	0.6	1.0	2.1
3	General Terrain	0.7	1.5	2.4	4.9
4	Truss Bridge	0.8	1.7	2.8	5.6
5	Mountain Top	6.7	13.4	22.2	44.5
6	POL Facility ⁽¹⁾	0.5	0.9	1.6	3.2
7	Mountain Storage Facility	0.6	1.3	2.1	4.2

Note: (1) Displacement based on vertical background

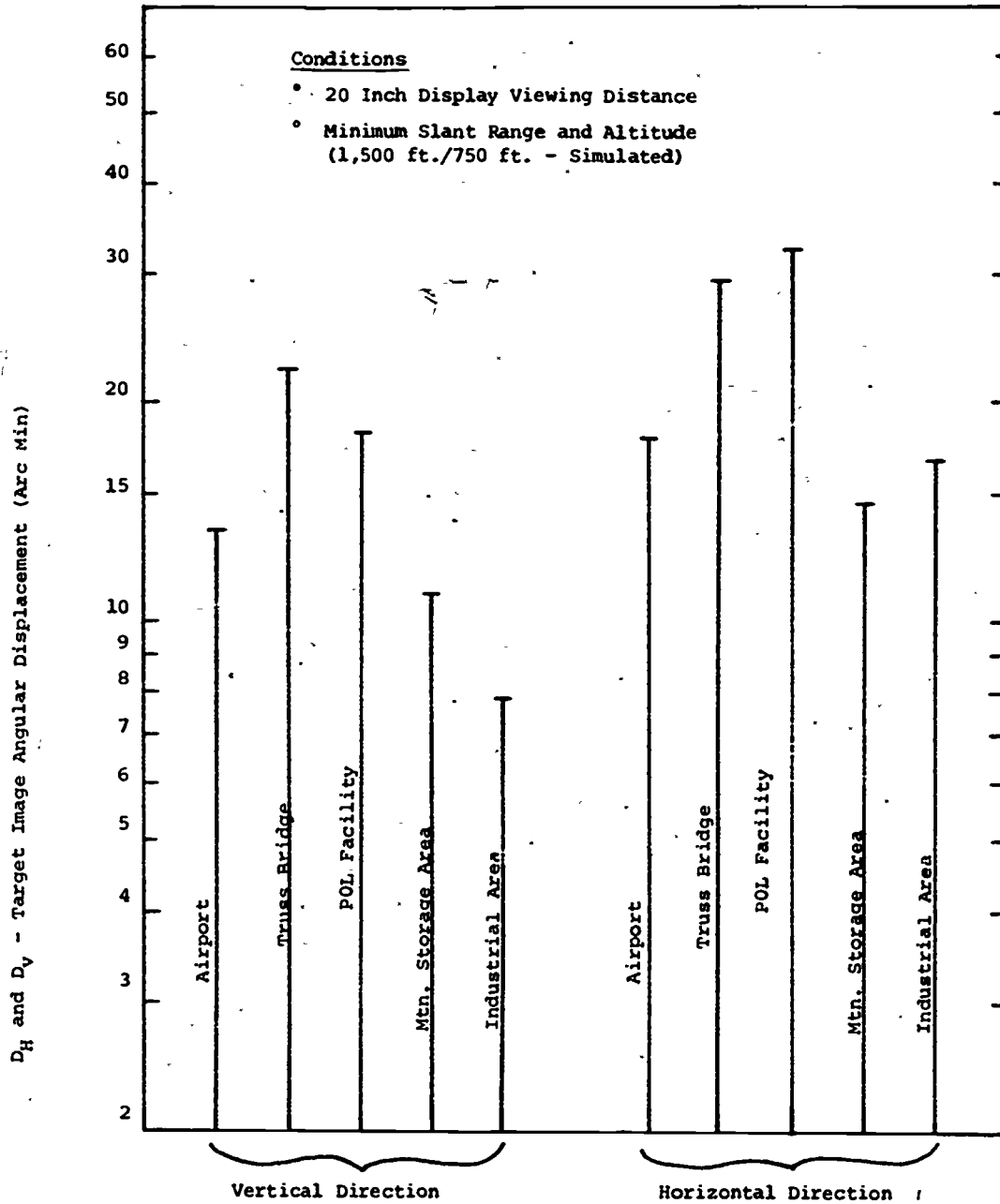


Figure 43. Vertical and Horizontal Displayed Target Angular Displacements - Dive Approach

The same data as above are plotted in Figures 44 and 45 as a function of target height and target-to-background separation, respectively.

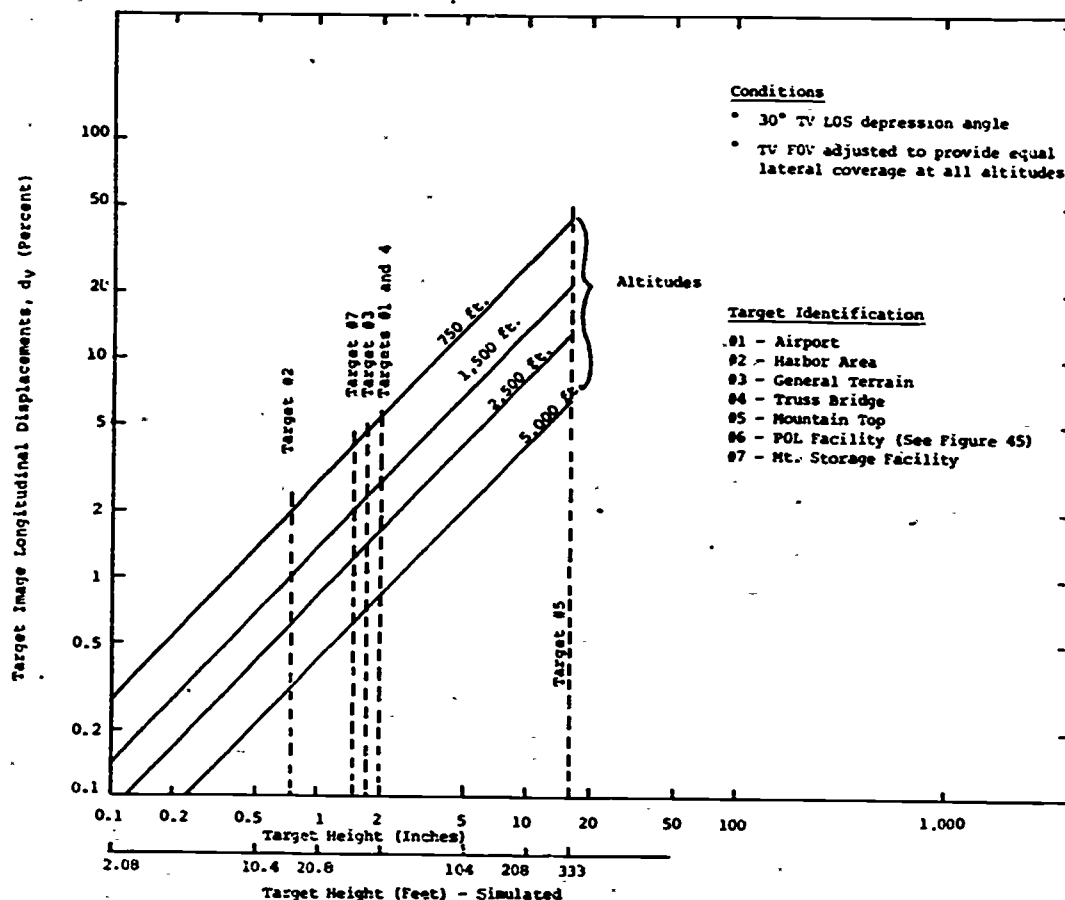


Figure 44. Percent Target Image Longitudinal Displacement versus Target Height for Different Altitudes - Constant Altitude Approaches - Flat Terrain Background Case

Displayed image angular displacements were computed using equation (11). Table 15 lists the resulting values for the seven targets and four sensor altitude conditions.

Figure 46 presents this same data in bar graph form.

3.2.2 Displayed Image Rate Calculations. Paragraph 2.3.3 describes two general categories of displayed image angular rates; viz., absolute and relative. Within the absolute rate category, there are two types of rates identified, based on whether the dynamic display imagery is generated by a DA or a CAA trajectory. The Dive Approach produces radial image expansion at an increasing rate, and the Constant Altitude Approach geometry produces a general downward movement of the image. Superimposed on these absolute rates is a relative rate generated by 3-D target/background motion-parallax effects. Again, these relative rates differ between the DA and CAA tests.

NAVTRAEQUIPCEN 70-C-0238-1

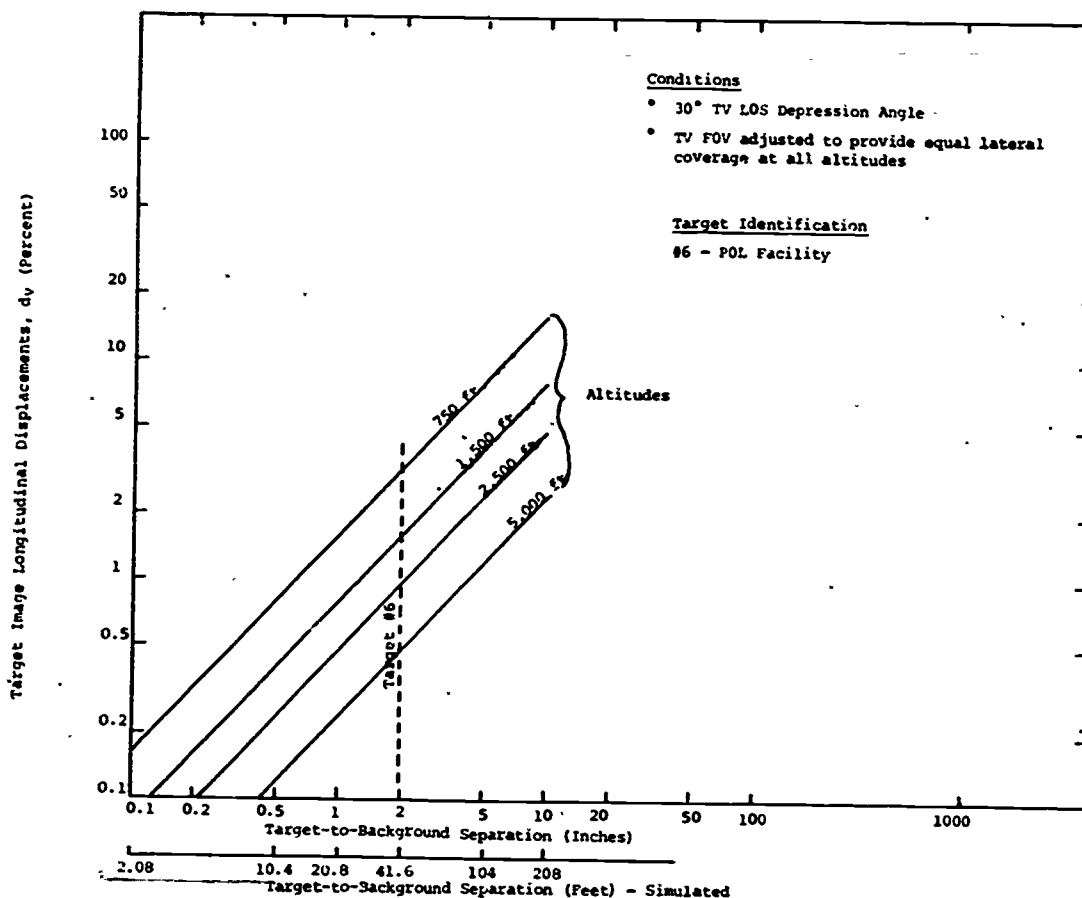


Figure 45. Percent Target Image Longitudinal Displacement versus Target-to-Vertical Background Separation for Different Altitudes - Constant Altitude Approaches - Vertical Background Case

TABLE 15. DISPLAYED IMAGE ANGULAR DISPLACEMENTS - CONSTANT ALTITUDE APPROACH

Target Area No.	Target Area	Vertical Displacement, D_y (arc minutes)			
		Altitude (feet)			
		Actual/Simul 20/5,000	Actual/Simul 10/2,500	Actual/Simul 6/1,500	Actual/Simul 3/750
1	Airport	6.6	13.2	22.0	44.0
2	Harbor Area	2.5	5.0	8.2	16.5
3	General Terrain	5.8	11.6	19.2	38.4
4	Truss Bridge	6.6	13.2	22.0	44.0
5	Mountain Top	53.0	106.0	175.0	350.0
6	POL Facility ⁽¹⁾	3.8	7.6	12.7	25.4
7	Mountain Storage Facility	5.0	10.0	16.5	33.0

Note: (1) Displacement based on vertical background

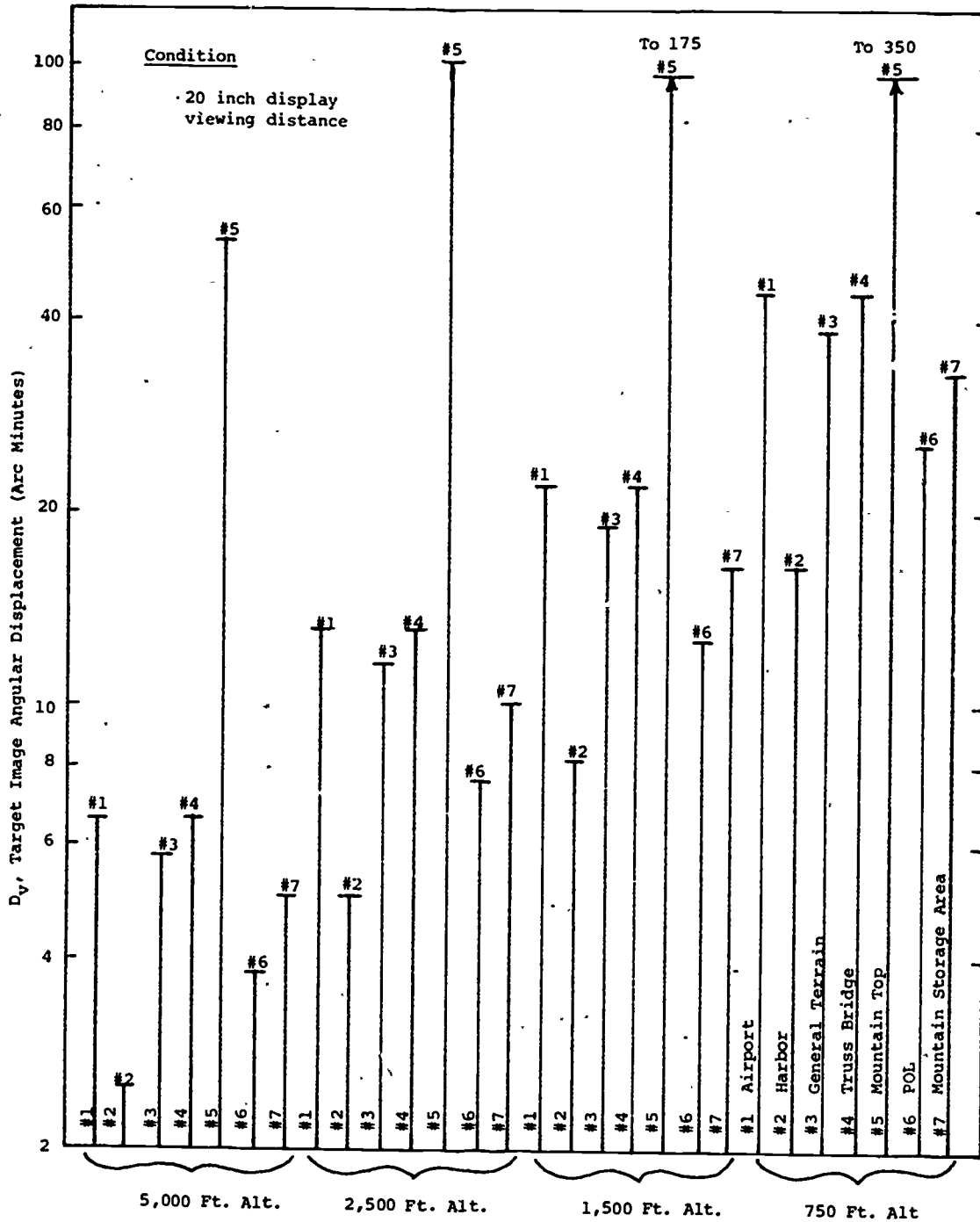


Figure 46. Displayed Target Image Angular Displacement versus Altitude - Constant Altitude Approach

NAVTRAEQUIPCEN 70-C-0238-1

The following sections include rate calculations based on typical test conditions. Detailed calculations were not performed since the behavioral analyses showed that velocity was not a significant factor in the perception of image dimensionality.

3.2.2.1 Dive Approach Rate Calculations. As previously noted, the maximum rate effects in the DA tests occur at the end of the run. Equation (19) was used to obtain a good approximation of the absolute radial image rate at the edges of the display under the following experimental conditions (also refer to Figure 39).

$V = 650$ feet/second (simulated) - Approach velocity

$t = 0.5$ second - Time before end of run

$R_{\min} = 1500$ feet (simulated) - Final slant range

$\Delta R = V \cdot t = 325$ feet (simulated) - Final range increment

$R_1 = R_{\min} + \Delta R = 1,825$ feet (simulated) - Range at 0.5 second prior to end of run

$\alpha_T = 6$ degrees }
 $\cong 105$ mr. } - Sensor horizontal FOV

From Paragraph 2.3.3.1 analysis:

$$\alpha_P = \frac{\alpha_T}{2} \cdot \frac{R_{\min}}{R_1} = \frac{105}{2} \cdot \frac{1,500}{1,825} = 43 \text{ mr.}$$

From Equation (19), the absolute displayed horizontal rate is:

$$\begin{aligned} \dot{\beta}_{DH} &= \frac{3}{2} \left(\frac{\alpha_T - 2\alpha_P}{t} \right) = \frac{3}{2} \left(\frac{105 - 86}{0.5} \right) \\ &= 57 \text{ mr/second} \\ &\cong 3.2 \text{ degrees/sec.} \end{aligned}$$

The corresponding vertical rate equals the horizontal rate multiplied by the display aspect ratio of 3 to 4; therefore:

$$\begin{aligned} \dot{\beta}_{DV} &= \frac{3}{4} \cdot 57 = 42 \text{ mr/second} \\ &\cong 2.4 \text{ degrees/second} \end{aligned}$$

NAVTRAEQUIPCEN 70-C-0238-1

A typical relative displayed image rate, \dot{D} , also experienced during the final half-second of the DA run, was calculated using equation (20) together with the following experimental conditions (see paragraph 2.3.3.1):

$$t = 0.5 \text{ second}$$

$$R_{\min} = 1,500 \text{ feet (simulated)}$$

$$D_{\min} = 29.3 \text{ arc minutes (calculated displayed angular displacement for the Truss Bridge target - see Table 13)}$$

$$V = 650 \text{ feet/second (simulated)}$$

From Paragraph 2.3.3.1 analysis:

$$t = \frac{R_c - R_{\min}}{V}$$

$$\text{Therefore, } R_c = t \cdot V + R_{\min}$$

$$= 325 + 1,500 = 1,825 \text{ feet.}$$

From equation (20), the relative displayed horizontal image rate is:

$$\dot{D}_H = \frac{D_{\min} \left(1 - \frac{R_{\min}}{R_c}\right)}{t} = \frac{29.3 \left(1 - \frac{1,500}{1,825}\right)}{0.5}$$

$$\cong 10.5 \text{ arc minutes/second}$$

In similar fashion, the corresponding vertical rate was calculated as:

$$\dot{D}_V \cong 8 \text{ arc minutes/second}$$

By picking range increments further away from the final minimum range, corresponding image rates were calculated to demonstrate the increasing rate effect as the end of the run is approached. These rates are summarized in Table 16.

3.2.2.2 Constant Altitude Rate Calculations. The average absolute rate for this test condition was calculated by using Equation (21).

$$\begin{aligned} \text{Here, } B_V &= 13.2 \text{ degrees (subtended total vertical display angle -} \\ &\quad \text{20 inch viewing distance)} \\ &= 230 \text{ mr} \end{aligned}$$

and $t = 3.5$ seconds (time required for top to bottom movement of displayed image)

NAVTRAEQUIPCEN 70-C-0238-1

TABLE 16. RELATIVE DISPLAYED IMAGE RATES DURING TERMINAL PHASE OF RUN - DIVE APPROACH

Time Prior to End of Run (seconds)	Simulated Slant Range (feet)	Displayed Image Rates (arc min/second)	
		Horizontal	Vertical
0.0	1,500	10.5	8.0
0.5	1,825	7.2	5.5
1.0	2,150	5.3	4.0

From Equation (21), the average vertical rate is:

$$\dot{\beta}_V = \frac{\beta}{t} = \frac{230}{3.5} = 66 \text{ mr/second}$$

$$\approx 3.8 \text{ degrees/second}$$

It will be noted that this rate is quite similar to the corresponding DA rate previously calculated.

A relative displayed image rate was calculated using Equation (22). Here, as in the DA case, the Truss Bridge target displacements (vertical direction) were used as representative values for these tests (see Table 14).

From Equation (22) the relative displayed vertical rates are:

Slant Range/Altitude(feet)	10,000/5,000	5,000/2,500	3,000/1,500	1,500/750
\dot{D}_V , Relative Rates (arc min/sec)	1.9	3.8	6.3	12.6

3.3 TARGET PERSPECTIVE CHANGE CALCULATIONS. As discussed in Paragraph 2.2, perspective changes were not significant clues to displayed image dimensionality, being overshadowed by movement parallax effects. The following calculations were performed in order to compare the magnitude of perspective change during a CAA run* with the calculated movement parallax change experienced with the same target(s). The Truss Bridge and the Airport targets were selected, since they both exhibited higher than average levels of movement parallax at the lower altitudes (and consequently should have generated higher than average perspective changes). The heights, h, of the identified critical elements in both cases were two inches above the terrain (approximately 40 foot simulated heights).

* The largest movement parallax effect should be produced with the CAA run geometry.

NAVTRAEQUIPCEN 70-C-0238-1

Equation (5) in Paragraph 2.2 was used to compute the percent perspective change, p , relative to the sensor vertical FOV. The following conditions were defined:

- Target height, $h = 2$ inches (42 feet simulated)
- Sensor depression angle, $\theta = 30$ degrees
- Sensor vertical FOV, $\alpha_{FV} = 13$ degrees (Note: This FOV value was selected but the absolute value of FOV is not critical to the calculation.)
- Slant range, $R = 6$ feet (1,500 feet simulated) - Note: This minimum range was picked to produce maximum perspective change.

From Equation (9),

$$\begin{aligned}
 p(\%) &= \frac{h \left(\cos \theta - \frac{\alpha_{FV}}{2} - \left(\cos \theta + \frac{\alpha_{FV}}{2} \right) \right)}{R \cdot \alpha_{FV} \text{ (radians)}} \times 100 \\
 &= \frac{2 \left((\cos 30^\circ - 6.5^\circ) - (\cos 30^\circ + 6.5^\circ) \right)}{6 \times 12 \times 0.23} \times 100 \\
 &= 1.4 \text{ percent}
 \end{aligned}$$

To compare the magnitude of this perspective change with the degree of change due to movement parallax, the value of $p(\%)$ was evaluated against the percent image displacements, d_v , produced by the same targets at the same simulated slant range and altitude. This latter data can be obtained from Figure 44. A value of approximately 5.5 percent displacement corresponds to the 750 foot altitude line. This is nearly four times as great as the perspective shift value. Therefore, these calculations support the contention that motion parallax was the most important clue to the dimensionality of the displayed image source.

APPENDIX H

SUBJECT INSTRUCTIONS

Subject instructions for both tests were prerecorded on audio tape and then presented to the subjects on an individual basis. The transcripts of the instructions are presented in this section.

1. DIVE APPROACH INSTRUCTIONS

On the TV monitor you will be presented a series of tape sequences. These sequences will simulate a view from a TV camera which would be mounted on the nose of an aircraft or a missile as it dives toward a target. There are five different target areas ranging from an oil dump or POL facility located in the desert to a built-up industrial area. There are two rates of closure, that is, the velocity at which you approach the target may simulate either 440 or 750 miles an hour. Each individual target area may vary in several respects. For example, one time the area may be shown under cloudy conditions, another time under sunny conditions. Also, as stated before, the speed with which you approach the target may be one of two rates. There is only one essential major difference, however, in the manner of presentation of these targets, and that difference is dimensionality. Each target will be presented either as a 2-dimensional target or a 3-dimensional target. For the 3-dimensional case, the target you will be viewing will be a display of an actual 3-dimensional target area. In actuality, you will be viewing the 250-to-1 scale model of the terrain and manmade objects which are located on that terrain. As you dive toward the target, the images displayed will behave exactly as they would in real life. The principle of motion parallax, which will be explained below, will make it possible to see the objects move with relationship to each other.

For the 2-dimensional case, the image displayed during the dive will be identical to a photograph or a 2-dimensional image. In this instance, the relationships of all objects would not change as you get closer.

The quality of each presentation is not a clue to its dimensionality. For example, some sequences were filmed under low light levels, and the images are of poor quality for both the 3-dimensional and 2-dimensional presentations.

Now, determination of whether a sequence is 2-D or 3-D, that is, determination of depth, involves a single essential clue, motion parallax. If you as an observer fixate on an object that is moving, the differential angular velocity exists between the lines of sight to the fixated moving object and some other stationary or moving objects. For example, when we look out a car window, nearer objects move across our field of vision more rapidly than objects that are farther away. For example, telephone poles move past quickly, while houses move slowly or seem not to move at all in the distance. This principle of motion parallax then enables us to distinguish actual depth in a 3-dimensional world. If, in our case, we approach an area or dive on a target, the nearer objects will move at a different

NAVTRAEQUIPCEN 70-C-0238-1

rate than objects farther away. If then, we watch the relationship between objects that are at different distances from our eye, we will see differences in relative movement which will result in the objects assuming different positions relative to each other as we get closer to them. If, on the other hand, we view a 2-dimensional display, for example, like a photograph, the relative positions of the viewed objects cannot change because they are fixed in that photograph or image plane.

Now, your task then is to view a series of TV tapes and attempt to determine which of these are 3-D and which are 2-D. Each run will vary from 8 to 14 seconds depending on the velocity. During the trial run, if you are able to determine that the image being presented to you is a 3-D image, then at the instant you determine that it is a 3-D, say "3-D" into the microphone that you are holding, and when you say this, please enunciate clearly. Again, if you think it is 3-D, as soon as you determine this say "3-D." If, on the other hand, you determine that the image is 2-dimensional, then report "2-D" at the time you decide. If you cannot tell whether it is 2-D or 3-D, then state "don't know." After each run, you will have a 10-second break. During this time period, you may also state your decision if you haven't during the run. For example, if you watch the total run and are uncertain as to the dimensionality, then during that 10-second break you would state "don't know" or you may evaluate the run and decide "3-D" or "2-D" after its completion. The object is to try and distinguish the dimensionality at the earliest possible time. So, if you do make a decision, state it immediately and clearly into the microphone.

You will have a series of 44 trials with a rest period of 5 minutes half way in between. After the trials are completed, you will be asked for your subjective comments about the test. To start, you will be given four practice runs, two will be 2-D and two will be 3-D. They are of a single area showing a large suspension bridge and an industrial area. The image quality will differ because of the lighting conditions and, again, you are warned that this is not a clue to dimensionality. There are several objects in the view that will offer you clues as to its dimensionality. For example, the relationship between the bridge tower and the car on the bridge roadway at the upper left of the picture you will see will change as you get closer to it. Another area is between the vertical walls of the buildings with the relationship to the sidewalks and the streets. Again, four practice trials will be given. If you have any questions, please ask them. After the practice trials, the actual trials will begin. During the practice trials, the test conductor will point out areas on the display where the cues to dimensionality may be seen or not seen. After you have viewed the four practice trials, the practice trials will be repeated and you will have an opportunity to give your answer into the microphone before proceeding ahead to the actual runs.

One final point: If you view the runs completely and have made a decision or have not been able to make a decision, you may, during this period either change your mind or make your decision during the interval. For example, if you thought it was 2-D during the run, and then at the end you change your mind, you have the option of doing this one time. If you

NAVTRAEQUIPCEN 70-C-0238-1

said it was 2-D, then at the end, change your mind and say "3-D" during this interval. Now, are there any questions?

2. CONSTANT ALTITUDE APPROACH INSTRUCTIONS

On the TV monitor, you will be presented a series of tape sequences. These sequences will simulate the view from a TV camera mounted on an aircraft as the aircraft flies over various terrain areas. There are five different terrain areas ranging from flat, almost featureless landscape with few manmade objects, to mountainous terrain with rapidly varying heights and topographical features. Some of the areas will also contain numerous manmade objects, such as an airport, industrial area, bridges and storage facilities. You will fly over the terrain at a simulated velocity of 200 feet per second, which is 138 miles an hour, and at one of four different simulated altitudes: 5,000, 2,500, 1,200 and 600 feet.

A few of the trials will be presented at a simulated velocity of 400 feet per second, or 276 miles an hour. The scenes that will be presented to you will be either 3-dimensionally based, that is, all the features are physical objects similar to those in the real world, or the scenes will be of a 2-dimensionally based nature; that is, they will be the same as viewing a photograph. The quality of the picture you will see will be identical whether it is 3-D or 2-D.

Your task will be to determine whether the scene is 2-dimensionally based or 3-dimensionally based and report this to the test conductor. Again, for the 3-D case, the target you will be viewing will be a display of an actual 3-D target area. In actuality, you will be viewing a 250-to-1 scale model of the terrain and manmade objects. As you fly over the different objects and general terrain features, the images displayed will behave exactly as they would in real life. The principles of motion parallax and other principles, such as perspective change which will be explained below, will make it possible to see objects move in relation to their backgrounds, or to change shape as the angle that you are viewing them changes as you fly over them. For the 2-D case, the image displayed during the flight will be identical to a photograph or 2-D image. In this instance, the relationship of all objects would not change as you got closer or change your viewing angle. Now, the determination of whether a sequence is a 2-D or a 3-D, that is, determination of depth, involves several cues.

One of the most important of these is motion parallax. If you, as an observer, fixate on an object that is moving, a differential angular velocity exists between the lines of sight to the fixated moving object and some other stationary or moving object. For example: when we look out the car window, nearer objects appear to move across our field of vision much more rapidly than objects that are farther away. For example, telephone poles race past while a house in the distance appears to move more slowly or not at all. This principle of motion parallax enables us to distinguish actual depth in a 3-dimensional world. If in our case we approach an area, the nearer objects will move at a different rate than objects farther away.

NAVTRAEQUIPCEN 70-C-0238-1

If then we watch the relationship between objects that are at different distances from our eye, we will see differences in relative movement which will result in the objects assuming different positions relative to each other as we get closer. If, on the other hand, we view a 2-D display, for example, like a photograph, the relative positions of the viewed objects cannot change because they are fixed in that photo or image plane. One other principle which will enable you to distinguish between 2-D and 3-D is that of perspective change. As you approach an object in a tangential manner, that is, not directly at it, but flying over it as in the case we have here, its shape or perspective as you view it will appear to change. For example, the vertical height of a building will decrease as you get closer to it. That is, the apparent height will decrease as you view it, and this change in height is another essential clue which aids in distinguishing depth.

In the 2-D case, the building could not change its apparent height since it is fixed at the perspective angle in which the photo was taken. Again, your task is to view a series of tapes and attempt to determine which of these are 3-D and which are 2-D. At the end of each trial, you will have a 10-second interval to respond. Wait until you have viewed the complete trial before responding. Then, either say, "2-D" or "3-D." If you cannot determine what the dimensionality is, then respond by saying, "don't know" during this blank interval. Each answer, that is, "2-D," "3-D," and "don't know," all have equal weight, so don't try to guess. We are interested in the perception of images as generated by either a 3-D or 2-D terrain model simulator. We are not interested in the individual performances of the subjects, except as these responses are used to tell us something about the different techniques of simulation. You will have a series of 37 trials, and will have a rest period of five minutes after the 23rd trial. To start, you will be given practice runs which will demonstrate the principles that we have been discussing. These will point out to you the features that we have been talking about. You may ask any questions now, or at that time.

Unclassified
Security Classification

DOCUMENT CONTROL DATA - R & D

(Security classification of title, body of abstract and indexing annotation must be entered when the overall report is classified)

1. ORIGINATING ACTIVITY (Corporate author) Martin Marietta Corporation Orlando, Florida 32605		2a. REPORT SECURITY CLASSIFICATION Unclassified	
		2b. GROUP	
3. REPORT TITLE RELATIVE EFFECTIVENESS OF TWO AND THREE DIMENSIONAL IMAGE STORAGE MEDIA			
4. DESCRIPTIVE NOTES (Type of report and inclusive dates) Final Report June 1970 - February 1972			
5. AUTHOR(S) (First name, middle initial, last name) King, Barry C., and Fowler, Frank D.			
6. REPORT DATE September 1972		7a. TOTAL NO. OF PAGES 118	7b. NO. OF REFS 3
8a. CONTRACT OR GRANT NO. N61339-70-C-0238		8b. ORIGINATOR'S REPORT NUMBER(S) OR11,796	
8b. PROJECT NO. 8424-B		8c. OTHER REPORT NO(S) (Any other numbers that may be assigned this report) NAVTRAEQUIPCEN 70-C-0238-1	
10. DISTRIBUTION STATEMENT Approved for public release; distribution is unlimited.			
11. SUPPLEMENTARY NOTES		12. SPONSORING MILITARY ACTIVITY Naval Training Equipment Center. Orlando, Florida	
13. ABSTRACT Experiments were conducted to evaluate subjects' ability to perceive the dimensionality of source material used to generate dynamic TV images of simulated military targets. The Dive Approach test series investigated the perception of motion-dependent depth cues during an approach to the target area at a constant dive angle. The stimulus material used in these behavioral tests were video recordings of runs made in the Martin Marietta Guidance Development Center (GDC) using 3-dimensional (3-D) and optically simulated 2-dimensional (2-D) target areas. The Constant Altitude Approach test series investigated the perception of motion dependent cues to dimensionality derived from simulated horizontal flight at various altitudes. Again, the stimulus materials used were video recordings of selected target runs made on the GDC terrain model. Results show that movement parallax normally provides useful depth cues only at very close ranges, both for constant dive angle and constant altitude approach geometries. This finding has significant implications for the design of visual simulation equipment to be used for training. Thus, for problems which require simulation of TV navigation and/or targeting imagery, serious consideration should be given to the use of relatively inexpensive 2-D storage devices for altitudes in excess of 750 feet.			

Unclassified

Security Classification

14	KEY WORDS	LINK A		LINK B		LINK C	
		ROLE	WT	ROLE	WT	ROLE	WT
	Target Identification Visual Simulation Closed Circuit TV Human Factors						

Unclassified

Security Classification

DISTRIBUTION LIST

NOTE

Mailing labels are prepared, when needed, as a computer listing, the source of which is updated on a weekly basis. It is not practical to prepare distribution lists each time labels are prepared. Therefore, such lists are prepared semiannually, and a slight discrepancy may exist between the addressees on this list and those appearing on the labels used to distribute this publication.

USAF HUMAN RES LAB AFHRL-DO OPERATION OFC BROOKS AFB TX 78235	1	DR JOHN MEYER HDQTRS AIR TRNG CMD XPT RANDOLPH AFB TX 78148	1
USAF HUMAN RES LAB AFHRL-TT TECH TRNG DIV LOWRY AFB CO 80230	1	USAF HUMAN RES LAB AFHRL-FT FLYING TRNG DIV WILLIAMS AFB AZ 85224	1
USAF HUMAN RES LAB PERSONNEL RSCH DIV LACKLAND AFB TX 78236	1	CHIEF NAVAL MATERIAL MAT 031M WASHINGTON DC 20360	1
USAF HUMAN RES LAB AFHRL-TR TRNG RES DIV WRIGHT-PATTERSON AFB OH 45433	1	JOSEPH J COWAN CH PERS RSCH BRANCH USCG HQ FO-1 STA 3-12 400 SEVENTH ST S W WASHINGTON DC 20226	1
CHIEF NAVAL RESEARCH PSYCHOLOGICAL SCIENCES CODE 450 NAVY DEPT ARLINGTON VA 22217	1	BUREAU NAVAL PERSONNEL ATTN PERS A3 ARLINGTON ANNEX WASHINGTON DC 20370	1
DR RALPH R CANTER DIR MIL MANPWR RSCH OASD M-RA MR-U PENTAGON RM 3-960 WASHINGTON DC 20301	1	DEPT OF PSYCHOLOGY UNIV OF IL AT URBANA-CHAMPAIGN PROF PSYCH J A ADAMS CHAMPAIGN IL 61820	1
NATL SCIENCE FDN ATTN DR HENRY S ODBERT 1800 G ST NW WASHINGTON DC 20550	1	CHIEF NAVAL OPERATIONS ATTN CDR H J CONNERY MSC OP-701E2 NAVY DEPT WASHINGTON DC 20350	1
CHIEF NAVAL OPERATIONS ATTN DR J J COLLINS OP-07T16 NAVY DEPT WASHINGTON DC 20350	1	INSTITUTE OF AVIATION UNIV OF IL URBANA-CHAMPAIGN SAVOY IL 61874	1

NAVTRAEQUIPCEN 70-C-0238-1

CHIEF NAV OPERATIONS ATTN M K MALEHORN OP-14C NAVY DEPT WASHINGTON DC 20350	1	COMMANDER NAVSHIPSSYSCMD CODE 03 WASHINGTON DC 20360	1
COMMANDER NAVELECTSYSCMD CODE 03 WASHINGTON DC 20360	1	CDR NAVSHIPS SYS CMD NAVSHIPS SYS CMD HQS SHIPS 03H GEO N GRAINE WASHINGTON DC 20360	1
NAV AEROSPACE MED INST NAV AEROSPACE MED CTR ATTN CH AVIA PSYCH DIV PENSACOLA FL 32512	1	COMMANDER NAVAIRSYSCMD CODE 03 WASHINGTON DC 20360	1
COMMANDER NAVSUPSYSCMD CODE 03 WASHINGTON DC 20360	1	CO NAVMED RSCH INST NATL NAVMED CTR ATTN TECH REF LIB BETHESDA MD, 20014	1
COMMANDER NAVORDSYSCMD CODE 03 WASHINGTON DC 20360	1	SCIENTIFIC TECHNICAL INFORMATION OFFICE NASA WASHINGTON DC 20546	1
HUMAN RES RSCH ORG DIV NO 1 SYS OPER 300 N WASHINGTON ST ALEXANDRIA VA 22314	1	BEHAVIORAL SCI DIV OFC CHIEF RSCH - DEVEL DEPT OF ARMY WASHINGTON DC 20310	1
CO NAV MISSILE CTR ATTN HD HUMAN FACTORS ENGRG BR POINT MUGU CA 93042	1	HUMAN RESOURCES RESCH ORGZTN DIV 6 AVIATION P O BOX 428 FORT RUCKER AL 36360	1
CH RSCH AND DEVLPMT CH BEHAVIORAL SCI DIV DEPT OF ARMY WASHINGTON DC 20310	1	HQS AF SYS CMD DLSL OFC SCIENTIFIC RSCH ANDREWS AFB WASHINGTON DC 20331	1
COMMANDING OFFICER NAVY MEDICAL NEUROPSYCHIATRIC RESCH UNIT SAN DIEGO CA 92152	1	COMMANDER NAVFAC ENGR CMD NAVFAC ENGR CMD HDQ ASST DIR R&D DIV(CODE 03) WASHINGTON DC 20390	1
DIR DEF RSCH - ENGRG ARPA BEHAVIORAL SCI DIV ATTN LCOL A W KIBLER WASHINGTON DC 20301	1	DIRECTOR US ARMY MOTIVATION & TNG LAB COMMONWEALTH BLDG 1300 WILSON BLVD ARLINGTON VA 22209	1

NAVTRAEQUIPCEN 70-C-0238-1

COMDT OF MARINE CORPS CODE A03C WASHINGTON DC 20380	1	DIR HUMAN RES RSCH ORG 300 WASHINGTON ST ALEXANDRIA VA 22314	1
CHIEF NAVAL RESEARCH ATTN CODE 458 DEPT NAV ARLINGTON VA 22217	1	CHIEF OF NAVAL TRNG CODE 017 NAS PENSACOLA FL 32508	1
COMMANDING OFFICER PERS-TRNG RSCH DEV LAB SAN DIEGO CA 92152	1	CDR NAVAIR DEVEL CTR ATTN HUMAN ENGRG BR WARMINISTER PA 18974	1
US ARMY BEHAVIORAL SCI RESEARCH LAB COMMONWEALTH BLDG RM 239 1320 WILSON BLVD ARLINGTON VA 22209	1	DR JOHN W WEISZ DIR HUMAN ENGRG LAB USA ABERDEEN RSCH DEVEL CTR ABERDEEN PROV GROUNDS MD 21005	1
EXECUTIVE EDITOR PSYCHO ABSTRACTS AMERICAN PSYCH ASSOC 1200 17TH ST NN WASHINGTON DC 20036	1	CO NAVAIR TECH TRNG NAS MEMPHIS ATTN DR G D MAYO HD RESEARCH BR MILLINGTON TN 38054	1
NAV PERSONNEL RSCH & DEVELOPMENT LAB ATTN LIBRARY BLDG 200 RM 3307 WNY WASHINGTON DC 20390	1	ERIC CLEARINGHOUSE ON EDUCATION MEDIA--TECH STANFORD UNIV STANFORD CA 94305	1
CHIEF OF NAVAL TECH TRNG NAVAL AIR STATION, MEMPHIS (75) MILLINGTON, TN 38054 (ATTN: DR. LARRY HARDING, CODE 34)	1		
NAVAL TRAINING EQUIPMENT CENTER ORLANDO, FLORIDA 32803			146
DEFENSE DOCUMENTATION CENTER CAMERON STATION ALEXANDRIA, VA 22314			12

Naval Training Equipment Center, Orlando, Florida

TR NAVTRAEQUIPCEN 70-C-0238-1 UNCLASSIFIED
AD

RELATIVE EFFECTIVENESS OF TWO AND THREE DIMENSIONAL IMAGE STORAGE MEDIA FINAL REPORT. 1972, 118 pp, 46 illus., 3 refs., 16 tables

Experiments were conducted to evaluate subjects' ability to perceive the dimensionality of source material used to generate dynamic TV images of simulated military targets. The Dive Approach test series investigated the perception of motion-dependent depth cues during an approach to the target area at a constant dive angle. The stimulus material used in these behavioral tests were video recordings of runs made in the Martin Marietta Guidance Development Center (GDC) using 3-dimensional (3-D) and optically simulated 2-dimensional (2-D) target areas. The Constant Altitude Approach test series

Martin Marietta Corp.
King, Barry C. and
Fowler, Frank D.
N61339-70-C-0238
NAVTRAEQUIPCEN
Project 8424-B

Naval Training Equipment Center, Orlando, Florida

TR NAVTRAEQUIPCEN 70-C-0238-1 UNCLASSIFIED
AD

RELATIVE EFFECTIVENESS OF TWO AND THREE DIMENSIONAL IMAGE STORAGE MEDIA FINAL REPORT. 1972, 118 pp, 46 illus., 3 refs., 16 tables

Experiments were conducted to evaluate subjects' ability to perceive the dimensionality of source material used to generate dynamic TV images of simulated military targets. The Dive Approach test series investigated the perception of motion-dependent depth cues during an approach to the target area at a constant dive angle. The stimulus material used in these behavioral tests were video recordings of runs made in the Martin Marietta Guidance Development Center (GDC) using 3-dimensional (3-D) and optically simulated 2-dimensional (2-D) target areas. The Constant Altitude Approach test series

Martin Marietta Corp.
King, Barry C. and
Fowler, Frank D.
N61339-70-C-0238
NAVTRAEQUIPCEN
Project 8424-B

KEY WORDS

Target Identification
Visual Simulation
Closed Circuit TV
Human Factors

Naval Training Equipment Center, Orlando, Florida

TR NAVTRAEQUIPCEN 70-C-0238-1 UNCLASSIFIED
AD

RELATIVE EFFECTIVENESS OF TWO AND THREE DIMENSIONAL IMAGE STORAGE MEDIA FINAL REPORT. 1972, 118 pp, 46 illus., 3 refs., 16 tables

Experiments were conducted to evaluate subjects' ability to perceive the dimensionality of source material used to generate dynamic TV images of simulated military targets. The Dive Approach test series investigated the perception of motion-dependent depth cues during an approach to the target area at a constant dive angle. The stimulus material used in these behavioral tests were video recordings of runs made in the Martin Marietta Guidance Development Center (GDC) using 3-dimensional (3-D) and optically simulated 2-dimensional (2-D) target areas. The Constant Altitude Approach test series

Martin Marietta Corp.
King, Barry C. and
Fowler, Frank D.
N61339-70-C-0238
NAVTRAEQUIPCEN
Project 8424-B

KEY WORDS

Target Identification
Visual Simulation
Closed Circuit TV
Human Factors

Naval Training Equipment Center, Orlando, Florida

TR NAVTRAEQUIPCEN 70-C-0238-1 UNCLASSIFIED
AD

RELATIVE EFFECTIVENESS OF TWO AND THREE DIMENSIONAL IMAGE STORAGE MEDIA FINAL REPORT. 1972, 118 pp, 46 illus., 3 refs., 16 tables

Experiments were conducted to evaluate subjects' ability to perceive the dimensionality of source material used to generate dynamic TV images of simulated military targets. The Dive Approach test series investigated the perception of motion-dependent depth cues during an approach to the target area at a constant dive angle. The stimulus material used in these behavioral tests were video recordings of runs made in the Martin Marietta Guidance Development Center (GDC) using 3-dimensional (3-D) and optically simulated 2-dimensional (2-D) target areas. The Constant Altitude Approach test series

Martin Marietta Corp.
King, Barry C. and
Fowler, Frank D.
N61339-70-C-0238
NAVTRAEQUIPCEN
Project 8424-B

KEY WORDS

Target Identification
Visual Simulation
Closed Circuit TV
Human Factors

investigated the perception of motion-dependent cues to dimensionality derived from simulated horizontal flight at various altitudes. Again, the stimulus materials used were video recordings of selected target runs made on the GDC terrain model.

The results show that movement parallax normally provides useful depth cues only at very close ranges, both for constant dive angle and constant altitude approach geometries. This finding has significant implications for the design of visual simulation equipment to be used for training. Thus, for problems which require simulation of TV navigation and/or targeting imagery, serious consideration should be given to the use of relatively inexpensive 2-D storage devices for altitudes in excess of 750 feet.

investigated the perception of motion-dependent cues to dimensionality derived from simulated horizontal flight at various altitudes. Again, the stimulus materials used were video recordings of selected target runs made on the GDC terrain model.

The results show that movement parallax normally provides useful depth cues only at very close ranges, both for constant dive angle and constant altitude approach geometries. This finding has significant implications for the design of visual simulation equipment to be used for training. Thus, for problems which require simulation of TV navigation and/or targeting imagery, serious consideration should be given to the use of relatively inexpensive 2-D storage devices for altitudes in excess of 750 feet.

investigated the perception of motion-dependent cues to dimensionality derived from simulated horizontal flight at various altitudes. Again, the stimulus materials used were video recordings of selected target runs made on the GDC terrain model.

The results show that movement parallax normally provides useful depth cues only at very close ranges, both for constant dive angle and constant altitude approach geometries. This finding has significant implications for the design of visual simulation equipment to be used for training. Thus, for problems which require simulation of TV navigation and/or targeting imagery, serious consideration should be given to the use of relatively inexpensive 2-D storage devices for altitudes in excess of 750 feet.

investigated the perception of motion-dependent cues to dimensionality derived from simulated horizontal flight at various altitudes. Again, the stimulus materials used were video recordings of selected target runs made on the GDC terrain model.

The results show that movement parallax normally provides useful depth cues only at very close ranges, both for constant dive angle and constant altitude approach geometries. This finding has significant implications for the design of visual simulation equipment to be used for training. Thus, for problems which require simulation of TV navigation and/or targeting imagery, serious consideration should be given to the use of relatively inexpensive 2-D storage devices for altitudes in excess of 750 feet.